

**The function of PTK7 during *Xenopus* neural crest migration**

PhD Thesis

in partial fulfillment of the requirements

for the degree “Doctor rerum naturalium (Dr.rer.nat)”

in the Molecular Biology Program

at the Georg August University Göttingen

Faculty of Biology

Submitted by

**Iryna Shnitsar**

Born in Smila, Ukraine

### **Affidavit**

Herewith I declare that I prepared the PhD thesis “The function of PTK7 during *Xenopus* neural crest migration” on my own and with no other sources and aids than quoted.

02.11.2009

Submission date

---

Iryna Shnitsar

## List of Publications

1. **Shnitsar I**, Wehner P, Podleschny M, Urlaub H and Borchers A. RACK1 interacts with PTK7 to regulate neural tube closure. In preparation
2. **Shnitsar I** and Borchers A. PTK7 recruits dsh to regulate neural crest migration. *Development*. 2008 Dec; 135(24):4015-24.
3. Koestner U, **Shnitsar I**, Linnemannstöns K, Hufton AL and Borchers A. Semaphorin and neuropilin expression during early morphogenesis of *Xenopus laevis*. *Dev Dyn*. 2008 Dec;237(12):3853-63
4. P.V. Pogribnoy, I.L. Lisovskiy, N.V. Markeeva, V.M. Shnitsar, **I.I. Zinchenko\*** and M.A. Soldatkina. Production of recombinant of hBD-2-human antimicrobial peptide expressed in cervical and vulval cancer. *Exp Oncol* 2003 March; 25 (1) : 36-39
5. V.M. Shnitsar, M.A. Soldatkina, **I.I. Zinchenko\***, N.V. Markeeva, N.V. Rodnin, S.V. Nespryadko, O.V. Turchak, A.B. Vinnitskaya and P.V. Pogrebnoy. Autoantibodies against human beta-defensin-2 in the blood serum of patients with vulval and cervical cancer. *Exp Oncol* 2003 June; 25 (2): 155-157

---

\* Married in June 2003, previous surname was Zinchenko

**Table of Contents**

Table of Contents.....	4
Acknowledgements .....	8
Abstract.....	9
List of Figures.....	10
List of Tables.....	12
1. Introduction .....	13
1.1 The neural crest and its derivatives.....	13
1.2 Neural crest induction.....	13
1.3 Neural crest migration.....	16
1.3.1 <i>Xenopus laevis</i> as a model system to study neural crest migration.....	17
1.3.1.1 The NC migratory pathways in <i>Xenopus</i> embryo .....	17
1.3.1.2. Methods to investigate neural crest migration in <i>Xenopus</i> embryo .....	18
1.3.2. Signaling pathways controlling neural crest migration.....	19
1.4 Planar cell polarity (PCP) is a Wnt signaling pathway, which controls the establishment of epithelial polarity and morphogenetic movements.....	26
1.5 Molecular mechanisms of PCP signaling .....	30
1.5.1 The “core” PCP genes .....	30
1.5.2 Upstream regulators of the PCP signaling .....	34
1.5.3 Small GTPases and other PCP downstream targets .....	35
1.5.4 Additional PCP regulators.....	37
1.5.5 Protein tyrosine kinase 7 (PTK7).....	39
1.6 The role of PCP signaling in neural crest migration.....	41
1.7 Aims.....	43
2. Materials .....	44
2.1 Model organism .....	44
2.2 Bacteria .....	44
2.3 Chemicals, solutions, media and buffers .....	44
2.3.1 Chemicals.....	44
2.3.2 Media and antibiotics .....	44
2.3.3 Buffers and Solutions .....	44
2.3.4 Unclassified chemical substances and reagents .....	45
2.4 Enzymes and Kits .....	45

2.5 Vectors and DNA Constructs.....	46
2.5.1 Vectors .....	46
2.5.2 Constructs.....	47
2.6 Oligonucleotides .....	52
2.7 Antibodies.....	55
2.8 Laboratory equipment and software .....	55
3. Methods .....	57
3.1 DNA methods .....	57
3.1.1 Plasmid DNA preparations.....	57
3.1.2 DNA concentration measurement .....	57
3.1.3 Agarose-gel electrophoresis .....	57
3.1.4 DNA restriction digest .....	57
3.1.5 Purification of the DNA fragments from agarose gel or restriction digest mixture.....	57
3.1.6 Polymerase chain reaction (PCR) .....	58
3.1.7 DNA-sequencing and sequence analysis.....	58
3.1.8 Molecular cloning .....	58
3.1.8.1 PCR-based cloning .....	58
3.1.8.2 Restriction-based cloning .....	59
3.1.8.3. Ligation into an expression vector.....	59
3.1.8.4 Chemical transformation .....	59
3.1.8.5 Transformation by electroporation .....	59
3.1.8.6 Verification of the a DNA fragment integration .....	60
3.2 RNA methods.....	60
3.2.1 Total RNA isolation .....	60
3.3.2 Reverse transcription and RT-PCR.....	60
3.2.3 <i>In vitro</i> transcription.....	61
3.2.3.1. In vitro transcription of the dioxigenin-labelled antisense RNA for the whole mount in situ hybridization (WISH).....	61
3.2.3.2. In vitro transcription of the capped-mRNA for microinjections .....	61
3.2.4 RNA analysis and concentration measurement.....	61
3.3. Protein methods .....	62
3.3.1 Protein electrophoresis under the denaturing conditions (SDS-PAGE).....	62
3.3.2 Western blotting .....	63
3.3.3 <i>In vitro</i> transcription-translation assay.....	63

3.3.4 Co-Immunoprecipitation .....	63
3.3.5 Investigation of the PTK7-dsh complex by glycerol gradient density centrifugation ..	64
3.3.6 Identification of PTK7-binding partners by tandem mass-spectroscopy .....	64
3.4 <i>Xenopus laevis</i> embryos injections and manipulations.....	65
3.4.1 Preparation of <i>Xenopus laevis</i> testis.....	65
3.4.2 Embryo injections and culture.....	65
3.4.3 Animal cap assay.....	65
3.4.4 Cranial neural crest (CNC) explants .....	66
3.5. Immunostaining and Whole-mount in situ hybridization (WISH) .....	66
3.5.1 Immunostaining of the animal caps (AC).....	66
3.5.2 Immunostain of the gelatin-albumin sections .....	67
3.5.3 Whole mount <i>in situ</i> hybridization (WISH).....	67
4. Results .....	71
4.1 PTK7 functions in PCP signaling by recruiting dsh to the plasma membrane.....	71
4.1.1 PTK7 recruits dsh to the plasma membrane via its kinase homology domain .....	71
4.1.2 PDZ domain of dsh is required for the co-localization with PTK7 .....	73
4.1.3 PTK7 is a part of a fz7/dsh complex.....	75
4.1.4 PTK7 loss of function affects fz7-mediated dsh membrane recruitment and hyperphosphorylation.....	76
4.1.5 Fz7 loss of function does not affect the PTK7-mediated dsh membrane recruitment ..	78
4.1.6 RACK1 is a novel PTK7-binding partner, identified by tandem mass-spectrometry...80	
4.1.7 Similar to PTK7, RACK1 regulates neural tube closure .....	81
4.1.8 PTK7 recruits RACK1 to the plasma membrane in animal cap cells.....	85
4.1.9 RACK1 is required for PTK7-mediated dsh membrane recruitment.....	87
4.1.10 RACK1 is required for the interaction between PTK7 and PKC $\delta$ 1 .....	89
4.1.11 RACK1 is not required for the fz7-mediated dsh localization.....	91
4.1.12 Both PTK7 and RACK1 can activate JNK phosphorylation .....	92
4.2. The function of PTK7 in neural crest migration.....	94
4.2.1 PTK7 is expressed in the area of the pre-migratory and migratory neural crest cells ..94	
4.2.2 PTK7 loss of function, but not the overexpression leads to defects in neural crest migration.....	94
4.2.3 Neural crest specific expression of $\Delta$ kPTK7 inhibits migration.....	98
4.2.4 Recruitment of dsh DEP domain by PTK7 is required for neural crest migration .....	101
4.2.5 PTK7 is necessary for the migration of explanted neural crest cells .....	101
4.2.6 PTK7 localizes at cell-cell contacts and possesses homophilic binding.....	104

4.2.7 PTK7, but not its kinase deletion mutant co-localizes with dsh in migrating neural crest cells .....	105
4.2.8 PTK7 may be required for contact inhibition of locomotion .....	108
4.2.9 RACK1 can also regulate neural crest migration.....	109
5. Discussion.....	111
5.1 PTK7 functions in PCP signaling .....	111
5.2 RACK1 is a novel PTK7 binding partner, which mediates its dsh membrane recruitment .....	113
5.3 The role of PTK7 and RACK1 in the regulation of PCP downstream effects. ....	115
5.4 The role of PTK7 and RACK1 in dsh hyperphosphotrylation. ....	116
5.5 PTK7 functions in neural crest migration.....	117
6. Conclusions .....	122
7. Bibliography .....	123
Curriculum vitae .....	139

## **Acknowledgements**

I would like to express a deep gratitude to my supervisor Dr. Annette Borchers, who provided me with an exciting project as well as great guidance and encouragement throughout my work.

I am very grateful to the members of my thesis committee, Prof. Dr. Andreas Wodarz and Prof. Dr. Michael Kessel, for critical evaluation and valuable advice for my project. In addition, I would like to thank Prof. Dr. Tomas Pieler for giving me an opportunity to join his department and for his very practical and constructive comments during my progress reports. Finally, I thank Dr. Halyna Shcherbata, Prof. Dr. Ernst Wimmer and Prof. Dr. Detlef Doennicke, who kindly agree to join my examination board.

I am very thankful to the entire Developmental Biochemistry team and especially to the people of the “Morphogenesis” group (Martina, Hanna and Gabrielle) for the great working atmosphere, support during the work and useful advice. A special gratitude goes to Ilona Wunderlich for her essential help during my experiments.

I am indebted to the Christiane Nüsslein-Volhard foundation, for providing me with an essential support for the childcare of my daughter, as well as to Göttingen Graduate School for Neurosciences and Biological sciences (GGNB) for giving me a stipend.

Furthermore, I would like to acknowledge the International MSc/PhD program in Molecular Biology, and particularly Dr. Steffen Burkhardt, for the excellent coordination and support during all these years.

Finally, I owe my coming to Göttingen to my parents and my husband. Therefore, I want to express a special gratitude to my family for their invaluable support, understanding and encouragement throughout all my life.



**Abstract**

PTK7 is a novel component of the planar cell polarity (PCP) signaling pathway, which regulates inner ear hair cell polarity and neural tube closure, however, its signaling mechanism is largely unknown. In *Xenopus* PTK7 is expressed in the closing neural tube as well as the migrating neural crest indicating a function in the regulation of these morphogenetic movements. For neural tube closure this has already been demonstrated, but the role of PTK7 in neural crest migration is unclear. The aim of this PhD project was to analyze if PTK7 affects neural crest migration and to characterize how it intersects with the PCP signaling pathway to regulate cell movements. Analyzing protein co-localization in *Xenopus* ectodermal explants, demonstrated that PTK7 recruits dsh to the plasma membrane. Further, co-immunoprecipitation experiments revealed that PTK7 is a component of the fz7-dsh complex, which is necessary for the fz7-dependent dsh membrane recruitment and phosphorylation. As our data indicated that the PTK7-dsh interaction is not direct, tandem mass-spectrometry analysis was employed to identify novel PTK7 binding partners. In the result, the receptor of activated PKC 1 (RACK1) was identified. RACK1 has a similar expression pattern like PTK7 and binds to PTK7 in immunoprecipitation experiments. Similar to PTK7, RACK1 loss of function disturbs neural tube closure. Furthermore, loss of function studies demonstrate that RACK1 is required for PTK7-mediated dsh localization. The analysis of protein-protein interactions and co-localization demonstrates that RACK1 interacts with PKC $\delta$ 1 and the complex with PKC $\delta$ 1 and RACK1 mediates PTK7-dependent dsh membrane recruitment. Loss of function studies demonstrate that PTK7 is required for neural crest migration. Expressing of the full-length PTK7 and its deletion constructs under the control of the neural crest-specific slug promoter shows that PTK7 is specifically required in migrating neural crest cells. Epistasis experiments indicate that PTK7 interacts with dsh to regulate neural crest migration.

**List of Figures**

Figure 1.1. The derivatives of trunk and cranial neural crest cells	13
Figure 1.2. Steps of neural crest induction	16
Figure 1.3. Pathways of NC migration in <i>Xenopus laevis</i> embryo	17
Figure 1.4. Methods to study NC migration in <i>Xenopus</i>	19
Figure 1.5. The role of cell adhesion molecules and metalloproteases in neural crest development	20
Figure 1.6. The expression of ephrin, semaphorin and slit/robo signaling components during NC migration	23
Figure 1.7. Different branches of Wnt signaling	27
Figure 1.8. Processes, controlled by PCP signaling	28
Figure 1.9. The convergent extension movements	29
Figure 1.10. The schematic structure of the dishevelled protein	31
Figure 1.11. In the PCP signaling cascade dsh activates two different classes of small GTPases	36
Figure 1.12. PTK7 is a PCP regulator	40
Figure 1.13. PCP signaling regulates neural crest migration via contact inhibition of locomotion	42
Figure 4.1. PTK7 recruits dsh to the plasma membrane	72
Figure 4.2. PTK7 and dsh co-localization is detected by glycerol-gradient centrifugation	73
Figure 4.3. The PDZ domain is necessary for PTK7-dependent membrane translocation of dsh	74
Figure 4.4. Fz7 and dsh are both required to co-precipitate PTK7	75
Figure 4.5. PTK7 is required for fz7-mediated dsh membrane recruitment	76
Figure 4.6. PTK7 is required for fz7-mediated dsh hyperphosphorylation	77
Figure 4.7. Loss of fz7 function does not affect the PTK7-dsh co-localization	79
Figure 4.8. RACK1 interacts with PTK7	80
Figure 4.9. RACK1 morpholino oligonucleotides	81
Figure 4.10. RACK1 loss of function phenotype	83
Figure 4.11. Targeted injection of RACK1 MO1 also results in neural tube closure defects	84
Figure 4.12. PTK7 recruits RACK1 to the plasma membrane	86
Figure 4.13. RACK1 is required for the PTK7-mediated dsh membrane localization	88
Figure 4.14. PKC $\delta$ 1 is recruited to the plasma membrane by PTK7 via RACK1	90

Figure 4.15. PKC $\delta$ 1 is required for PTK7-dsh co-localization	91
Figure 4.16. RACK1 does not affect the fz7-dependent dsh membrane recruitment and phosphorylation	92
Figure 4.17. Both RACK1 and PTK7 act upstream of dsh to activate JNK phosphorylation	93
Figure 4.18. In <i>Xenopus laevis</i> embryo PTK7 is expressed in the area of pre-migratory and migrating neural crest	94
Figure 4.19. Loss of PTK7 function causes neural crest migration defects	96
Figure 4.20. PTK7 overexpression does not affect neural crest migration	97
Figure 4.21. Neural-crest-specific expression of PTK7 and dsh constructs	99
Figure 4.22. PTK7 is required for <i>in vitro</i> neural crest migration	102
Figure 4.23. PTK7 is enriched at the area of cell-cell contacts	103
Figure 4.24. PTK7 possess homophilic binding	104
Figure 4.25. PTK7 co-localizes with dsh in migrating neural crest	106
Figure 4.26. PTK7 mediates contact inhibition of locomotion	107
Figure 4.27. RACK1 loss of function affects the migration of explanted neural crest cells	108
Figure 4.28. RACK1 co-localizes with PTK7 at cell contacts	109
Figure 5.1. The model of PTK7 intersection with PCP signaling	113
Fig. 5.2. The model of PTK7 role of in neural crest migration	117

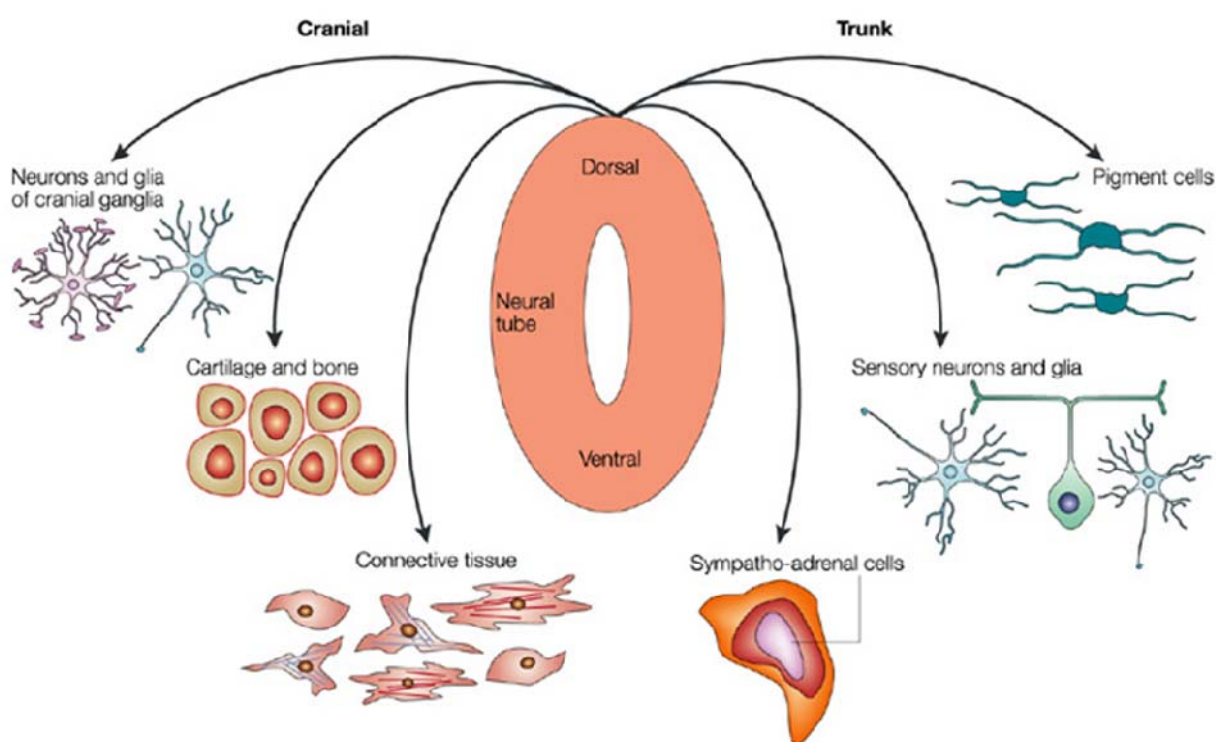
**List of Tables**

Table 2.1. DNA constructs	48-50
Table 2.2 Linearization and in vitro transcription of the DNA constructs	51
Table 2.3 RT-PCR primers	52
Table 2.4 Sequencing primers	53
Table 2.5 Morpholino blocking oligonucleotides	54
Table 2.6 Antibodies and their working dilutions	55
Table 3.1. The correlation between protein size and percentage of the correspondent acrylamide gel	62
Table 3.2 Separating gel	62
Table 3.3 Stacking gel	62
Table 3.4. Rehydration of embryos	68
Table 3.5 Proteinase K treatment	68
Table 3.6 Acetylation	68
Table 3.7 Washing and RNase treatment	69
Table 3.8 Blocking and antibody incubation	69
Table 3.9. Coloring reaction	70
Table 3.10. Bleaching of embryos	70

## 1. Introduction

### 1.1 The neural crest and its derivatives

The neural crest (NC) is a group of cells, induced at the border between the epidermis and neural plate of a developing embryo. In accordance with their anterior-posterior position within an embryo the neural crest can be subdivided into cranial and trunk NC. Neural crest cells are considered to be pluripotent cells, and after being specified they delaminate from the neural tube and migrate through the whole organism, differentiating in a wide variety of the cell types, including skin melanocytes, cartilage cells, sensory neurons and glial cells. In addition, the NC cells are important for the formation of adrenal gland and heart. Here the derivatives of the neural crest are briefly summarized in Figure 1.1.



**Figure 1.1. The derivatives of trunk and cranial neural crest cells.** The cranial neural crest gives rise to the neurons and glia of the cranial ganglia, cartilage and bone cells as well as connective tissue. The trunk neural crest differentiates into pigment cells, sensory neurons and ganglia as well as sympatho-adrenal cells. Adapted from Knecht, 2002

### 1.2 Neural crest induction

As it was mentioned above, the NC originates at the border between the neural plate and the surrounding epidermis. Its formation is thereby regulated by a unique combination of signals coming from both of the tissues as well as from the underlying mesoderm (Fig. 1.2). Indeed,

studies of the past decades strongly support this hypothesis (Mancilla and Mayor, 1996; Mayor et al., 1995; Selleck and Bronner-Fraser, 1996). It was shown, that neural plate borders are specified by a gradient of bone morphogenetic protein (BMP) established between the epidermis and the neural plate. At later stages three other types of signaling molecules, derived from the endomesoderm, namely fibroblast growth factor (FGF), retinoic acid (RA) and Wnt, lead to the induction of the NC (Fig.1.2) (Barembaum and Bronner-Fraser, 2005; Steventon et al., 2005).

Until now it is not entirely clear, how the cross-talk between BMP, FGF, RA and Wnt signaling pathways controls the activation of the specific gene cascades responsible for NC formation. However, according to R. Mayor, several phases can be delineated in this process (reviewed in (Kuriyama and Mayor, 2008)). At the first step an initial set of genes, called *cell specification* or *neural plate border specifier genes*, is induced at the border of the neural plate. These genes are expressed in a domain, which is wider than the prospective neural crest and also includes neural plate and epidermal cells. The expression of the neural plate border specifier genes is primarily controlled by the BMP gradient established by selective inhibition of BMP in the neural plate (Marchant et al., 1998; Mayor et al., 1995). The inhibition of the BMP signal occurs via BMP-binding molecules chordin, noggin and follistatin and additionally by the downregulation of the BMP expression levels via Wnt signaling (Baker et al., 1999; Fainsod et al., 1994). It is considered that intermediate BMP levels are required for the NC induction however it is not sufficient to induce the NC cell specification genes (Marchant et al., 1998; Mayor et al., 1995). The second group of molecules, namely FGF, RA and Wnt, known to be involved in the anterior-posterior (AP) patterning of the neural tube, are able to induce the NC-fate in the neural folds. Therefore, only the combination of BMP, FGF, RA and Wnts is thought to induce the expression of neural plate border specifier genes (Fig. 1.2) (Delaune et al., 2005; Linker and Stern, 2004; Sauka-Spengler and Bronner-Fraser, 2008; Steventon et al., 2005).

The group of neural plate border specifier genes includes transcription factors, Msx, Dlx, Pax3, Myc, Zic and AP2- $\alpha$ , which upregulate the expression of another group of genes, named *NC specified* or *cell survival genes* (Sauka-Spengler and Bronner-Fraser, 2008; Steventon et al., 2005). These genes are expressed in the area of the NC and necessary for NC proliferation and survival. The transcription factors Snail and Slug were among the first discovered NC specifier genes. They are necessary for the induction and maintenance of neural crest fate in chick, mouse and *Xenopus* embryo (Mayor et al., 1995; Nieto et al., 1994). The Snail/Slug proteins induce expression of other NC survival genes, including Id3, FoxD3, the Sox group of genes and Twist (Fig.1.2) (Aybar and Mayor, 2002; Aybar et al., 2003; Honore et al., 2003; LaBonne and Bronner-Fraser, 2000; Sauka-Spengler and Bronner-Fraser, 2008). However, Slug/Snail function is not exclusively restricted to NC maintenance. These transcription factors initiate the

epithelial-mesenchymal transition (EMT), a process leading to the delamination of NC cells from the neural tube and migration (Rukstalis and Habener, 2007; Savagner et al., 1997; Tucker, 2004). Interestingly, the signaling mechanisms, controlling epithelial-mesenchymal transition of the neural crest is very similar to the ones, occurring during malignant transformation and tumor metastasis. Therefore, investigation of NC induction and migration also helps to shed light on malignant transformation processes (Kuriyama and Mayor, 2008; Thiery, 2002).

Finally, the last group of genes, involved in the NC formation, is the *NC effector or migration/differentiation genes*. This is the most diverse group, which includes transmembrane signaling molecules, like cadherins, integrins and neuropilins, secreted matrix metalloproteases, as well as intracellular proteins, like RhoB, involved in cytoskeletal rearrangements. The function of all those proteins is to promote delamination and migration of the neural crest cells (Fig. 1.2) (reviewed in (Kuriyama and Mayor, 2008; Sauka-Spengler and Bronner-Fraser, 2008).

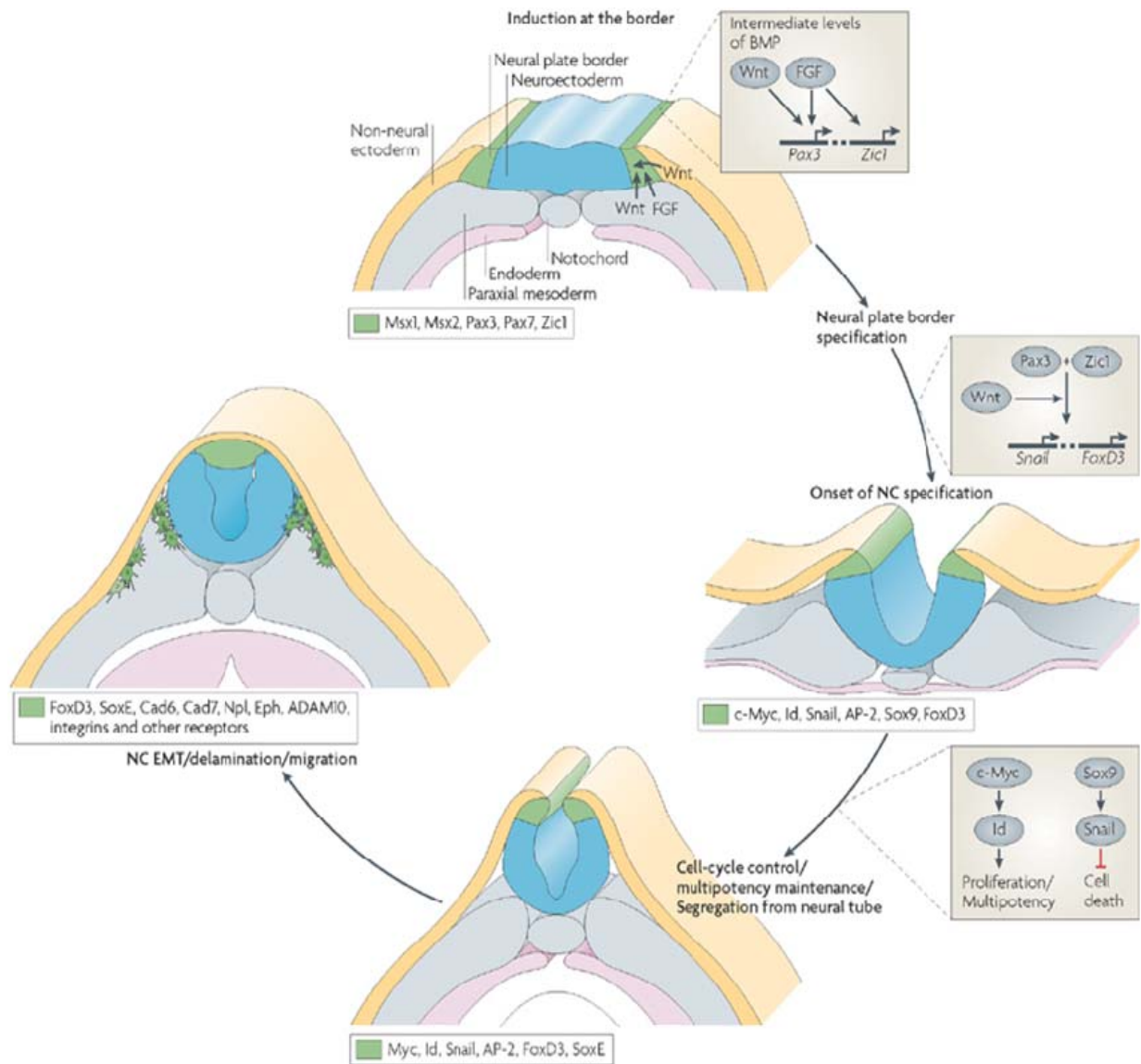


**Figure 1.2. Steps of neural crest induction.** First, the neural plate border specifier genes are induced by the intermediate levels of BMP signaling. Then, Wnts together with FGF, secreted by underlying tissues (endo- and mesoderm), induce the neural crest specifier genes. Finally, the neural crest specifier genes induce the epithelial-mesenchymal transition and NC migration. Adapted from Bronner-Fraser, 2008

### 1.3 Neural crest migration

Upon delamination from the neural tube, neural crest cells start to migrate. The NC travels very long distances by following specific pathways and colonizing nearly every organ in the developing organism, and therefore they are often called “the explorers of the embryo”. Since the migration of the neural crest is a complicated process, occurring relatively early during organism development, it is difficult to study in organisms with internal development, like for example mouse. Therefore, the major investigations of neural crest migration were carried out in chicken, zebrafish and *Xenopus* embryos.



### 1.3.1 *Xenopus laevis* as a model system to study neural crest migration

The main advantages of *Xenopus* as a model system are the external development and big embryo size, which makes it an ideal system to perform embryo manipulations, like microinjections, NC transplantation and explantation, as well as lineage tracing experiments. In *Xenopus* embryos the neural crest is formed at stages 15-16, after neural tube closure is completed. Upon the induction, neural crest cells start to delaminate and migrate. Neural crest migration starts in the cranial region at late neurula stages and then progresses as a wave along the embryo, finishing by stage 46 (Collazo et al., 1993; Krotoski et al., 1988; Mayor et al., 1999).

#### 1.3.1.1 The NC migratory pathways in *Xenopus* embryo

Neural crest migrates on defined pathways and according to the anterior-posterior position, two segments, named cranial and trunk neural crest, are distinguished. Each of the neural crest segments gives rise to distinct cell types. For instance, pigment cells originate predominantly from the trunk neural crest, while the head cartilage arises from the cranial segments (Mayor et al., 1999). In *Xenopus* embryos the migrating cranial NC forms three different branches, namely

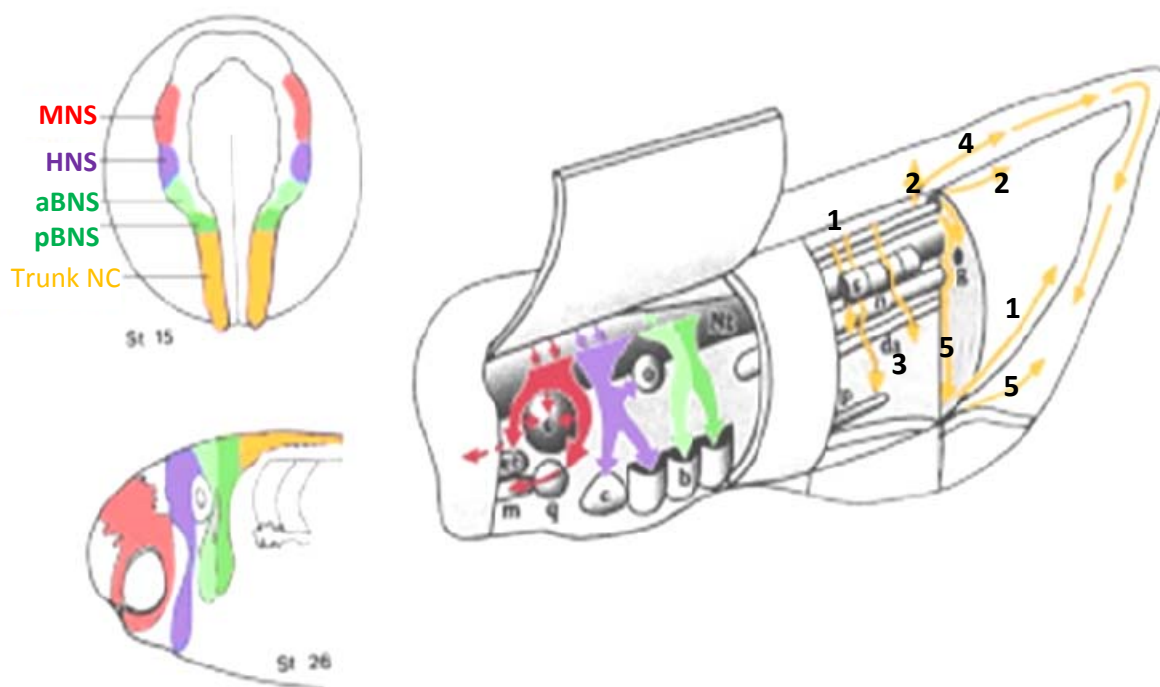


**Figure 1.3. Pathways of NC migration in *Xenopus laevis* embryo.** Mandibular neural crest (MNS) is depicted in red, hyoid (HNS) - in purple and branchial neural crest branch (aBNS – anterior and pBNS – posterior branchial arches respectively) – in green. The migratory pathways of the trunk neural crest are shown by yellow arrows. 1 -ventral pathway; 2 – dorsal pathway; 3 – lateral pathway; 4 – pathway around the tail; 5 – enteric pathway. Adapted from Mayor, 1999

the mandibular, the hyoid and the branchial branch (Fig. 1.3). The mandibular branch (Fig. 1.3, in red) is the most caudal and participates in the formation of Meckel's cartilage as well as profundus, gasserian and geniculate ganglion, and Schwann cells of related nerves and ganglionic cell bodies. The cells of the hyoid branch (Fig. 1.3, in purple) migrate to the bottom of the pharynx and differentiate into the ceratohyal cartilage. In addition, they also participate in the formation of the otic tissues and the muscles, which connect distinct parts of the cartilage. Finally, the branchial branches (Fig. 1.3, in green) contribute to the formation of the branchial arches, giving rise to the cartilage tissues (Mayor et al., 1999; Sadaghiani and Thiebaud, 1987). The trunk NC follows five different pathways (Fig. 1.3, in yellow): the ventral pathway between neural tube notochord and somites (Fig. 1.3, 1), the lateral pathway between somites and epidermis (Fig. 1.3, 3), the pathway around the tail (Fig. 1.3, 4) and finally the dorsal (Fig. 1.3, 2) and enteric pathways (Fig. 1.3, 5) into the dorsal and ventral fin respectively (Collazo et al., 1993; Krotoski and Bronner-Fraser, 1986; Krotoski et al., 1988). The NC cells following the ventral pathway contribute to the formation of the root ganglia, supporting cells for peripheral neurons, chromaffin cells, enteric ganglia, gut pigment cells, pronephric duct and posterior part of the dorsal aorta. At the same time, the major part of the pigment cells is formed by cells following the lateral pathway. In the pathway around the tail cells migrate along the dorsal fin and turn at the tip of the tail towards the ventral part (Fig. 1.3). Finally, cells following the dorsal and enteric migratory pathways participate in the formation of the fin (reviewed in (Mayor et al., 1999)).

#### **1.3.1.2. Methods to investigate neural crest migration in *Xenopus* embryo**

The methods to study *Xenopus* NC migration are briefly summarized in Figure 1.4. The most direct and easiest way to observe neural crest migration is a lineage tracing analysis, which can be performed by targeted microinjection of labeled substances or fluorescently tagged proteins into defined parts of the embryo. Alternatively, the microinjection technique can be applied to address the function of a certain protein in the neural crest migration. For this purpose mRNA of the protein or a translation blocking morpholino oligonucleotide (MO) can be injected dorsally in one blastomere at the 2-cell stage, resulting in an effect at one side of the embryo, while the other side will serve as an internal control (Fig. 1.4 A). Following injection, NC migration defects can be analyzed by whole mount *in situ* hybridization (WISH) with neural crest specific antisense probes (e.g. Slug, Twist, AP-2). This approach also allows observing the effects on specific NC subpopulations. In this case subpopulation-specific WISH probes can be used. In addition, tissue specific staining can be performed. For instance, cartilage formation can be visualized by Nile-blue staining of the embryos at stage 45-50 (Carl et al., 1999; Klymkowsky and Hanken,

1991). The trunk neural crest can be marked by an antisense probe to gremlin (Hsu et al., 1998), while both cranial and trunk NC can be marked with Twist (Hopwood et al., 1989).

To target the expression of selected proteins specifically to the neural crest, their constructs may be injected as a plasmid, in which the expression is controlled by the NC-specific Slug-promoter (Vallin et al., 2001). Finally, to investigate the direct influence of selected molecules on the migratory behavior of the neural crest, NC cells can be excised from embryos and explanted on fibronectin coated dishes, where their migration can be observed over a period of several hours (Fig. 1.4 B, D). Alternatively, cells can be labeled with fluorescent dyes and transplanted into the wild type embryo, where their migratory behavior can be analyzed *in vivo* by fluorescent microscopy (Fig. 1.4B, C) (Borchers et al., 2000).

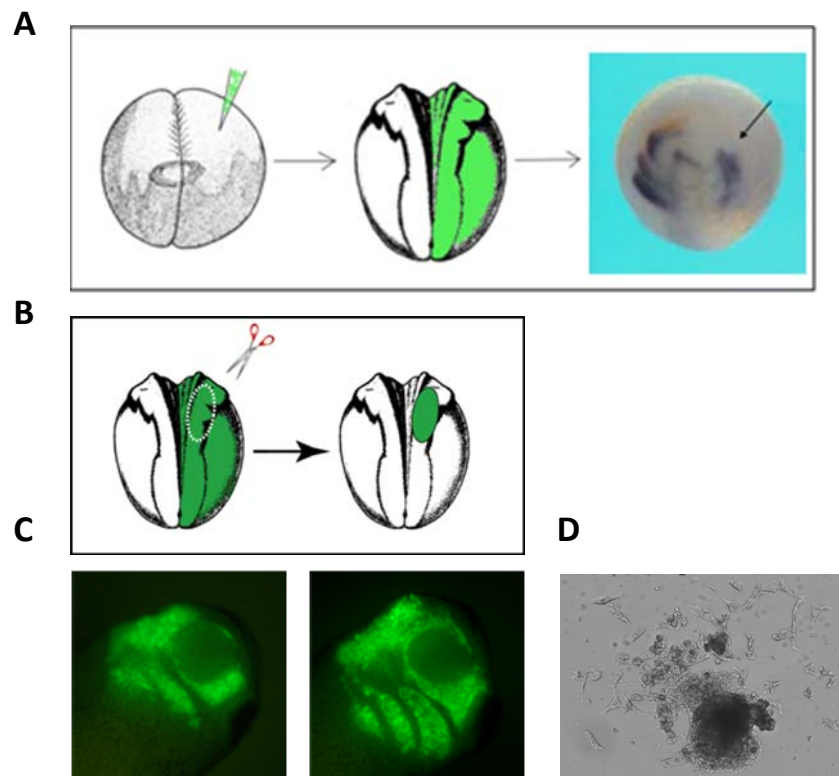


**Figure 1.4. Methods to study NC migration in *Xenopus*.** (A) Schematic representation of the microinjection experiment followed by the whole mount *in situ* hybridization. (B) NC transplantation experiment. To perform NC explants the same region is excised and placed on fibronectin coated dish. (C) The analysis of the migration of transplanted neural crest by fluorescent microscopy. (D) Explanted neural crest cells, migrating on fibronectin.

### 1.3.2. Signaling pathways controlling neural crest migration

Upon specification neural crest cells undergo an epithelial-mesenchymal transition (EMT), a process, during which they gain the ability to delaminate from the neural tube and migrate. EMT results in massive changes of gene expression inside of the NC cells. In particular, the neural

crest cells change the type of cell adhesion molecules and cell junctions. They start secreting matrix metalloproteases, which allow them to invade other tissues, and cytoskeletal modulators to increase their motility (summarized in Figure 1.5). From the other side, the neural crest cells are guided through the organisms by several distinct signaling cascades, which include Ephrin/EphR, Slit/Robo, Semaphorin/Neuropilin (summarized in Figure 1.6) and PCP signaling pathways, which will be described below.

The neural crest cells migrate in a tight space between the epithelial and mesodermal sheets and during the initial steps of migration they remain in close contact with each other. Their movements are thought to be regulated by two classes of adhesion molecules: **cadherins**, which facilitate the interaction between cells, and **integrins**, which are responsible for the interaction with the extracellular matrix (Fig. 1.5 B).

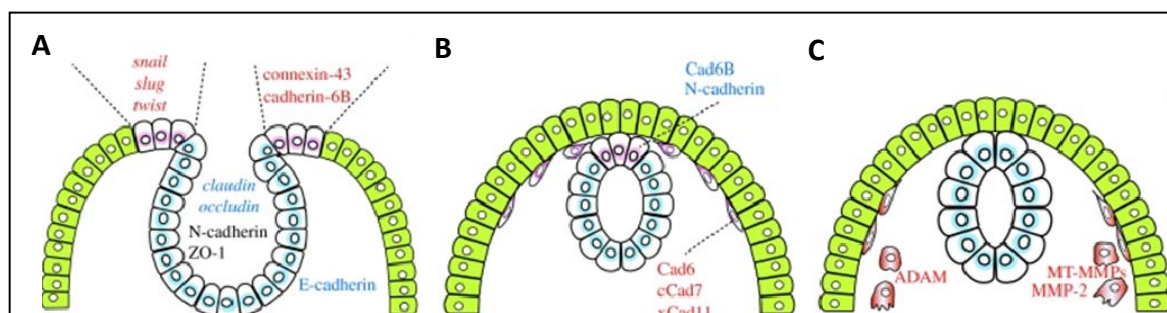


**Figure 1.5. The role of cell adhesion molecules and metalloproteases in neural crest development.** (A) The neural crest induction leads to the change from adherent to the gap junctions. The expression of occluding is downregulated, while connexin 43 expression levels increase in the area of Slug expression. (B) Prior to migration the neural crest cells need to undergo the changes in cadherin expression. Type I cadherins, like N-cadherin, are substituted by type II cadherins, like xCad11, Cad6 and Cad7. (C) Upon the migration NC cells secrete metalloproteases, like ADAM and MMP, which allow them to cross tissue boundaries. Adapted from Mayor and Kuriyama, 2008

The **cadherin** proteins are calcium-dependent adhesion molecules, which can be subdivided into 6 types: type 1 and type 2 cadherins, protocadherins, desmosomal and atypical cadherins, and cadherin-like molecules (Taneyhill, 2008; Tanihara et al., 1994). But only two types of the cadherins, namely type 1 and type 2, play a major role in the regulation of neural crest migration. Type 1 cadherins are usually expressed on epithelial cells and associated with stable cell assemblies (Chu et al., 2006; Sauka-Spengler and Bronner-Fraser, 2008). When cells undergo EMT they switch to the expression of type 2 cadherins, which are typical for mesenchymal cells. The expression of type 2 cadherins results in a decrease of cell adhesiveness and an increase in cell motility (Chu et al., 2006; Hadeball et al., 1998; Nakagawa and Takeichi, 1998; Sauka-Spengler and Bronner-Fraser, 2008). In particular, it was shown, that prior to EMT neural crest

precursors express E-cadherin, which is repressed at the start of EMT (Fig. 1.5). The NC-specific transcription factors, Snail1 and Snail2/Slug, directly bind to the E-cadherin promoter and repress its expression (Batlle et al., 2000; Cano et al., 2000; Sauka-Spengler and Bronner-Fraser, 2008). Once the NC delamination starts, the expression of N-cadherin and cadherin 6B is induced. However, in the migrating neural crest cells the expression of both molecules is downregulated by Slug and FoxD3 transcription factors (Sauka-Spengler and Bronner-Fraser, 2008). Interestingly, the blocking of N-cadherin functions in both chick and mice results in neural crest migration defects. But the knockdown of cadherin 6B leads to earlier emigration of neural crest cells in the chick embryo (Cheung et al., 2005; Hatta et al., 1987; Taneyhill, 2008; Taneyhill et al., 2007). Migrating neural crest cells upregulate the expression of cadherin 7, a typical type 2 cadherin. This cadherin was shown to promote neural crest cells motility. But similarly to other cadherins, the overexpression of cadherin 7 leads to clustering of the neural crest cells and inhibition of their migration (Cheung et al., 2005; Nakagawa and Takeichi, 1995, 1998; Taneyhill, 2008). In *Xenopus* another cadherin, cadherin11, is shown to be expressed in the area of the migrating neural crest cells (Hadeball et al., 1998). The neural crest transplantation experiments revealed that cadherin 11 expression is necessary for neural crest migration (Borchers et al., 2001). Interestingly, during neural crest migration, cadherin 11 is cleaved by ADAM metalloproteases (McCusker et al., 2009). Following the cleavage, its membrane bound cytoplasmic part promotes protrusive activity of cranial neural crest cells via the interaction with Trio guanine nucleotide exchange factor (Trio-GEF) (Kashef et al., 2009). Two other cadherins, cadherin 19 and 20, are also found in the mammalian migrating neural crest cells. However, their role remains to be elucidated (Taneyhill, 2008).

**Integrins** are heteromeric transmembrane receptors, which bind both extracellular matrix proteins and cytoskeletal intracellular components, promoting thus cell migration on the extracellular matrix. These proteins show interaction with laminin, collagen and fibronectin and promote cell migration. Integrins can regulate migration processes by switching between two conformations: low-affinity and high-affinity conformation. In addition cell migration can be regulated by altering integrins redistribution on the cell surface, their clustering and protein expression levels. In *Xenopus* at least 4 integrins, namely  $\alpha3\beta1$ ,  $\alpha5\beta1$ ,  $\alpha6\beta1$  and  $\alpha v$  are expressed at a suitable place and time to function in the neural crest migration (Joos et al., 1995; Kil et al., 1996; Lallier et al., 1996; Ransom et al., 1993; Whittaker and DeSimone, 1993). However, so far only  $\alpha5\beta1$  integrin was shown to have an influence on neural crest migration on fibronectin (Alfandari et al., 2003). Additionally, experiments on chick embryos demonstrated the emerging role of  $\beta1$  integrin/fibronectin interaction for the cranial NC migration *in vitro* (Strachan and Condic, 2003, 2008).

During their migration neural crest cells need to invade extracellular matrixes (ECM) and cross tissue borders. To move through the ECM without delay neural crest cells, similarly to metastatic cells, require proteolytic activity of both membrane bound and secreted **matrix metalloproteases (MMP)**. However, in contrast to tumor cells, the invasive behavior of neural crest cells is thought to be tightly regulated by MMP natural inhibitors, the tissue inhibitors of metalloproteases (TIMPs). Matrix metalloproteases are produced as precursor proteins, pro-MMPs. To be activated, the pro-MMP needs to undergo the proteolytic cleavage by other metalloproteases, for instance, the MMP2. Interestingly, both MMP2 and its natural inhibitor TIMP2 are required for cardiac neural crest migration and their expression is upregulated by Snail transcription factor (Cai et al., 2000; Cantemir et al., 2004; Erickson et al., 1992; Kuphal et al., 2005).

Another class of MMPs, a metalloprotease/disintegrin family (ADAM), was also shown to be crucial for neural crest migration (reviewed in (Kuriyama and Mayor, 2008)). ADAM metalloproteases are glycoproteins, bound to the cell surface, which act by ECM remodeling as well as mediating cell adhesion (Sauka-Spengler and Bronner-Fraser, 2008). ADAM10, for example, cleaves the extracellular part of CD44, inhibiting thus CD44-mediated matrix adhesion in the developing cornea. This inhibition allows then the NC cells to invade cornea and to differentiate into corneal precursors (Huh et al., 2007). In *X. laevis*, ADAM13 is expressed in the area of pre- as well as migratory neural crest cells, where it is thought to facilitate NC delamination from the neuroepithelium. Subsequently, it can promote further migration of the NC cells by modulation of the extracellular matrix (Alfandari et al., 2001; Kee et al., 2007). ADAM19 also has a function in both NC induction and migration (Neuner et al., 2009). And another MMP, MMP-2, was shown to play a role in the migration of the enteric neural crest (Anderson, 2009). In addition, the chemical inhibition of MMP2 and 14 activities blocks melanophore migration in *X.laevis* (Tomlinson et al., 2009).

**Ephrins and Ephrin receptors (EphR)** are transmembrane molecules, acting as a signaling pair. (Orioli and Klein, 1997; Pasquale, 1997; Tuzi and Gullick, 1994; Zisch and Pasquale, 1997). EphR are receptor tyrosine kinases, which dimerise and autophosphorylate upon ligand binding (Himanen et al., 2004; Zisch and Pasquale, 1997). Ephrin downstream signaling results in cytoskeletal remodeling and affects cell motility (Arvanitis and Davy, 2008; Davy and Soriano, 2007; Kuriyama and Mayor, 2008). In *Xenopus* EphA4 and EphB1 as well as their ephrinB2 ligand are expressed in the area of migrating cranial neural crest (Fig. 1.6). Overexpression of the EphA truncated forms demonstrates, that EphR/ephrin signaling is necessary for proper NC migration from the third arch as well as for avoiding the intermingling between the NC cells derived from two different arches (Helbling et al., 1998; Robinson et al.,

1997; Smith et al., 1997). In addition, the migration of mouse cranial neural crest cells is guided by the EphA/ephrinB interaction (Mellott and Burke, 2008) (Adams et al., 2001; Davy and Soriano, 2007; Smith et al., 1997). Mutations of ephrins B1 and B4 in humans were also associated with the failure of NC migration (Merrill et al., 2006; Twigg et al., 2004).

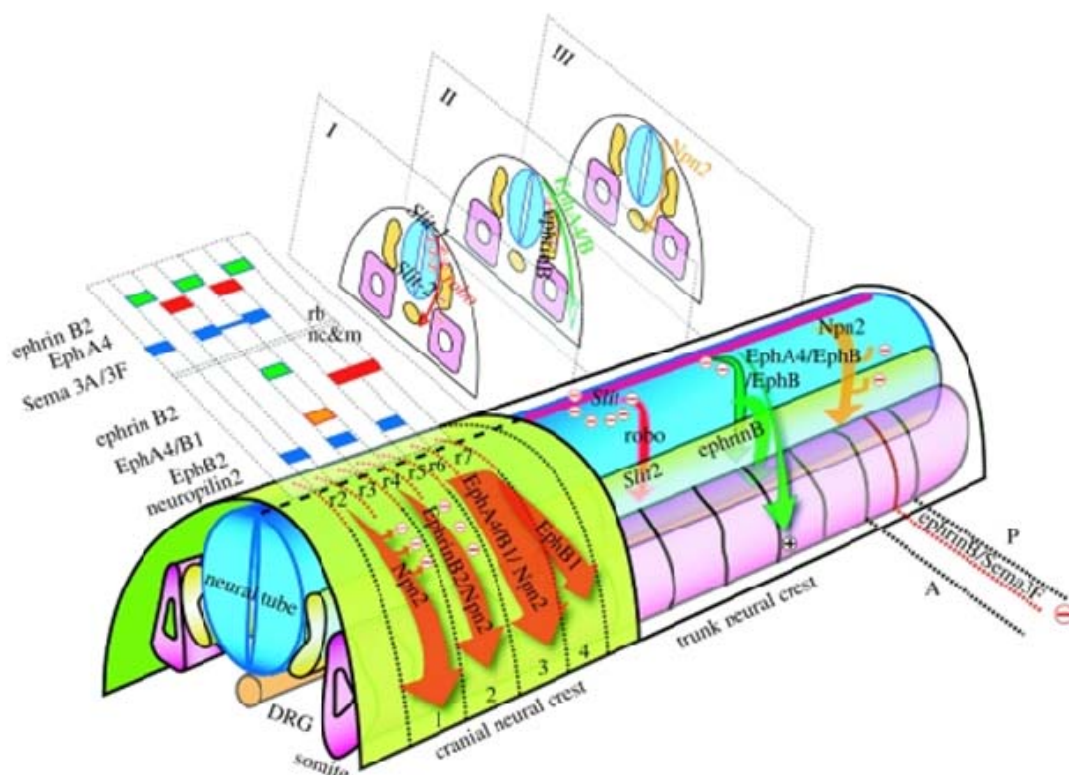


**Figure 1.6. The expression of ephrin, semaphorin and slit/robo signaling components during NC migration.** Ephrin B2 and its correspondent receptors EphA4/B1 are expressed in a specific pattern in the area of both cranial and trunk neural crest, enabling proper NC guidance. Sema3A/3F together with Npn2 are expressed in a conserved patterns in migrating NC. Slit and Robos are expressed and required for trunk NC migration. Adapted from Kuriyama and Mayor, 2008.

EphR/ephrin signaling is acting not only in cranial but also in trunk neural crest migration (Fig. 1.6). It was shown, that avian EphB3/ephrin B1 prevents neural crest cells from the invasion of the posterior part of the somite, thus forcing them to migrate through the anterior part. Ephrin signaling also controls the choice between dorsoventral and medial pathways of the NC (Bronner-Fraser et al., 1991; Koblar et al., 2000; Krull et al., 1997; McLennan and Krull, 2002; Wang and Anderson, 1997). In addition ephrin B1 prevents early migratory NC cells to enter the dorsoventral pathway, but once they are committed to the melanocyte cell lineage ephrinB1 promotes their migration across the same pathway (Santiago and Erickson, 2002). Thus, Ephrins serve rather as repelling guidance cues during both cranial and trunk neural crest migration.

**Semaphorins** are glycoproteins, which can be either secreted or membrane associated. According to their structure and amino acid similarity, semaphorins are subdivided into 8 classes: class 1 and 2 is found in invertebrates, class 3-7 - in vertebrates while class 8 is represented by viral semaphorins. The characteristic feature of all semaphorin proteins is the presence of a 400 aa “Sema” domain, followed by PSI (plexin semaphorin integrin) domain. In class 2, 3, 4 and 7 semaphorins the PSI domain is followed by an immunoglobulin-like domain, whereas class 5 semaphorins have 7 thrombospondin domains instead. Class 2 and 3 as well as viral semaphorins are secreted, while class 1, 4, 5, 6 and 7 are membrane bound. Individual semaphorin names are designed by the addition of letter code to the class name (for instance semaphorin3A or Sema6D4). Semaphorins are predominantly interacting with **Plexin and Neuropilin** transmembrane receptors. The interaction between semaphorins and plexins/neuropilins leads to cytoskeletal reorganizations, caused by the activation of small GTPases, like Rho and Rac (reviewed in (Kruger et al., 2005)).

Semaphorins were initially identified as molecules, involved in neural system development and, particularly, in axonal guidance (Kolodkin, 1998). However, recent studies add evidence, that semaphorin/plexin/neuropilin signaling plays an important role in neural crest migration (Tamagnone and Comoglio, 2004; Yu and Moens, 2005). The expression domains of semaphorin 3F and its neuropilin 2 (Npl2) receptor are conserved within the neural crest area in zebrafish *Xenopus*, chick and mice embryo. And their interaction was shown to be important for the proper migration of both cranial and trunk neural crest cells. (Gammill et al., 2007; Koestner et al., 2008; Osborne et al., 2005; Schwarz et al., 2009a; Schwarz et al., 2009b; Schwarz et al., 2008). Sema 3D was also shown to regulate both cranial and trunk NC migration by the proliferation control. (Berndt and Halloran, 2006).

The particular importance of semaphorin/neuropilin/plexin signaling was demonstrated for the cardiac NC, which lies between cephalic and trunk neural crest. In many species semaphorins of group 3, 4 and 6 together with plexins and neuropilins are required for proper cardiac NC migration (Brown et al., 2001; Gitler et al., 2002; Lepore et al., 2006; Sato et al., 2006; Toyofuku et al., 2008; Vallejo-Illarramendi et al., 2009), reviewed in (High and Epstein, 2007). In *X.laevis* embryo a number of additional semaphorins and the corresponding plexin and neuropilin receptors are expressed at the right time and place to have function in both cranial and trunk NC migration (Koestner et al., 2008).

**Slit/Robo signaling** was originally identified in *Drosophila*, where it controls axonal guidance. Slits are secreted proteins which share similar domain structure: 4 leucine repeats, followed by 7-9 epidermal growth factor-like domains, a laminin G domain and a cyteine-rich domain. Robos are transmembrane proteins comprised of 5 immunoglobulin-like and 3 fibronectin type-3-like



domains in the extracellular part, single transmembrane domain and cytoplasmic tail with unknown function (reviewed in (Dickson and Gilestro, 2006), (Kuriyama and Mayor, 2008)). Slit/Robo signaling acts primarily in the regulation of trunk neural crest migration (Fig. 1.6). Robo 1 and 2 are found to be expressed on early migrating neural crest cells and Slit2 inhibits their migration both *in vitro* and *in vivo*. It is thought, that Slit2, which is expressed in the dermamyotome, prevents the migration of Robo1/2-positive cells via the dorsolateral route before they committed to be pigment cells (Jia et al., 2005). Slit2 also regulates the migration of cardiac and vagal NC cells and has a function during trigeminal ganglion formation (Calmont et al., 2009; De Bellard et al., 2003; Shiao et al., 2008).

Interestingly, all previously described pathways, Semaphorins, Slit/Robo and Ephrins, guide the NC migration by repelling them from certain areas, while no clear chemoattractant cues were identified for the NC cells so far. Several studies demonstrated, that neural crest cells may be attracted by **glial cell line derived neurotrophic factor (GDNF)** and **netrin/deleted colon cancer gene (DCC) signals**. However, the data from the *in vitro* experiments do not fully support these findings (Jiang et al., 2003; Natarajan et al., 2002; Wells and Ridley, 2005; Young et al., 2001). Another molecule, thought to serve as NC attractant, was **stroma-derived factor 1 (SDF-1)**. But the recent data also demonstrate that SDF-1 rather increases NC motility, than regulates its directional migration (Belmadani et al., 2005; Kuriyama and Mayor, 2008). Several ECM molecules, like **fibronectin, collagen or laminin** can serve as permissive cues for neural crest migration. However, their role as directional NC migration cues was not demonstrated so far (reviewed in (Kuriyama and Mayor, 2008)). Finally, the proteoglycan **Syndecan 4** was shown to have a function in the neural crest migration in both *Xenopus* and zebrafish embryos. Syndecan 4 regulates directionality of neural crest migration by activation of the small GTPase Rac and interacts with planar cell polarity signaling, which will be discussed below (Matthews et al., 2008b).

Another way to guide the neural crest migration is to simultaneously polarize all cells towards the same direction of movement. Indeed, the migrating neural crest cells exhibit polarization, since they migrate as a group of cells, in which lamellipodia and filopodia are formed only at the leading edge. Since the **planar cell polarity (PCP)** pathway is known to control morphogenetic movements of polarized tissues, it becomes more and more the focus of studying directionality of NC migration (Kuriyama and Mayor, 2008). The molecules, involved in PCP signaling as well as their possible role in the regulation of neural crest migration will be described in two next chapters.

#### **1.4 Planar cell polarity (PCP) is a Wnt signaling pathway, which controls the establishment of epithelial polarity and morphogenetic movements**

The Wnt signaling consists of several conserved pathways, which regulate a wide variety of cellular processes, including motility, polarity, primary axis formation, cell fate determination, organogenesis, malignant transformation and stem cell renewal (Komiya and Habas, 2008; Logan and Nusse, 2004). The abbreviation Wnt is the fusion of the gene names, *wingless* and *integrated (int-1)*, which encode the ligands of this pathway in *Drosophila* and human cells respectively. Wnt proteins are secreted glycoproteins, which interacts with frizzled receptors. Currently, 19 different Wnt molecules and 10 frizzled receptors are identified in human, while *Drosophila* has 7 Wnt ligands and two different frizzled receptors (Komiya and Habas, 2008; Montcouquiol et al., 2006). A basic mechanism of the Wnt signaling includes the interaction of a Wnt ligand with a frizzled receptor, which, in turn, results in the complex formation and activation of the dishevelled (dsh) protein. At the level of dsh Wnt signaling branches into three major pathways, the  $\beta$ -catenin, the Wnt-calcium and the planar cell polarity (PCP) pathways (Fig. 1.7). Since the  $\beta$ -catenin signaling was discovered first, it is also named canonical Wnt signaling, while two other pathways are classified as non-canonical Wnt signaling pathways (Montcouquiol et al., 2006; Veeman et al., 2003a).

The **canonical** Wnt signaling pathway (Fig. 1.7A) was originally identified from *Drosophila* genetic screens, and, subsequently, its signaling components were found in vertebrates. This pathway has important roles during embryogenesis, particularly in the axis formation, anterior-posterior patterning, cell fate determination and organogenesis, as well as in the stem cells renewal (Angers and Moon, 2009; Komiya and Habas, 2008; Montcouquiol et al., 2006). The hallmark of this pathway is the accumulation of the stabilized  $\beta$ -catenin (armadillo in *Drosophila*) in the nucleus, where it interacts with TCF/LEF family transcription factors and causes a transcriptional response (Behrens et al., 1996; Hart et al., 1999; Molenaar et al., 1996).

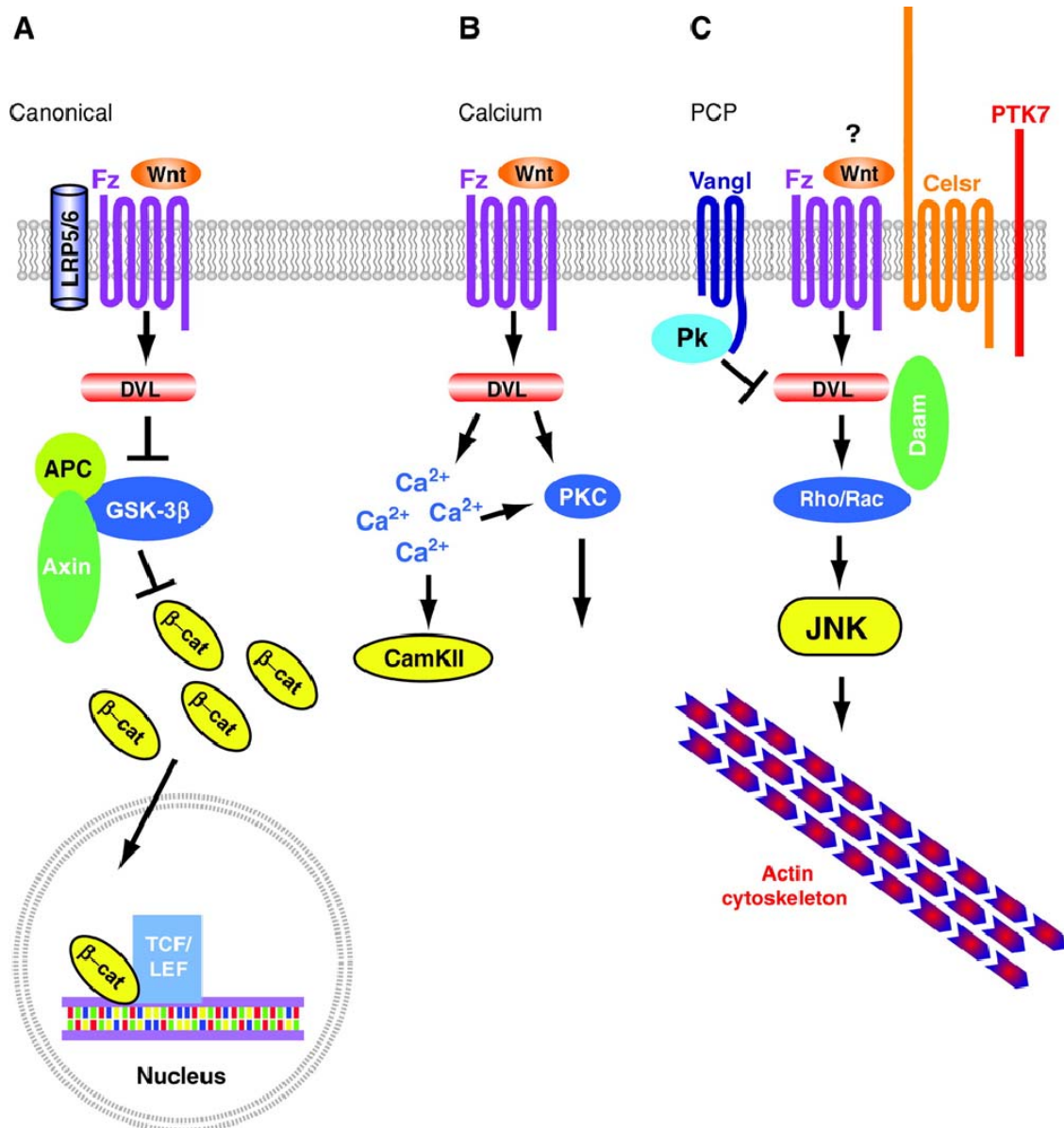


**Figure 1.7. Different branches of Wnt signaling.** (A) Canonical Wnt signaling/ $\beta$ -catenin signaling. (B) Calcium Wnt signaling. (C) Planar cell polarity signaling.  $\beta$ -Cat is  $\beta$ -catenin, dvl is dishevelled, Pk is prickles, celsr is flamingo, Vangl corresponds to strabismus. Adapted from Montcouquiol, 2006

Without the Wnt signal,  $\beta$ -catenin localizes primarily at the adherent junctions, while the cytoplasmically localized  $\beta$ -catenin is phosphorylated by glycogen synthase kinase 3  $\beta$  (GSK3 $\beta$ ) and targeted for proteasomal degradation. During the activation of canonical Wnt signaling a Wnt forms a complex with a fz receptor and LRP 5/6 co-receptor (arrow in *Drosophila*), resulting in the phosphorylation and activation of dsh, which leads to GSK-3 $\beta$  inhibition and stabilization of the  $\beta$ -catenin (Angers, 2008; Angers and Moon, 2009; Huang and Klein, 2004; Itoh et al., 1998; Kishida et al., 1999; MacDonald et al., 2009; Perrimon and Mahowald, 1987; Sussman et al., 1994; Wehrli et al., 2000).

Although a detailed mechanism of this process is not completely understood, it is known that  $\beta$ -catenin can be phosphorylated by GSK3 $\beta$  only when this kinase complexes with Axin and APC (Itoh et al., 1998). Upon Wnt signaling activation Axin is recruited to the plasma membrane and phosphorylated by LRP6. Next, it, most probably interacts with dsh, than the Axin-GSK-3 $\beta$ -APC complex dissociates and the activated dsh prevents GSK-3 $\beta$  from  $\beta$ -catenin phosphorylation (Angers and Moon, 2009; Kishida et al., 1999; MacDonald et al., 2009; Smalley et al., 1999). As a result  $\beta$ -catenin accumulates in the cytoplasm and subsequently translocates to the nucleus with a help of Ran GTPase (Fagotto et al., 1998; Komiya and Habas, 2008; Montcouquiol et al., 2006). In the nucleus the  $\beta$ -catenin/TCF-complex promotes the expression of other transcription factors, like for instance Twin or Siamois, which are responsible for the expression of organizer-specific genes (De Robertis, 2006; De Robertis and Kuroda, 2004). Thus, the activation of canonical Wnt signaling results in the stabilization of nuclear  $\beta$ -catenin, which activates transcriptional responses.

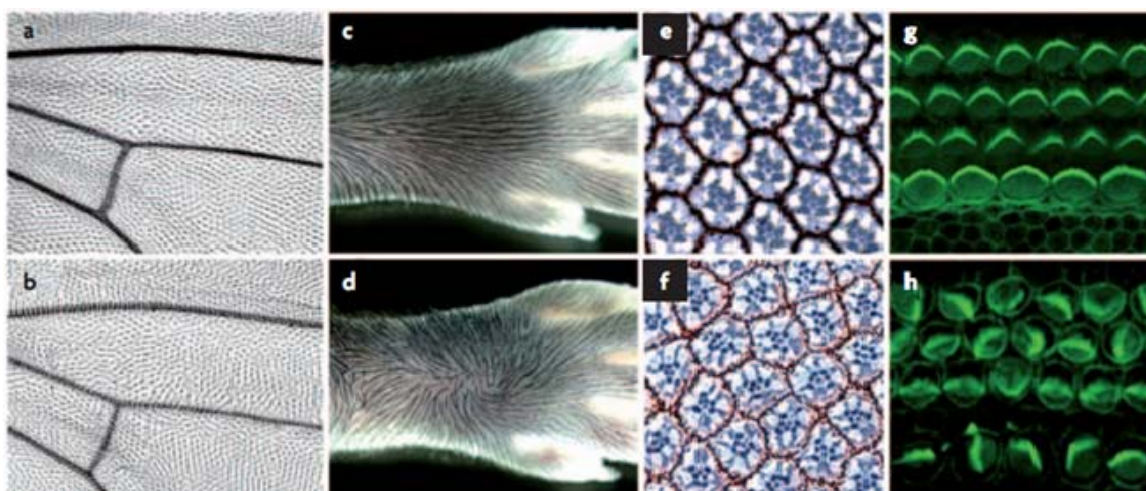


**Figure 1.8. Processes, controlled by PCP signaling.** (A) Normal polarity of *Drosophila* wing hair cells. (B) The polarity is disturbed upon disregulation of the PCP signaling. (C) Normal and (D) affected polarity of mice hair cells. (E) Normal and (F) affected polarity of the rhabdomeres in ommatidia. (G, H) Polarity of inner ear hair cells in normal situation and during the disregulation of the PCP signaling. Adapted from Seifert and Mlodzik, 2007

In contrast, non-canonical Wnt-signaling pathways, like the PCP pathway, are  $\beta$ -catenin independent. The planar cell polarity (PCP) signaling pathway comprises a branch of Wnt signaling, which is responsible for the establishment of epithelial polarity and morphogenetic movements (Fig. 1.7 C). The components of the PCP pathway were originally identified in *Drosophila*, where they are responsible for the establishment of polarity in the wing hair cells, the rhabdomeres in the ommatidia, (Figure 1.8, a, b, e, f) as well as hairs on the abdomen and

notum (Adler, 2002; Klein and Mlodzik, 2005; Lawrence et al., 2004; Mlodzik, 1999; Simons and Mlodzik, 2008; Strutt, 2003).

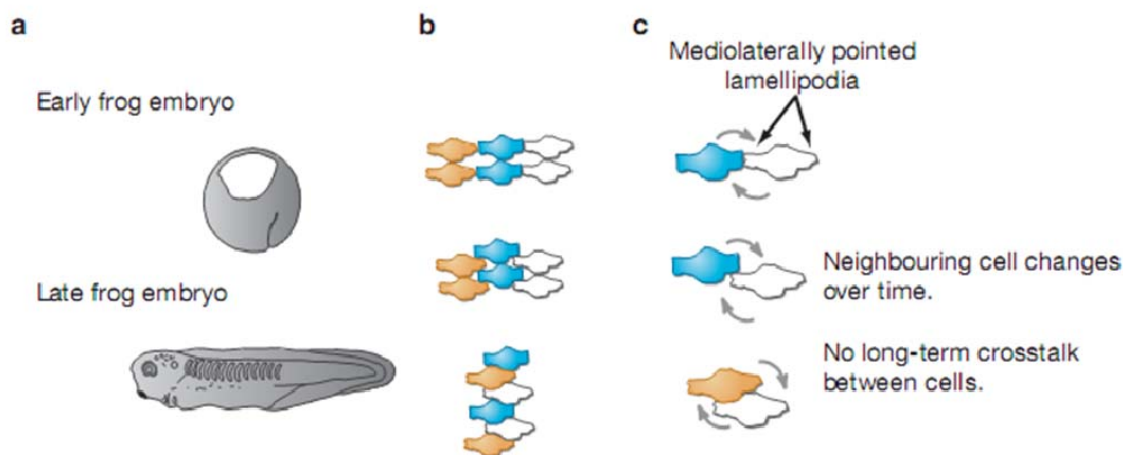


**Figure 1.9. The convergent extension movements.** (A) During the development vertebrate embryos require CE movements for gastrulation, neural tube closure as well as to gain an elongated shape. (B) The polarized cells interdigitation is a driving force of the convergent extension movements. (C) The polarization of cells and local lamellopodia formation is crucial for this process. During CE movement lamellipodia are stabilized specifically at the mediolateral cell faces. Lamellipodia formation is driven by the intercellular interactions. It is thought, that PCP signaling and, particularly, dsh redistribution functions in the local lamellipodia formation. Adapted from Wallingford, 2004

Later, vertebrate orthologues of *Drosophila* PCP genes were shown to regulate the polarization within epithelial sheets and morphogenetic movements. Originally, studies in *Xenopus* and zebrafish embryos demonstrated that PCP genes regulate convergent extension movements: a process during which cells intercalate in between each other, resulting in the narrowing and extension of the tissue (Figure 1.9). Convergent extension movements occur during both gastrulation and neural tube closure (Hamblet et al., 2002; Jessen et al., 2002; Kibar et al., 2001; Marlow et al., 1998; Montcouquiol et al., 2003; Tada and Smith, 2000; Wallingford et al., 2000). Similar to *Drosophila*, vertebrate PCP signaling components also establish epithelial polarity, like the polarization of inner ear hair cells, hair orientation in the mouse skin (Figure 1.8, c, d, g, h) as well as cilia polarization in the *Xenopus* epidermis (Park et al., 2006; Wang and Nathans, 2007).

Finally, recent studies revealed the emerging role of PCP signaling during cell migration, axonal guidance and oriented cell divisions during kidney tubules formation (Bacallao and McNeill, 2009; Kuriyama and Mayor, 2008; Simons and Mlodzik, 2008; Simons and Walz, 2006; Singla

and Reiter, 2006; Wallingford and Habas, 2005). Despite sharing similar fz, wnt and dsh molecules with canonical Wnt signaling the PCP pathway results rather in cytoskeletal rearrangements, than transcriptional activity. Currently, it is not entirely clear, how the choice between different Wnt signaling pathways is made, but each Wnt signaling branch has specific regulatory molecules in addition to frizzled receptors and dsh protein (Fig. 1.7). In the next chapter a known PCP regulatory mechanisms will be summarized and discussed in a more detail.

### 1.5 Molecular mechanisms of PCP signaling

In addition to the standard Wnt signaling components, like fz and dsh, the PCP signaling contains a variety of specific regulators like prickle, strabismus or flamingo (Fig. 1.7 C). Some of these regulators are crucial for the PCP activation, while other acts in a tissue specific context. Therefore, PCP signaling components can be subdivided into the “core” PCP genes and additional regulators. Furthermore, the PCP pathway is regulated by the upstream signals, and results in the activation of specific downstream effectors, which lead to the cytoskeleton remodeling. Thus, the following chapters will summarize the knowledge regarding upstream PCP activators, “core” genes and downstream effectors as well as its additional modulators.

#### 1.5.1 The “core” PCP genes

In both vertebrates and *Drosophila* the core PCP cassette includes the following proteins: Frizzled (Fz), Flamingo (Fmi, Starry night, Stan, Celsr in mouse), Dishevelled (Dsh, Dvl in mammals), Prickle, Strabismus (Stbm, Van/Gogh or Vang in mouse) and Diego (Dgo, Diversin and Inversin in vertebrates) in accordance with (Klein and Mlodzik, 2005; Simons and Mlodzik, 2008; Veeman et al., 2003a). Originally Frizzled and disheveled were identified as key molecules, causing downstream PCP effects, while Flamingo, Prickle, Diego and Strabismus are thought to be necessary for the proper localization of Fz/Dsh complex and modulation of its activity (Jenny et al., 2003; Jenny et al., 2005; Strutt, 2003).

**Frizzleds** are serpentine seven-pass transmembrane receptors, 500-700 amino acid residues in length. The extracellular part of Fz consists of a highly conserved cyteine-rich domain (CRD), which binds Wnt ligands, and hydrophilic linker sequence. The cytoplasmic tail of different frizzleds is very variable with an exception of the KTXXXW consensus sequence, which is situated just after the last transmembrane domain and necessary for dishevelled (dsh) binding. Frizzled molecules can act in both canonical and non-canonical/PCP signaling pathways. In PCP signaling frizzled acts by recruiting dsh to the plasma membrane, and facilitates its interaction with downstream PCP effectors (Huang and Klein, 2004; Strutt, 2003). Originally, several frizzleds, including frog Frizzled 7 (xFz7) and mouse Frizzleds 3 and 6, were thought to play a role exclusively in PCP signaling. In *Xenopus* Fz7 is expressed in the tissues, which undergo

convergent extension (CE) movements, and its miss-expression severely affects CE. The mouse knockouts of Fz3 and Fz6 also exhibit typical PCP defects, including craniorachischisis, a NT closure defect, where neural tube remains opened from the mid-hindbrain boundary towards the tail, and disturbed polarity of inner ear hair cells (Djiane et al., 2000; Guo et al., 2004; Vinson and Adler, 1987; Wang et al., 2006b; Wang et al., 2006c). However, recent studies have demonstrated that at certain conditions xFz7 can also activate canonical Wnt signaling, while the miss-expression of other frizzled molecules results in PCP-specific defects (Abu-Elmagd et al., 2006; Dearnorff et al., 1998; Kemp et al., 2007).

**Dishevelled** is a cytoplasmic regulatory protein, involved in three main Wnt signaling branches (Fig. 1.7 and 1.10) and thought to serve as a branch point between different Wnt signaling cascades. Like most PCP genes it was originally identified in *Drosophila* and subsequently its homologues were found in vertebrate organisms. Dishevelled is a 500-600 aa protein with a typical modular structure (Fig. 1.10). At the N-terminus dishevelled has the Dishevelled-Axin binding (DIX) domain, which functions primarily in canonical wnt signaling, The DIX domain is followed by the PSD-95-Discs-Large-ZO (PDZ) domain, which is involved in protein-protein interactions and required for both Wnt canonical, Wnt-Ca<sup>2+</sup> as well as PCP signaling cascades. Finally, the DEP domain (Dsh, EGL-10, Plekstrin), situated at the C-terminal part, is required for activation of the PCP pathway. The DEP domain was also shown to be crucial for the frizzled-mediated dsh membrane recruitment in response to Wnt treatment. In addition to the distinct domains, dishevelled proteins share several conserved motifs, which include a basic region and Ser-Thr-rich stretches between the DIX and PDZ domains, a proline-rich region with a potential SH3-binding site after the PDZ domain as well as a conserved C-terminal region (Fig. 1.8). Since dsh was shown to interact with more than 30 different proteins, its primary function is thought to be a scaffolding of different signaling pathways. However, the detailed mechanisms of dsh signaling remain to be elucidated (Axelrod et al., 1998; Boutros et al., 1998; Capelluto et al.,

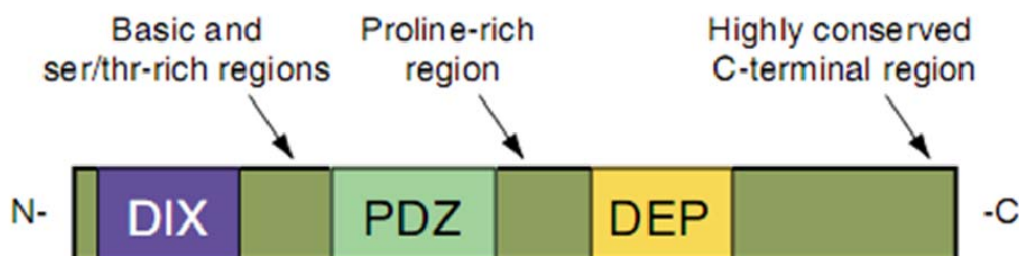


**Figure 1.10. The schematic structure of the dishevelled protein.** The dishevelled proteins have three major domains, namely the DIX, the PDZ and the DEP domains and several conserved motifs, including a basic ser/thr-rich region, a proline-rich region and a conserved C-terminal region. Adapted from Wallingford, 2005

2002; Moriguchi et al., 1999; Penton et al., 2002; Rothbacher et al., 2000; Tada and Smith, 2000; Wallingford et al., 2000; Wong et al., 2003; Wong et al., 2000), reviewed in (Wallingford and Habas, 2005).

Upon activation of Wnt signaling dsh needs to become activated in order to further transduce the signal. It is also known, that for PCP signaling the “active” state of dsh is associated with its membrane recruitment and hyperphosphorylation, which can be detected on the SDS gel by the appearance of a second higher molecular weight band. However, the detailed mechanisms of this process remain poorly understood. It is known, that dsh can be phosphorylated upon the co-expression with various frizzleds, for instance frizzled 7, or upon Wnt treatment (Lee et al., 1999; Rothbacher et al., 2000; Takada et al., 2005; Yanagawa et al., 1995). Several kinases, like casein kinase 1 and 2, as well as PAR1, were shown to phosphorylate dsh. At the same time other kinases, like PKC- $\delta$ , do not cause dsh hyperphosphorylation upon co-expression, however, their loss of function leads to the inhibition of dsh phosphorylation. Therefore, it is thought, that they are required for dsh phosphorylation, perhaps, by initializing the whole process (Cong et al., 2004; Kinoshita et al., 2003; Ossipova et al., 2005; Sun et al., 2001; Willert et al., 1997).

During development dishevelled is involved in various processes, like the establishment of segmental polarity in *Drosophila* embryo and vertebrate dorso-ventral axis patterning (Harland and Gerhart, 1997; Miller et al., 1999; Nusslein-Volhard and Wieschaus, 1980; Perrimon and Mahowald, 1987; Wallingford and Habas, 2005). But despite the multiple effects of dsh on development, many studies demonstrated PCP-specific defects during dsh loss-of-function or miss expression. Thus, it was shown, that *dsh*<sup>1</sup> allele, which harbors a single mutation in the DEP domain causes polarity defects in the fly wing (Axelrod, 2001; Theisen et al., 1994). In *Drosophila* eyes dsh is necessary for normal chirality and overall orientation (Boutros et al., 1998; Cooper and Bray, 1999; Strutt et al., 2002; Theisen et al., 1994). In vertebrates dsh was shown to be involved in convergent extension (CE) movements. During CE movements dsh regulates lamellipodia formation and governs cell movements into the right direction. In this context the dsh function is relevant for both gastrulation and proper neural tube closure. It was shown, that the expression of dominant negative dsh constructs (dsh lacking the PDZ or the DEP domains) or disruption of *dvl1/2* genes result in neural tube closure defects in fish, amphibians, chicken and mouse (Ewald et al., 2004; Hamblet et al., 2002; Kinoshita et al., 2003; Matsui et al., 2005; Sokol, 1996; Tada and Smith, 2000; Wallingford and Harland, 2002; Wallingford et al., 2000; Wang et al., 2006a). Moreover, the DVL-mutant mice phenotype is reminiscent of the human neural tube closure defect, craniorachischisis (Kirillova et al., 2000; Saraga-Babic et al., 1993). Dsh was shown to be involved in the formation and stability of the lamellipodia, and



consistent with this finding it also has a function in cell migration, for example of cardiomyocytes, Chinese hamster ovary (CHO) cells, Saos 2 (osteogenic, sarcoma-derived) cells as well as the neural crest cells (Carmona-Fontaine et al., 2008; De Calisto et al., 2005; Endo et al., 2005; Kinoshita et al., 2003; Phillips et al., 2005; Wallingford and Habas, 2005; Wallingford et al., 2000; Wiggan and Hamel, 2002). Finally, a function of dsh in PCP signaling was also demonstrated during kidney tube development, where it regulates polarized cell divisions (reviewed in (Bacallao and McNeill, 2009; Wallingford and Habas, 2005)).

**Strabismus and Prickle** are the PCP regulators in *Drosophila*, which antagonize Fz-Dsh activity. Strabismus (Stbm in *Drosophila*; Vang, Ltap in mouse) is a four transmembrane domain protein with conserved serine-threonine rich (STH) motif, implicated into dsh binding. Prickle (PK) is a cytoplasmic protein with 3 LIM and a PET domain, which physically interact with both Stbm and dsh (Seifert and Mlodzik, 2007). Prickle is recruited to the plasma membrane by Stbm, where it interacts with dsh and inhibits fz-mediated dsh membrane recruitment (Jenny et al., 2003; Jenny et al., 2005; Taylor et al., 1998; Tree et al., 2002; Wolff and Rubin, 1998). There is also a line of evidences, indicating that prickle can induce the degradation of dsh, by targeting cytoplasmically localized dsh to the proteasome, while membrane recruited dsh is protected from the degradation (Carreira-Barbosa et al., 2003). The opposing localization of Fz-dsh versus Stbm-Pk was nicely demonstrated in *Drosophila* wing hair cells, where Fz and dsh accumulates on the distal side, while Stbm-Pk is localized on the proximal side. The differential localization of these components is also observed in ommatidia (Bacallao and McNeill, 2009; Simons and Mlodzik, 2008). In vertebrates both Pk and dsh localize to specific sites of cells during CE movements (Ciruna et al., 2006; Yin et al., 2008). In mouse inner ear hair cells Stbm/Vang and dsh also display opposing localization. However, Vang co-localizes with Fz3 and 6 (Montcouquiol et al., 2003; Wang et al., 2006b), reviewed in (Simons and Mlodzik, 2008), (Seifert and Mlodzik, 2007). Additionally, during mouse development, dsh can asymmetrically localize Pk by targeting its degradation in Par6-dependent manner via Smurf ubiquitine ligases (Narimatsu et al., 2009).

As typical PCP genes, Vang and Pk regulate convergent extension movements in vertebrates. CE movements in zebrafish are severely affected in Vang (trilobite) and Pk mutants (Carreira-Barbosa et al., 2003; Jessen et al., 2002; Veeman et al., 2003b). Similarly, in *Xenopus* both Strabismus and Prickle are necessary for convergent extension (Goto et al., 2005). In mice the knockdown of Vang leads to craniorachischisis and disturbed inner ear hair cell polarity, while the heterozygous mice (loop-tail mice) also demonstrate mild NT closure defects, caused by affected CE movements (Kibar et al., 2003; Kibar et al., 2001; Montcouquiol et al., 2003).

The **Flamingo** (Fmi) protein, which mouse ortholog is named Celsr, is an atypical cadherin with seven-pass transmembrane features. Fmi is a homophilic binding molecule, and its loss-of-function in *Drosophila* results in typical PCP defects. Subsequently, mouse knock-out of Fmi/Celsr also demonstrates NT closure defects as well as disturbed polarity in the inner ear. Interestingly, Fmi/Celsr does not show asymmetric localization either in *Drosophila* or in vertebrate cells. Therefore it is thought to be required for the stabilization of core PCP components on the membrane. However, the particular function of Fmi in PCP signaling remains to be elucidated (Das et al., 2002; Shimada et al., 2001; Usui et al., 1999), reviewed in (Bacallao and McNeill, 2009; Montcouquiol et al., 2006; Seifert and Mlodzik, 2007; Simons and Mlodzik, 2008).

Finally, **Diego (Dgo)**, together with its vertebrate orthologs diversin/inversin and ankyrin repeat domain 6 (ankrd6), are cytoplasmic ankyrin repeat domain proteins, which can be recruited to the membrane by Fz and directly interact with dsh. Dgo is thought to be a positive regulator of Fz-dsh signaling. It was shown, that dgo competes with Pk for dsh binding, increasing thus a pool of active dsh on the membrane (Wu et al., 2008). In addition, dgo/diversin in vertebrates mediates dsh downstream signaling towards the small Rho-like GTPases and c-Jun N-terminal kinases. Interestingly, the mutation K44M in the DEP domain of vertebrate dsh, which mimics the classical *Drosophila* PCP-specific mutation, results in the inhibition of dsh-diversin interaction (Moeller et al., 2006). On the other hand, diversin can act as a molecular switch between canonical and PCP signaling. It was shown, particularly, that diversin can target a cytoplasmic pool of disheveled, which is necessary for canonical wnt signaling, for degradation (Simons et al., 2005). Moreover, by interacting with several  $\beta$ -catenin upstream regulators, including CKI $\epsilon$  and Axin, it promotes  $\beta$ -catenin degradation and inhibition of canonical Wnt signaling (Schwarz-Romond et al., 2002). At the same time diversin promotes CE movements in *Xenopus* and zebrafish embryos and can activate small Rho-GTPases and JNKs, which indicates that it functions as a PCP activator (Moeller et al., 2006).

### 1.5.2 Upstream regulators of the PCP signaling

It is unclear how the Fz/Dsh distribution as well as their activity is established. One hypothesis is that it is controlled by morphogen gradients. Originally, frizzleds were identified as receptors for Wnt molecules, therefore Wnts are good candidates to regulate Fz/dsh localization. Wnts comprise a family of secreted glycoproteins, which can specifically activate different branches of downstream signaling (Angers and Moon, 2009). The analysis of zebrafish wnt mutants, *pipetail* (*Wnt5a*) and *silberblick* (*Wnt11*), demonstrated that both *Wnt5a* and *Wnt11* affect convergent extension movements and activate downstream PCP signaling (Heisenberg et al., 2000; Lele et al., 2001). In accordance with zebrafish data, the same effects were shown for *Xenopus* embryos

as well as for human cell culture (Du et al., 1995; Moon et al., 1993; Tada and Smith, 2000). In addition, it was also demonstrated, that a Wnt5a gradient is necessary for the proper localization of Prickle in tissues undergoing CE movements (Veeman et al., 2003b).

Other Wnt ligands, namely Wnt4 and mouse Wnt7a, are also involved in the regulation of PCP signaling. Wnt4 can affect CE movements (Ungar et al., 1995), while mouse Wnt7a regulates stereocilia formation and polarity (Dabdoub et al., 2003). Recently it was also shown, that Wnt9b activates PCP signaling during kidney tubule formation (Karner et al., 2009). In addition, increasing evidence supports the idea, that different Wnt molecules can act in a context-dependent manner to activate either canonical or PCP signaling pathways. For instance, Wnt3a can also activate PCP downstream molecules, like JNK (Endo et al., 2005), while Wnt5a can lead to  $\beta$ -catenin stabilization upon the co-expression with human Frizzled5 (He et al., 1997).

Surprisingly, the localization of Fz7/dsh in *Drosophila* wing hair cells was not shown to be controlled by Wnt/Wg ligands. However, another group of PCP regulators, consisting of large protocadherins Fat (Ft), Dachshous (Ds) and Four-jointed (Fj), was recently identified in *Drosophila*. The dysfunction of any of these components also results in polarity defects and therefore all three protocadherins seems to establish another PCP signaling system, the FAT-system (Matakatsu and Blair, 2004; Rawls et al., 2002; Strutt et al., 2004; Zeidler et al., 1999), reviewed in (Bacallao and McNeill, 2009; Simons and Walz, 2006). The components of the FAT system demonstrate a genetic interaction with Fz/dsh signaling (Yang et al., 2002). Although it is not entirely clear, how FAT components affect the distribution of Fz-Dsh complex in wing hair cells and ommatidia, the one hypothesis is that the FAT system is required for proper localization of Fz7-Dsh and STBM/Pk at least within the wing hair cells. Furthermore, the investigation of the polarity establishment in the *Drosophila* abdomen leads to the hypothesis that both pathways act in parallel to each other (Casal et al., 2006; Lawrence et al., 2004), reviewed in (Lawrence et al., 2007; Simons and Walz, 2006).

### **1.5.3 Small GTPases and other PCP downstream targets**

Once dsh is properly localized and “activated” it promotes remodeling of the actin cytoskeleton. Despite the fact that the detailed mechanism of the dsh-induced cytoskeletal remodeling is not completely understood, it is known that disheveled can affect cytoskeletal reorganization via two distinct small-GTPase-dependent pathways, namely the Rho- and the Rac-pathways (Fig. 1.11) (Keller, 2002; Wallingford and Habas, 2005).

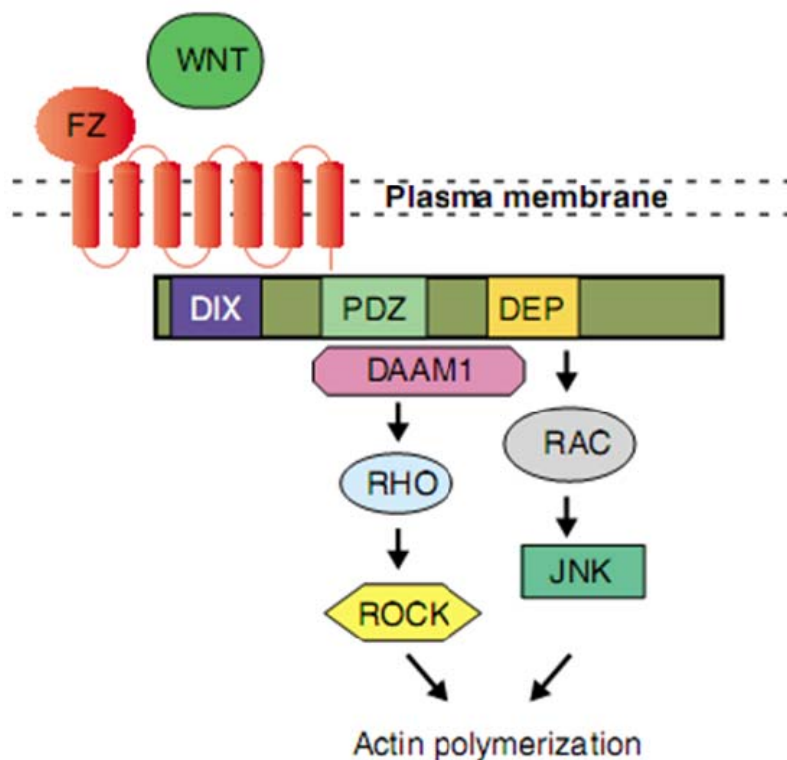


**Figure 1.11. In the PCP signaling cascade dsh activates two different classes of small GTPases.** (A) During the Rho-pathway dsh interacts with formin homology domain protein DAAM, which recruits and subsequently activates Rho small GTPase. The Rho small GTPase, in turn causes the activation of ROCK kinase and remodeling of the actin cytoskeleton. (B) During the Rac-pathway dsh activates Rac small GTPase and, subsequently, c-Jun-N-terminal kinases (JNK), which also cause actin remodeling. Adapted from Wallingford, 2005

In the **Rho-pathway** disheveled interacts with the formin-homology-domain protein DAAM (disheveled-associated-activator-of-morphogenesis), which mediates the Rho-dsh interaction (Habas et al., 2001; Matusek et al., 2006). The Rho protein, in turn, activates Rho kinase (ROCK, Rok), which facilitates cytoskeletal rearrangements, and particularly stress fiber contraction (Habas et al., 2003; Katoh et al., 2001a; Katoh et al., 2001b; Winter et al., 2001) (Fig. 1.11, A). Experiments with dominant negative zebrafish Rok2 show, that the Rho-pathway may be required for proper mediolateral elongation, intercalation and alignment of cells. It is assumed that the Rho-pathway facilitates shortening and development of lamellipodia traction and inhibition of lamellipodia formation (Keller, 2002; Marlow et al., 2002). Interestingly, dsh might regulate cytoskeleton remodeling only via DAAM, because formin-domain proteins can directly induce cytoskeletal rearrangements (Sagot et al., 2002; Watanabe and Higashida, 2004). In contrast to Rho, **Rac activity** is associated with large lamellipodia formation. The Rac pathway is also activated via dsh and leads to the activation/phosphorylation of c-Jun-N-terminal kinases (JNK), which mediate cytoskeletal remodeling (Boutros et al., 1998; Habas et al., 2003) (Fig. 1.11, B). Furthermore, there is an evidence to support the hypothesis, that Rho and Rac

pathways antagonize each other, forming thereby a polarized cell with Rac promoting the lamellipodia at the leading edge and Rho inhibiting their formation at cell-cell contacts (Carmona-Fontaine et al., 2008; Yamaguchi et al., 2001). All PCP downstream effectors, including Rac, Rho as well as DAAM, Rok and JNK were shown to regulate convergent extension movements, polarity establishment in *Drosophila* wings and eyes, as well as cell migration (Eaton et al., 1996; Fanto et al., 2000; Habas et al., 2003; Habas et al., 2001; Kim and Han, 2005; Strutt et al., 1997; Tahinci and Symes, 2003). Finally, it was shown that upon activation of noncanonical Wnt/PCP signaling JNK kinases become not only phosphorylated but also translocated to the nucleus, where they phosphorylate their downstream target Jun, which can be used as a readout for PCP activity (Tahinci et al., 2007; Yamanaka et al., 2002).

Another small GTPase, **CDC-42**, was also shown to function in CE movements. In frog constitutively active CDC-42 rescues the effect of inhibitory Fz7 isoform and vice versa. CDC-42 might regulate anterior and posterior filopodia activity and act in PCP as well as Wnt-Ca<sup>2+</sup> pathway (Choi and Han, 2002; Djiane et al., 2000; Winklbauer et al., 2001). In *Drosophila*, missharpen, a Ste-20-like kinase, was also shown to act downstream of dsh and regulate cell polarity in the eyes (Boutros et al., 1998; Paricio et al., 1999).

#### 1.5.4 Additional PCP regulators

In addition to key PCP factors and their upstream and downstream effectors, a number of molecules, which regulate distinct aspects of the PCP signaling, have been identified. This group consists of different classes of signaling molecules and includes secreted proteins, transmembrane receptors, kinases and scaffold proteins.

**Glypican 4/6**, which was identified by mutational analysis in zebrafish as **knypek** (kny), is a heparane sulfat proteoglycan, associated with the plasma membrane via GPI-anchor. Knypek was shown to bind wnt5a, wnt11 as well as frizzled 7 and enhance PCP signaling. In zebrafish and *Xenopus* embryos knypek was shown to regulate CE movements (Ohkawara et al., 2003; Topczewski et al., 2001). Interestingly, during gastrulation kny is interacting with canonical wnt-signaling molecule Dickkopf (Dkk), thereby mediating Dkk function during morphogenetic movements (Caneparo et al., 2007). In *Drosophila* no homologues of knypek were identified so far, therefore it is thought to be a vertebrate-specific PCP modulator (Simons and Mlodzik, 2008). Another protein, which is functionally related to knypek is **Down syndrome critical region protein 5 (Dscr5)**. The Dscr5 protein is a predicted component of the GPI-N-acetylglucosaminyltransferase (GPI-GnT) complex, which is involved in glypicans procession. Dscr5 was shown to regulate convergent extension movements. Furthermore, Dscr5 knockdown results in the disruption of knypek membrane localization, enhanced Fz7 endocytosis and increased dsh degradation (Shao et al., 2009).

**Fuzzy** is a four-pass transmembrane protein which physically and genetically interacts with a cytoplasmic adaptor protein **inturned** (Seifert and Mlodzik, 2007; Simons and Mlodzik, 2008). In the *Drosophila* wing fuzzy and inturned are required for the proper localization of Frizzled and Stbm and their disfunction leads to wing polarity defects (Adler et al., 2004; Collier and Gubb, 1997; Park et al., 1996b; Yun et al., 1999). In *Xenopus* embryos fuzzy and inturned loss-of-function affects convergent extension movements and ciliogenesis (Park et al., 2006). In *Drosophila* two other genes, **fritz** and the **multiple wing hair** (mwh) protein, demonstrate genetic interaction with fuzzy and inturned. Fritz is a WD40 coiled protein and mwh is predicted to be a G-protein-binding-formin-homology domain protein (GBD-FH3). Loss of function of either fritz or mwh results in the disturbed wing hair cell polarity. However, in vertebrates no homologues for either of these proteins were identified so far (Adler et al., 2004; Collier et al., 2005; Seifert and Mlodzik, 2007; Wong and Adler, 1993; Yan et al., 2008).

A number of kinases were also shown to regulate PCP signaling. This group includes **casein kinase 1  $\epsilon$**  (**CKI $\epsilon$** )/ **discs overgrowth** (**dco**), **nemo/nemo-like kinase** (**Nlk**) and vertebrate **protein kinase C  $\delta$**  (**PKC $\delta$** ). CKI $\epsilon$  is a serine-threonine kinase, which acts positively on fz-dsh signaling. It is known to phosphorylate dsh and regulate its localization. The disruption of the casein kinase function leads to wing and eye polarity defects in *Drosophila* as well as CE defects in vertebrates (Klein et al., 2006; McKay et al., 2001; Seifert and Mlodzik, 2007; Strutt et al., 2006). Nemo-like kinase is a Ser/Thr-kinase of the MAPK (mitogen-activated protein kinases) superfamily. It was shown to enhance fz-dsh signaling, by acting on both the  $\beta$ -catenin and the PCP signaling pathways. However, the detailed mechanism of Nlk function remains to be elucidated. It was shown that *Drosophila* nemo is required for polarity establishment in the eye, while Nlk acts together with Wnt11 to promote convergent extension movements in zebrafish (Choi and Benzer, 1994; Thorpe and Moon, 2004). Finally, another Ser/Thr kinase, PKC $\delta$ , was shown to have a function in *Xenopus* convergent extension. PKC $\delta$  interacts directly with dsh and is necessary for its Fz7-dependent membrane recruitment and phosphorylation. Thus, PKC $\delta$  also acts as a positive regulator of PCP signaling (Kinoshita et al., 2003).

Recently, a number of vertebrate-specific PCP regulators have been identified in zebrafish, frog and mice. Surprisingly, no abundant PCP-defects were demonstrated for their *Drosophila* orthologs. For the majority of these proteins their exact function in the PCP signaling remains to be further elucidated. This group includes Bardet-Biedl syndrome proteins, neurotrophin receptor related protein and protein tyrosine kinase 7. In addition, orphan receptor ROR2 and receptor tyrosine kinase Ryk have been shown to affect PCP signaling in vertebrates. The possible interactions of these proteins with PCP signaling as well as their roles in embryogenesis will be summarized below.

First of all, knockout studies in mice revealed that a structurally diverse group of **Bardet-Biedl syndrome (Bbs) proteins**, namely Bbs1, 2 and 6, displays PCP-specific defects in the polarity of inner ear hair cells as well as during the neural tube closure (Ross et al., 2005; Wang and Nathans, 2007). Another molecule, which demonstrates PCP defects in inner ear epithelium and neural tube is the cytoplasmic adaptor protein **scribble 1 (Scbr1)**. In addition, scribble demonstrates genetic interaction with Stbm/Vangl, which provides even stronger evidence for its PCP function (Montcouquiol et al., 2003; Murdoch et al., 2003; Murdoch et al., 2001). However, in *Drosophila* scribble is responsible only for the establishment of the apical-basal polarity, but not PCP (Bilder and Perrimon, 2000).

The **neurotrophin receptor related protein (NRH1)** was initially isolated in a screen for *Xenopus* posterior neuroectoderm genes. Lately, it was shown, that NRH1 regulates CE movements and activates small GTPases and JNKs. Interestingly, the effect of NRH1 on JNK does not depend on dsh, which suggests, that NRH1 could act downstream of dsh (Sasai et al., 2004).

Two other molecules, namely receptor **ROR2** and non-functional receptor tyrosine kinase **Ryk**, which can bind Wnt molecules, were also implicated to have a function in PCP signaling. It was shown, that Ryk is essential for convergent extension movements in *Xenopus*. Ryk interacts with both Wnt11 and  $\beta$ -arrestin-2 and promotes Wnt-11 stimulated endocytosis of the Fz7-dsh complex, which leads to activation of noncanonical Wnt signaling (Kim et al., 2008). The receptor ROR2 was shown to regulate CE movements. It also interacts with Wnt5a and leads to JNK activation. However, at the same time the Wnt5a/ROR2 pathway is classified as a distinct branch of noncanonical Wnt signaling. Additionally, the Wnt5a/ROR2 pathway results in transcriptional activation and causes the expression of **paraxial protocadherin (XPAPC)** (Schambony and Wedlich, 2007). XPAPC is thought to promote convergence during CE movements in *Xenopus* and acts through RhoA, Rac1 and JNK (Unterseher et al., 2004). During the gastrulation XPAPC interacts with another CE regulator **Sprouty (Spry)**, a negative inhibitor of PCP signaling. Upon binding XPAPC Spry is inhibited, which leads to PCP activation and progression of CE movements (Wang et al., 2008). Finally, protein tyrosine kinase 7 is another newly identified vertebrate PCP signaling regulator (Lu et al., 2004), which will be described in detail in the next chapter

### 1.5.5 Protein tyrosine kinase 7 (PTK7)

Protein tyrosine kinase 7 (PTK7), also called colon carcinoma kinase 4 (CCK4), was originally isolated from colon carcinoma and is overexpressed primarily in tumors with high metastatic potential. PTK7 belongs to the family of receptor tyrosine kinases and comprises a transmembrane molecule with seven immunoglobulin-like domains in the extracellular part and kinase homology domain in the cytoplasmic tail (Fig. 1.12, A) (Mossie et al., 1995; Park et al.,

1996a). The PTK7 kinase homology domain demonstrates high conservation among different species beginning from *Hydra* to human. However, the DFG triplet, which is necessary for the catalytic activity, within the kinase domain is mutated in all known PTK7 orthologs. (Boudeau et al., 2006; Grassot et al., 2006). The experiments with PTK7 in chick (KLG) and Hydra (Lemon) did not reveal any signs of the catalytic activity (Chou and Hayman, 1991; Miller and Steele, 2000). Interestingly, *Drosophila* ortholog of PTK7, off-track (Otk), was originally purified with a kinase activity, but it was not further proven that the kinase activity was specific to Otk (Pulido et al., 1992). For a long time PTK7 was thought to be an orphan receptor without any known downstream cascades. But lately it was shown, that *Drosophila* off-track can interact with semaphorins and plexins, thus regulating axonal guidance (Winberg et al., 2001). In addition, Off-track overexpression in *Drosophila* leads to the activation of JNK kinases (Bakal et al., 2008).

Knockout studies in mice revealed that, as many other PCP genes, PTK7 is required for proper

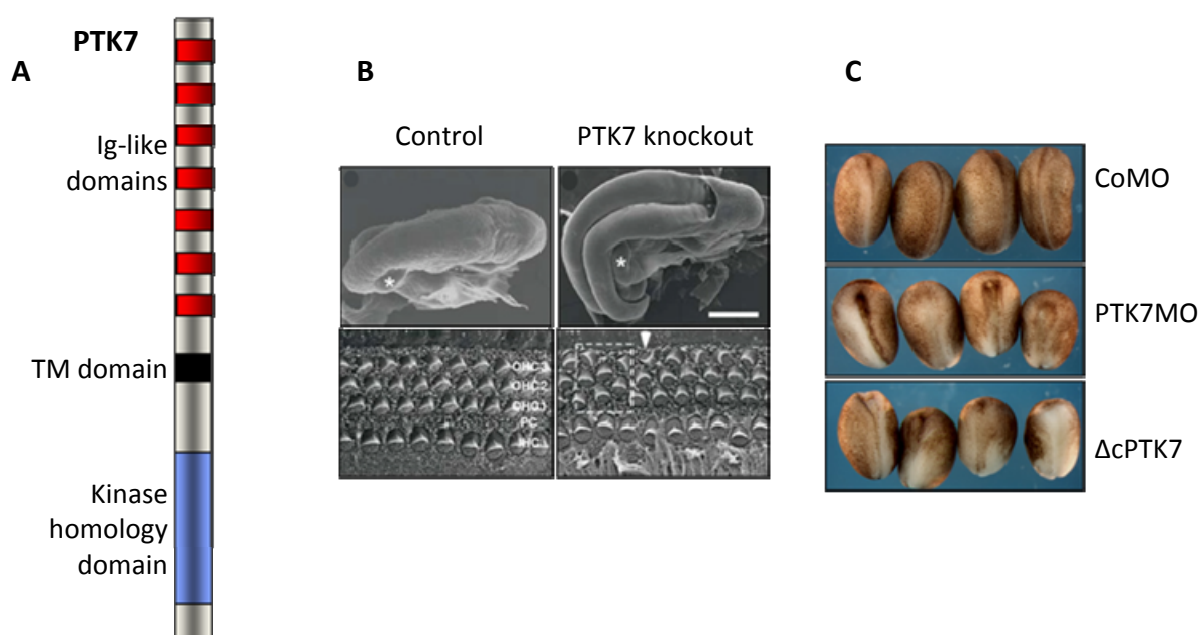


**Figure 1.12. PTK7 is a PCP regulator.** (A) The schematic structure of PTK7: PTK7 is a transmembrane molecule, consisting of 7 Ig-like domains (in red) and kinase homology domain (in blue). (B) PTK7 loss of function results in craniorachischisis (mouse embryonic stage E.9) and disturbed inner ear hair cell polarity (mouse embryonic stage E. 17.5). (C) The PTK7 loss-of-function, as well as overexpression of the PTK7 deletion mutant lacking the C-terminal part in *Xenopus* also causes neural tube closure defects. Adapted from Lu et al., 2004

neural tube closure and establishment of the inner ear hair cell polarity (Fig. 1.12, B). Moreover, PTK7 knockout mice demonstrate genetic interaction with loop-tail/Vangl mice, indicating a role in the regulation of PCP signaling. In addition, it was shown, that in mice PTK7 regulates cell motility and CE movements during gastrulation (Yen et al., 2009). The loss of PTK7 function in *Xenopus* also leads to neural tube closure defects, caused by improper CE movements.



Interestingly, the overexpression of xPTK7 lacking the conserved kinase homology domain leads to similar defects (Fig. 1.9, C), suggesting that the intracellular part of the PTK7 protein is involved in the regulation of the PCP signaling (Lu et al., 2004).

### **1.6 The role of PCP signaling in neural crest migration**

Several PCP components, including Wnts, frizzled receptors and dsh, are expressed in the area of the neural crest (De Calisto et al., 2005; Matthews et al., 2008a; Sisson and Topczewski, 2009). As PCP signaling has been implicated to regulate the directional migration of certain group of cells, it is likely that it functions in neural crest migration. Indeed, several studies support this hypothesis. First, it was shown, that overexpression of dsh mutants, lacking PCP activity, inhibits the migration of neural crest cells. Second, two Wnt ligands, namely Wnt11 and Wnt11-R, are expressed in the area of migrating neural crest and inhibition of both affects neural crest migration, but not NC induction. Moreover, Wnt11 inhibition can be rescued by intracellular activation of PCP signaling (De Calisto et al., 2005; Matthews et al., 2008a; Sisson and Topczewski, 2009). Thus these data support a function of PCP signaling in the regulation of NC migration.

Neural crest cells were shown to possess contact inhibition of locomotion and this phenomenon seems also to be regulated by PCP signaling (Carmona-Fontaine et al., 2008). Contact inhibition of locomotion was originally demonstrated for mouse fibroblasts, which reverse their migration direction upon contact with each other (Abercrombie and Heaysman, 1953, 1954). Similarly, upon explantation on fibronectin *Xenopus* neural crest cells start to migrate as a group, in which leading cells are followed by trailing cells. After a certain period of time, single cells start leaving the explant and migrate alone. It was shown that when such cells contact other NC cells they change their direction of migration. Interestingly, in migrating NC cells dsh is asymmetrically localized and detected in cell-cell contacts, where it co-localizes with Frizzled 7 and Wnt11, as well as in the lamellipodia at the leading edge.

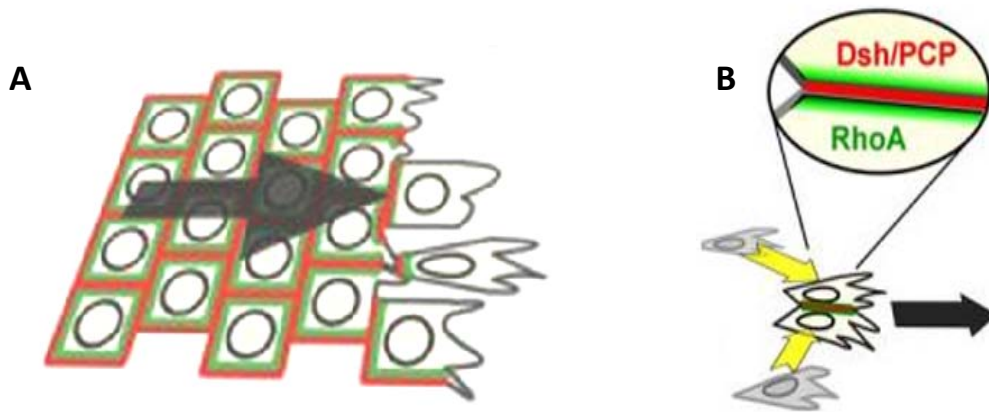


**Figure 1.13. PCP signaling regulates neural crest migration via contact inhibition of locomotion.** (A) During neural crest migration dsh together with fz7 and Wnt11 (in red) is localized to cell contacts, where it activates RhoA (in green). (B) During the establishment of contact between two neural crest cells, dsh is localized to this area and activates RhoA. The RhoA activation, in turn, causes cytoskeletal rearrangements resulting in changing the direction of movement. Yellow arrows indicate the direction of movement before the contact, black arrow – after the contact

When migrating NC cells establish a contact with each other, dsh localizes to cell-cell contacts and activates Rho, which in turn leads to the cytoskeletal remodeling, causing a change in the direction of migration. In contrast, cytoplasmic dsh in the lamellipodia activates Rac, which further promotes lamellipodia formation and, thus, cell migration in the same direction (Fig. 1.13). Moreover, overexpression of the dsh mutant, lacking PCP activity ( $\Delta$ DEP dsh) in neural crest cells affects their contact inhibition of locomotion. Therefore, PCP signaling is thought to be a pathway, implicated in the directional migration of the neural crest cells (Carmona-Fontaine et al., 2008).

### 1.7 Aims

PTK7 was identified as a PCP regulator, necessary for neural convergent extension and the establishment of inner ear hair cell polarity, however its intersection with the PCP signaling pathway remains poorly understood. Thus the first aim of the work is to characterize how PTK7 intersects with PCP signaling. For this purpose a candidate approach will be used to test for interaction with known PCP partners. This will be done using binding assays as well as analyzing protein-co/localization in ectodermal explants. To identify novel PTK7 interaction partners without previous knowledge of their function in PCP signaling, tandem mass-spectrometry analysis will be employed.

Since PCP signaling controls various types of morphogenetic movements in vertebrates, like the migration of neural crest cells and in *Xenopus laevis* embryos PTK7 is expressed in the area of migrating neural crest, the second aim of this work is to elucidate the role of PTK7 during *Xenopus* neural crest migration. Gain- and loss-of-function analysis will be used to elucidate the function of PTK7 in *Xenopus* embryos. If phenotypes are observed, then neural crest explants as well as targeted expression using the neural crest-specific slug promoter in combination with different PTK7 deletion constructs will be used to further elucidate this function.

## 2. Materials

### 2.1 Model organism

*In vivo* experiments of the given work were done on *Xenopus laevis* (Pipidae, Anura) embryos. The embryos were obtained by *in vitro* fertilization and staged according to Niewkoop and Faber (Niewkoop P.D., 1956). Adult frogs were provided by Nasco (Ft. Atkinson, USA).

### 2.2 Bacteria

The cloning work was done in *E.coli* strains XL1-Blue (RecA1, endA1, gyrA96, thi-1, hsdR17, supE44, relA1, lac[F'proAB, ZΔM15, Tn10(Tet<sup>f</sup>)]<sup>c</sup> (Stratagene)) and XL10- Gold (endA1 glnV44 recA1 thi-1 gyrA96 relA1 lac Hte Δ(mcrA)183 Δ(mcrCB-hsdSMR-mrr)173 tet<sup>R</sup> F'[proAB lacI<sup>q</sup>ZΔM15 Tn10(Tet<sup>R</sup> Amy Cm<sup>R</sup>)]<sup>C</sup> (Stratagene)).

### 2.3 Chemicals, solutions, media and buffers

#### 2.3.1 Chemicals

All chemicals, used in the given work, were obtained from the following companies: Roth (Karlsruhe), Sigma (Munich), Biomol (Hamburg) and Applichem (Darmstadt)

#### 2.3.2 Media and antibiotics

Media were prepared using deionized water (MiliQ) and autoclaved 20 min at 120°C. Antibiotics were added to the cooled solution.

**Luria-Bertani (LB)-Medium:** 1% (w/v) Bacto-Trypton (DIFCO), 0.5 % (w/v) yeast extract (DIFCO), 1% (w/v) NaCl, pH 7,5

**LB-Agar:** 1,5% (w/v) agar (DIFCO) in liquid LB-medium

Ampicillin: 50 mg/ml in H<sub>2</sub>O, 500x Stock (Biomol); Kanamycin: 50mg/ ml in H<sub>2</sub>O, 1000x Stock (Biomol)

#### 2.3.3 Buffers and Solutions

**Alkaline phosphatase buffer (APB):** 100 mM Tris-HCl (pH 9.5), 50 mM MgCl<sub>2</sub>, 100 mM NaCl, 0.1% Tween-20

**Ca<sup>2+</sup>-Mg<sup>2+</sup>-free medium:** 88 mM NaCl, 1 mM KCl, 2.4 mM NaHCO<sub>3</sub>, 7.5 mM Tris-HCl (pH 7.6)

**Cystein solution:** 2% L-Cystein-HCl, pH 7.8

**Danylchik's for Amy (DFA) medium:** 53 mM NaCl, 5 mM Na<sub>2</sub>CO<sub>3</sub>, potassium gluconate 4,5 mM, sodium gluconate 32 mM, MgSO<sub>4</sub> 1 mM, CaCl<sub>2</sub> 1 mM, BSA 0.1%

**Ficoll:** 10% (w/v) Ficoll PM 400 (Sigma), sterile filtered

**Hybridization mix (Hyb-mix):** 50% (v/v) Formamid; 5xSSC; 1 mg/ml Torula RNA (Sigma); 100 μg/ml Heparin (Sigma); 1x Denhards; 0.1 % (v/v) Tween-20; 0.1 % (w/v) CHAPS (Sigma)

**Injection buffer:** 1x MBS, 1% Ficoll

**Laemli running buffer (10x) (Gel running buffer):** 250 mM Tris-base, 2.5 M Glycine, 0,1% SDS

**Laemmly loading buffer (4x):** Tris-HCl pH 6.8 200 mM,  $\beta$ -merkaptoethanol 400 mM, Glycerol 40%, SDS 4%, Bromphenolblue 0.05%

**MAB:** 100 mM Maleinic acid; 150 mM NaCl, pH 7.5

**MBSH Buffer (1x):** 10 mM Hepes (pH 7,4), 88 mM NaCl, 1 mM KCl, 2.4 mM NaHCO<sub>3</sub>, 0.2 mM MgSO<sub>4</sub>, 0.41 mM CaCl<sub>2</sub>, 0.66 mM KNO<sub>3</sub>

**MEM:** 100 mM MOPS, 2 mM EGTA, 1 mM MgSO<sub>4</sub>

**MEMFA:** 1x MEM with 3.7% Formaldehyde

**Nile blue:** 0.01% (w/v) Nile blue in 0.1x MBSH

**NOP-buffer (co-immunoprecipitation buffer):** 20 mM Tris-HCl pH 7.5, 150 mM NaCl, 0.5% NP-40 substitute (Fluka)

**PBS (10x):** 8% (w/v) NaCl, 2% (w/v) KCl, 65 mM Na<sub>2</sub>HPO<sub>4</sub>, 18 mM KH<sub>2</sub>PO<sub>4</sub>, pH 7. 4

**S100-Buffer:** 50 mM Tris-HCl (pH 8.0), 50 mM KCl, 0,1 mM EDTA, 5 – 25% Glycerol

**SSC:** 150 mM NaCl, 15 mM Na-Citrate, pH 7.2-7.4

**TAE (Tris/Acetate/EDTA):** 40 mM Tris-Acetate (pH 8.5), 2 mM EDTA

**TBS/Tween:** 20 mM Tris-HCl (pH 7.5), 150 mM NaCl, 0.05% Tween

**TE-Buffer:** 10 mM Tris-HCl pH8.0, 1 mM EDTA

**Tris-HCl (pH 6.8, 7.5, 8.2, 8.8, or 9.5):** 1 M Tris-HCl, pH adjusted with 37% HCl

**Western blotting buffer:** 3.03 g Tris-base, 14,4g Glycine, 200 ml methanol, 800 ml H<sub>2</sub>O

**X-gal staining solution:** 1 mg/ml X-gal, 5 mM K<sub>3</sub>Fe (CN)<sub>6</sub>, 5 mM K<sub>4</sub>Fe (CN)<sub>6</sub>, 2 mM MgCl<sub>2</sub>

### 2.3.4 Unclassified chemical substances and reagents

Agarose  $\alpha$ -myc beads: A7470-1ML, Sigma;

Bovine fibronectin: F4759-5MG, Sigma;

Complete, EDTA-free Protease Inhibitor Cocktail tabs, Roche Diagnostics;

DNA ladder: Low, Middle, High-Range, MBI Fermentas;

Human chorionic gonadotropin (HCG), Sigma;

NBT and BCIP (NBT: C<sub>40</sub>H<sub>30</sub>Cl<sub>2</sub>N<sub>10</sub>O<sub>6</sub>, BCIP: C<sub>8</sub>H<sub>6</sub>NO<sub>4</sub>BrClIP x C<sub>7</sub>H<sub>9</sub>N), Roche;

Nonfat Dry Milk (NDM), Sucofin;

Protein A Sepharose beads: CL4B-beads, 17-0780-01, GE Healthcare;

Protein ladder: PageRuler Prestained Protein Ladder #SM0671, MBI Fermentas;

X-gal (5-Bromo-4-chloro-3-indolyl  $\alpha$ -D-galactopyranoside), Roche.

### 2.4 Enzymes and Kits

Big Dye Terminator v1.1 Cycle Sequencing Kit, Applied Biosystems;

DNase I (1 U/ $\mu$ l): MBI Fermentas;

DreamTaq Polymerase (5 U/ $\mu$ l): MBI Fermentas;  
 ECL Kit Super Signal Dura West, Pierce;  
 High Fidelity PCR Enzyme Mix (5 U/ $\mu$ l), MBI Fermentas;  
 Illustra™ Plasmid Prep Midi Flow Kit, GE Healthcare;  
 Illustra™ Plasmid Prep Mini Spin Kit, GE Healthcare;  
*Pfu* DNA Polymerase (2.5 U/ $\mu$ l), MBI Fermentas;  
 Proteinase K (20mg/ml), Merck;  
 Pyrophosphatase (0,1U/ $\mu$ l), Fermentas;  
 Restriction Endonucleases, MBI Fermentas and New England Biolabs (NEB);  
 Reverse Transkriptase (50U/ $\mu$ l), Applied Biosystems;  
 RNA *In Vitro* Transcription Kit, Stratagene;  
 RNase A (100U/ $\mu$ l), Sigma;  
 RNase Out (40 U/ $\mu$ l), Invitrogen;  
 RNase T1 1000U/ $\mu$ l, MBI Fermentas;  
 RNeasy Mini Kit, Qiagen;  
 Shrimp Alkaline Phosphatase, MBI Fermentas;  
 SP6, T3 and T7 mMACHINE Kits, Ambion Inc.;  
 SP6, T3, T7 RNA Polymerases (20U/ $\mu$ l), Fermentas;  
 T4 DNA Ligase (1 U/ $\mu$ l), MBI Fermentas;  
 T4 Polynukleotide Kinase (10 U/ $\mu$ l), MBI Fermentas;  
 TnT-Coupled Reticulocyte Lysate System, Promega;  
 Zymoclean Gel DNA Recovery Kit, Zymo Research, Hiss.

## 2.5 Vectors and DNA Constructs

### 2.5.1 Vectors

**PCS2+** is a multipurpose expression vector originally designed for the work in *Xenopus*, which is based on the pBlueskript II KS+ backbone. The vector contains a strong enhancer/promoter (simian CMV IE94) followed by a polylinker and a simian deficiency virus (SV40) polyadenylation site. The presence of the SP6 promoter at the 5' untranslated region allows *in vitro* transcription of the messenger RNAs.

**PCS2+ with myc tag (pCS2+MT)** was generated from pCS2+ by the insertion of the 6X myc tags (Klisch et al., 2006).

**PCS2+ with hemagglutinin tag (pCS2+HA)** was generated from the pCS2+ vector by insertion of the hemagglutinin tag (HA) via the XbaI site (Damianitsch et al., 2009).

Both pCS2+MT and HA share all properties and features of pCS2+.

PCS105 vector is a modified version of the pCS2

**BS I-Sce-II KS (Meganuclease) vector** was generated for *Xenopus* transgenesis (Pan et al., 2006).

**Sce-Slug vector** was generated from the BS I-Sce-II KS by the insertion of the minimal slug promoter (Vallin et al., 2001) via SpeI and BamHI restriction sites.

The **pCMV-Sport6** vector was designed for cell culture experiments. **pGEM-T** (Promega) is a cloning vector.

### **2.5.2 Constructs**

In the present work the following constructs were used for DNA injection into *Xenopus* embryos, cell transfection, preparation of mRNA for microinjections and generation of antisense RNA for whole mount *in situ* hybridization (Table 2.1).

**Table 2.1. DNA constructs**

<b>Construct Name</b>	<b>Insert</b>	<b>Accession number</b>	<b>Vector</b>	<b>Cloning strategy/Reference</b>
Dsh-GFP	Dishevelled ( <i>X.laevis</i> ) GFP	U31552	pCS2+	(Yang-Snyder et al., 1996)
Dsh-myc	Dishevelled ( <i>X.laevis</i> )	U31552	pCS2+ MT	(Sokol, 1996)
Dsh $\Delta$ DEP-GFP	Dishevelled ( <i>X.laevis</i> ), lacking the DEP domain, GFP	U31552	pCS2+	(Miller et al., 1999)
Dsh $\Delta$ DIX-GFP	Dishevelled ( <i>X.laevis</i> ), lacking the DIX domain, GFP	U31552	pCS2+	(Miller et al., 1999)
Dsh $\Delta$ PDZ-GFP	Dishevelled ( <i>X.laevis</i> ) lacking the PDZ domain, GFP	U31552	pCS2+	(Miller et al., 1999)
Frizzled 7	Frizzled 7 ( <i>X.laevis</i> )	AJ243323	pCS2+	(Medina et al., 2000)
Frizzled7-myc	Frizzled 7 ( <i>X.laevis</i> )	AJ243323	pCS2+ MT	(Winklbauer et al., 2001)
hRACK1	Receptor of activated PKC-1 (RACK1), human	BC032006	pCMV Sport6	Obtained from Open Biosystems: catalogue number IRAT40C14750184, SO#95799
hRACK1-HA	Receptor of activated PKC-1 (RACK1), human	BC032006	pCS2+ HA	Cloned by Ilona Wunderlich
mGFP	GFP with GAP43 myristilation signal, membrane associated		pCS2+	Provided by Dr. Alexandra Schambony
mRFP	RFP with K-ras myristylation signal, membrane associated		pCS2+	Provided by Ying Gog
PKC $\delta$ 1-	PKC $\delta$ 1	AB109739	pCS2	(Sivak et al., 2005)



GFP	( <i>X.laevis</i> ) GFP			
PTK7	PTK7 ( <i>X.laevis</i> ), MGC68806	AAH60500	pCMV- Sport6	Obtained from RZPD: catalogue number IMAGp998I099552
PTK7 $\Delta$ E- myc	PTK7 ( <i>X.laevis</i> ), lacking the extracellular part	AAH60500	pCS2+ MT	Cloned by Ilona Wunderlich
PTK7 $\Delta$ K- GFP	PTK7 ( <i>X.laevis</i> ), lacking the kinase homology domain, GFP	AAH60500	pCS2+	Cloned by Hanna Peradziryi
PTK7 $\Delta$ K- myc	PTK7 ( <i>X.laevis</i> ), lacking the kinase homology domain	AAH60500	pCS2+ MT	Amplified from PTK7-MT construct, excluding the kinase homology domain, with the following primers: 5'- CTTGTCGCCAGAGCTGTGTC-3' (Tm 56°C) and 5'-TCTTCTGGCAGCAAG ACACAAG-3' (Tm 55°C). Following the PCR reaction the original DNA template was destroyed by DpnI treatment, the construct was ligated and transformed into <i>E.coli</i>
PTK7- GFP	PTK7 ( <i>X.laevis</i> ), GFP	AAH60500	pCS2+	Cloned by Hanna Peradziryi
PTK7-HA	PTK7 ( <i>X.laevis</i> ), HA-tag	AAH60500	pCS2+	Was generated from PTK7-MT. The myc tag was excised by the digestion with ClaI and XbaI and the HA-tag, which was generated by the annealing of the primers: 5'-CGATATCCCTACGATG TTCCAGATTATGCATGATAA and 5'- CTAGTTGCGTAATCCGGTACATCG TAAGGGTAGT, was inserted instead. Prior to the insertion the primers were <i>in vitro</i> phosphorylated by PNK (Fermentas).
PTK7-myc	PTK7 ( <i>X.laevis</i> )	AAH60500	pCS2+	Cloned by Ilona Wunderlich
Slug	<i>Xenopus</i> zinc finger transcription factor Slug- $\alpha$	AF368041		(Mayor et al., 1995)
Slug-Dsh- GFP	Disheveled, GFP	U31552	BSI-Sce- II KS	Generated by restriction-based blunt- ended cloning of dsh-GFP (pCS2+) into the BSI-Sce-II KS vector. Dsh-GFP was excised from pCS2+ via HindIII and XhoI sites, blunted and inserted into

				blunted BSI-Sce-II KS, linearized with BamHI
Slug-Dsh $\Delta$ DEP-GFP	Dishevelled, lacking the DEP domain, GFP	U31552	BSI-Sce-II KS	Generated by restriction-based blunt-ended cloning of dsh $\Delta$ DEP-GFP (pCS2+) into the BSI-Sce-II KS vector.
Slug-Dsh $\Delta$ DIX-GFP	Dishevelled, lacking the DIX domain, GFP	U31552	BSI-Sce-II KS	Generated by restriction-based blunt-ended cloning of dsh $\Delta$ DIX-GFP (pCS2+) into the BSI-Sce-II KS vector.
Slug-Dsh $\Delta$ PDZ-GFP	Dishevelled, lacking the PDZ domain, GFP	U31552	BSI-Sce-II KS	Generated by restriction-based blunt-ended cloning of dsh $\Delta$ PDZ-GFP (pCS2+) into the BSI-Sce-II KS vector.
Slug-GFP	GFP with minimal Slug-promoter		BSI-Sce-II KS	Cloned by Ilona Wunderlich from the published slug promoter construct (Vallin et al., 2001)
Slug-PTK7	PTK7	AAH60500		Cloned by Ilona Wunderlich
Slug-PTK7 $\Delta$ k	PTK7, lacking the cytoplasmic tail	AAH60500		Cloned by Ilona Wunderlich
Sox10	Sox10 ( <i>X. laevis</i> )	AY149116	pCS2+	(Aoki et al., 2003)
xRACK1	Receptor of activated PKC 1 (RACK) ( <i>X. laevis</i> )	BC041541	pCS105	obtained from the NIBB/ XDB3 <a href="http://xenopus.nibb.ac.jp">http://xenopus.nibb.ac.jp</a> clone XL422i22ex
xRACK1-HA	Receptor of activated PKC 1 (RACK) ( <i>X. laevis</i> )	BC041541	pCS2+ HA	Generated by PCR cloning with the following primers: forward 5'-GAA TTCATGACTGAGCAAATGACACTT CAG (with EcoRI restriction site); reverse 3'-CTCGAGACGAGTGCCA ATAGTGACCTG (with XhoI restriction site), inserted into pCS2+ HA vector via EcoRI and XhoI restriction sites
xTwist	Twist, ( <i>X. laevis</i> )	BC123238	pGEM-T	(Hopwood et al., 1989)

In order to generate sense RNA for microinjections as well as antisense labeled RNA probes for whole mount *in situ* hybridization the constructs were linearized and *in vitro* transcription was performed. The enzymes, used for the linearization as well as the polymerases used for *in vitro* transcription are listed in Table 2.2.

**Table 2.2 Linearization and in vitro transcription of the DNA constructs**

Construct Name	<i>In vitro</i> Transcription		
	Lin.Enzyme	Pol.	direction
Dsh-GFP	NotI	SP6	sense
Dsh-myc	NotI	SP6	sense
Dsh $\Delta$ DEP-GFP	NotI	SP6	sense
Dsh $\Delta$ DIX-GFP	NotI	SP6	sense
Dsh $\Delta$ PDZ-GFP	NotI	SP6	sense
Frizzled 7	NotI	SP6	sense
Frizzled7-myc	NotI	SP6	sense
hRACK1	NotI	SP6	sense
hRACK1-HA	NotI	SP6	sense
mGFP	NotI	SP6	sense
mRFP	NotI	SP6	sense
PKC $\delta$ 1-GFP	NotI	SP6	sense
PTK7	SexAI	T7	antisense
	EcoRV	T7	antisense
PTK7 $\Delta$ E-myc	NotI	SP6	sense
PTK7 $\Delta$ K-GFP	NotI	SP6	sense
PTK7 $\Delta$ K-myc	NotI	SP6	sense
PTK7-GFP	NotI	SP6	sense
PTK7-HA	NotI	SP6	sense
PTK7-myc	NotI	SP6	sense
Slug	ClaI	SP6	antisense
Sox10	ClaI	T7	antisense
	NotI	SP6	sense
xRACK1	NotI	SP6	sense
xRACK1-HA	NotI	SP6	sense
xTwist	EcoRI	T7	antisense

## 2.6 Oligonucleotides

The oligonucleotides used in the following work include DNA primers for cloning, RT-PCR detection and sequencing, as well as morpholino blocking oligonucleotides. The DNA oligonucleotides were ordered in the lyophilized form from Sigma Aldrich and subsequently diluted till 100 $\mu$ M with HPLC-pure water (Roth). The morpholino blocking oligos (MO) were produced by Gene Tools. Upon arrival the oligos were diluted to a final concentration of 8g/10nl and stored at -80°C. The MO were dissolved and heated up at 65°C for 5 min prior to the use. The RT-PCR primer are listed in the Table 2.3, sequencing primers – in the Table 2.4, morpholino oligonucleotides – in the Table 2.5, while cloning primers are indicated in the Table 2.1 together with the corresponding constructs.

**Table 2.3 RT-PCR primers**

Gene name ( <i>X.laevis</i> )	Forward primer 5'→3'	Tm °C	Reverse primer 5'→3'	Tm °C
Frizzled 4	AGATCGCTGACCTTGTT GTAC	53	CTTCACAGAAGGCACATCC	53
Frizzled 7	ATGTCCTCTACAGTCTCG CTG	52	AAGCCGAACTTGTTTCATGAG	52
Frizzled 8	AACTGTCCTGCCAAGAG ATC	50	GTAGTAGTCCATACACAGGGT GTC	50
ODC	GCCATTGTGAAGACTCT CTCCATTC	48	TTCGGGTGATTCCTTGCCAC	48
PKC $\delta$ 1	ACATCCTCACATCAGCC TAAG	61	ATGACCATCTCTGTCCAACA	61
PTK7	CCTGGTCAGCTTCAAGA TAG	50	ATGTAGTGTGGTTCTGCCTC	50
RACK1	CGTCACACAAATAGCAA CTACC	60	CGCAGGATACAATGATAGGA	60

**Table 2.4 Sequencing primers**

<b>Construct/vector</b>	<b>Primer name</b>	<b>Sequencing primer 5'→3'</b>
BS I-Sce-II KS	<b>T7</b>	TAATACGACTCACTATAGGG
	<b>T3</b>	AATTAACCCTCACTAAAGGG
Dishevelled	<b>D1</b>	AAAGTGATGTACCATCTGGAT
	<b>D2</b>	AGCAGGTTTCAGCAGTTCC
	<b>D3</b>	CCTCCGGTGTCACTCTTC
	<b>D4</b>	TCCGGAGTAGCGGGAGTG
GFP	<b>GFPPr</b>	CAACGAGAAGCGCGATCACATG
pCMV-Sport6	<b>SP6</b>	TTAGGTGACACTATAGAATAC
	<b>T7</b>	TAATACGACTCACTATAGGG
pCS2+	<b>SP6</b>	TTAGGTGACACTATAGAATAC
	<b>T7p</b>	TCTACGTAATACGACTCACTATAG
	<b>T3</b>	AATTAACCCTCACTAAAGGG
pGEM-T	<b>T7gemtF</b>	TCTACGTAATACGACTCACTATAG
	<b>T7gemtR</b>	GCTAGTTATTGCTCAGCGG
PTK7	<b>AB0</b>	AGAACTAGGAGTCGATGC
	<b>AB1</b>	TTCAGAGATGGGACGCCGTTA
	<b>AB2</b>	TGGAGGTGGTATTCAAACCC
	<b>AB3</b>	AGGGATGCTGGGAACTACAC
	<b>AB4</b>	CCATTGTTCTCTCTGTGGTTG
	<b>AB5</b>	GCATCTGGCTAACAGTCG
	<b>AB7</b>	TCCTATTGCCCTTAGTAGTGC
Sce-Slug	<b>SlugFw</b>	CCCAAGGAAGAAAGCTCAG
	<b>T3</b>	AATTAACCCTCACTAAAGGG

**Table 2.5 Morpholino blocking oligonucleotides**

<b>Gene name</b>	<b>Morpholino sequence 5'→3'</b>	<b>Working concentrations</b>	<b>Comments/References</b>
Frizzled 7a MO	GCGGAGTGAGCAGAAATCGGCTGA	20-40ng/10nl	(Abu-Elmagd et al., 2006)
Frizzled 7b MO	CCAACAAGTGATCTCTGGACAG CAG	20-40ng/10nl	(Winklbauer et al., 2001)
PKCδ1 MO	TTCCTGCCCCGGATCCTCTCACTGC	20ng/10nl	(Kinoshita et al., 2003)
PTK7 MO2 MO3	TGCATCGCGGCCTCTCCCCTCA TTCCTGCCCCGGATCCTCTCACTGC	10-20ng/10nl	Both morpholinos bind within 5'-UTR. The higher knockdown efficiency in reached by the combination of MOs
PTK7 5MM2 5MM3	TGgATCcCGcCCTCTgCCgTCA TTgCTcCCCCGcATCCTgTCAgTGC	10-20ng/10nl	5 base pair mismatch morpholinos, which correspond to PTK7 MO2 and 3, used as a control to PTK7MO
RACK1 MO1 MO2	CCCGAAGTGTCATTTGCTCAGTCAT CTGAAACCGCTCCACCGACTAAGGA	10-20ng/10nl	MO1 targets CDS, starting from the translation start (ATG); MO2 targets 5'-UTR
Standard MO	CCTCTTACCTCAGTTACAATTTATA	10-40ng/10nl	

## 2.7 Antibodies

The antibodies used in the following work, as well as their working concentrations are summarized in the Table 2.6.

**Table 2.6 Antibodies and their working dilutions**

Name	Produced in	purpose	dilution	Company/cat. number
$\alpha$ -actin	mouse	WB	1:10000	Millipore,C4
$\alpha$ -GFP	mouse	WB	1:2000	Roche, 11814460001
$\alpha$ -GFP	rabbit	IF	1:1000	Abcam, AB290
$\alpha$ -goat-HRP	donkey	WB	1:5000	Santa Cruz, SC-2020
$\alpha$ -HA	mouse	IF IP WB	1:150 1:150 1:1000	Covance, MMS-101P
$\alpha$ -mouse-Alexa 488	goat	IF	1:200	Invitrogen, A11029
$\alpha$ -mouse-Alexa 596	goat	IF	1:200	Invitrogen,
$\alpha$ -mouse-Cy5	goat	IF	1:200	Abcam, AB6563
$\alpha$ -mouse-HRP	goat	WB	1:10000	Santa Cruz Biotechnology, sc-2005
$\alpha$ -myc	mouse	IF IP WB	1:500 1:500 1:5000	Sigma, 9E10
$\alpha$ -myc	goat	WB	1:3000	Abcam, ab19234
$\alpha$ -myc-Cy3		IF	1:150	Sigma, C6594
$\alpha$ -pJNK	mouse	IF WB	1:25 1:1000	Santa Cruz Biotechnology, G-7
$\alpha$ -rabbit-HRP	goat	WB	1:10000	Dianova
$\alpha$ -rabbit-FITC	goat	IF	1:200	Sigma, F7367
$\alpha$ -S6	mouse	WB	1:3000	Ref. Patrick K. Arthur
$\alpha$ - $\beta$ 1Integrin	mouse	IF	1:100	DSHB, 1C8

## 2.8 Laboratory equipment and software

### Microinjection

Microinjector 5242, Eppendorf; Needle puller, Leitz

**Equipment for the work with DNA/Protein**

Cooling centrifuge: Biofuge Fresco, Heraeus

Documentation of agarose gels: Chemi Doc, BioRad, supplied with SONY Video Graphic Printer, UP-895CE

Electrophoresis/Western Blotting chamber: Mini Protean Tetra Cell with Power Pac Basic Power Supply, BioRad

Mass spectrometry: linear ion trap mass spectrometer 4000 Qtrap; Applied Biosystems' coupled to an Agilent 1100 nanochromatography system

Nanodrop: ND-1000 Spectrophotometer, Coleman Technologies Inc.

PCR-machines: UNOII Thermo block, Biometra, Gottingen; TRIO Thermo block, Biometra, Gottingen

Sequencing machine: ABI 3100 Automated Capillary DNA Sequencer, ABI-Prism

Spectrophotometer: Ultrospec 1100 pro, Amersham

Table centrifuge: Eppendorf centrifuge 5415D

Ultracentrifuge: Optima™ Ultracentrifuge, Optima

Water Bath: GFL 1092, GFL

X-ray films: SuperRX, Fuji Medical X-ray film, 100NIF 18x14, Fujifilm; High performance chemiluminiscent film, Hyperfilm<sup>R</sup>, Amersham

**Optics**

Fluorescent microscope: Imager M1, UV-lamp: HXP120, Carl Zeiss, MicroImaging

Fluorescent microscope: Lumar V12 SteReo, UV-lamp: HBO100, Carl Zeiss, MicroImaging

Fluorescent microscope: SZX12, UV-lamp: U-RFL-T, Olympus

Laser scanning confocal microscope: LSM510 META, Carl Zeiss, MicroImaging

Stereo Microscope: Steni 2000, Zeiss

**Histology**

Vibratome, Type 1000, Pelco International;

**Software:**

Microsoft office 2003-2007

Vector NTI (Invitrogen)

SeqMan (DNASTAR Inc., Madison, USA)

BLAST online system (Altschul et al., 1990)

Adobe Photoshop 7 (Adobe systems Europe Ltd., Edinburgh, Scotland).

AxioVision ver.4.7.2, Zeiss

NanoDrop 3.01.1 Coleman Technologies Inc.



### **3. Methods**

#### **3.1 DNA methods**

##### **3.1.1 Plasmid DNA preparations**

Isolation of plasmid DNA in analytical amounts was performed using Illustra™ Plasmid Prep Mini Spin Kit, GE Healthcare, while for the isolation of plasmid DNA in preparative amount Illustra™ Plasmid Prep Midi Flow Kit, GE Healthcare, was employed. The DNA isolation was carried out according to the manufacturer's instruction with an exception of the final elution, where HPLC-pure water was used.

##### **3.1.2 DNA concentration measurement**

DNA quantification was performed by measurement of the absorption values at 260 nm ( $OD_{260}$ ) using the NanoDrop. The DNA concentration in a given sample was calculated according to the following ratio:  $OD_{260} = 1$  corresponds to 50  $\mu\text{g}$  of dsDNA. In addition the purity of the DNA sample was estimated by  $OD_{260}/OD_{280}$  for protein contamination (optimal values: 1.6-1.8) and  $OD_{260}/OD_{230}$  for salt contamination (optimal values: higher than 2, 0).

##### **3.1.3 Agarose-gel electrophoresis**

DNA or RNA fragments were size-separated in a horizontal electrical field being embedded into agarose-matrix. Depending on the expected sizes of DNA/RNA fragments, 0.7 to 2 % (w/v) agarose gels were prepared in TAE buffer. Gels always contained 0.5  $\mu\text{g}/\text{ml}$  ethidium bromine to visualize nucleic acids. Before loading samples into gel slots, nucleic acids were mixed with 5/1 (v/v) of DNA loading dye (6x, Ambion). The electrophoresis was run in the standard TAE-running buffer at 100-121 V in a house made horizontal electrophoresis chamber (Sharp et al., 1973). After the electrophoresis, DNA bands were visualized with UV-transilluminator (Herolab) and documented with ChemiDoc video documentation system (EASY view). The DNA fragments were sized according to the standard DNA ladder run in parallel (High, Middle or Low Range, Fermentas)

##### **3.1.4 DNA restriction digest**

For the analytical or preparative digest of plasmid DNA, 0.5-1  $\mu\text{g}$  of the DNA sample was incubated with 2-10 U of a chosen enzyme in the corresponding buffer. The total reaction volume was varied from 10 to 50  $\mu\text{l}$ , and the digest was performed for 1-12 h at 37°C

##### **3.1.5 Purification of the DNA fragments from agarose gel or restriction digest mixture**

The isolation of the DNA fragments from agarose gels was performed with the use of Zymoclean Gel Band DNA Recovery Kit (Zymogen) according to the manufacture's instruction.

DNA from restriction digest mixture was purified with the Zymoclean Gel Band DNA Recovery Kit (Zymogen) according to the manufacture's instruction, with an exception, that initial agarose

dilution step was substituted with addition of 3 volumes of MDB buffer to 1 volume of DNA mixture.

### **3.1.6 Polymerase chain reaction (PCR)**

To amplify desired DNA fragments, a standard PCR reaction was used, which contains the following components: 1x PCR buffer, supplemented with 2mM MgCl<sub>2</sub>/MgSO<sub>4</sub> (corresponding to the polymerase used); 0.2 mM each dNTPs; 0.2 mM each primer; 1-100 ng DNA template; 0.5-1 U DreamTaq or 2 U Pfu polymerase or 2U High Fidelity;

The initial DNA denaturation step was performed for 2min at 95 °C, and all subsequent DNA denaturation steps - at 94°C, annealing temperatures were calculated with a help of VectorNTI for each given pair of primers. The elongation steps of the fragments less than 1000bp were done with the DreamTaq at 72°C, while the fragments more than 1000bp were amplified with either the High Fidelity or Pfu Polymerase with the elongation carried at 68°C (Mullis et al., 1986).

### **3.1.7 DNA-sequencing and sequence analysis**

To carry out the sequence analysis of the selected constructs the ABI 3100 Automated Capillary DNA Sequencer was used (Sanger et al., 1977).

The protocol for sequencing with the Big Dye Terminator Kit (Applied Biosystems) is given below. The Reaction Mix contains 200ng plasmid DNA, 1 µl sequencing primer (10µM), BigDyeSeq Buffer 2 µl, Ready Reaction Premix 1.5 µl. The reaction components were mixed in a thin-walled PCR tube, and the volume was adjusted till 10µl with HPLC-pure water (Roth). The sequencing PCR was performed under the following conditions: 96 °C 2 min; 26X (96 °C 30 sec, 50 °C 20 sec, 60 °C 4 min); 12 °C. Following the PCR the labeled DNA fragments were purified according to the following protocol: 10µl of PCR reaction were mixed with 1 µl of 3 M sodium acetate (pH 5), 1 µl of 125 mM EDTA and 50 µl of 100% ethanol. The sample was incubated in 1.5 ml Eppendorf tube at room temp for 5 min and subsequently centrifuged at room temperature for 20 min at maximal speed. The supernatant was discarded and the pellet was washed with 200 µl of 70% ethanol. Thereafter the pellet was dried and diluted in 15µl of HiDi mix.

Sequence reactions were run and documented in the in-house sequencing lab (A. Nolte). The analysis of the received sequence computer files was done by Vector NTI (Invitrogen) software.

### **3.1.8 Molecular cloning**

#### **3.1.8.1 PCR-based cloning**

During the PCR based cloning a fragment was amplified from either cDNA or another template. The obtained product was separated by horizontal agarose gel electrophoresis and band of the correspondent size were excised from the gel and purified. If the further cloning procedure included the insertion of the fragment via restriction sites, then the same sites were inserted into

the PCR primers. After the purification, both an insert and a vector were digested with correspondent restriction enzymes, gel-purified and ligated (see below). When blunt-end cloning was performed, the purified fragment was subjected to the ligation directly after PCR.

#### **3.1.8.2 Restriction-based cloning**

Restriction-based cloning includes the excision of the given gene from one and insertion into a different vector with the help of restriction endonucleases. The restriction digest was set up, as described above and the obtained fragment was gel-purified and ligated into the correspondent vector. When the restriction sites of the insert did not coincide with the restriction sites of the vector, a blunt-ended cloning was applied. For this purpose endonucleases were heat-inactivated for 10 min at 65°C and then 0.5U of the Klenow Fragment (Fermentas) together with 1mM dNTP are added to the mixture and the reaction is carried out for 10 min at room temperature to create “blunt”-ends. The blunt ended construct was purified via agarose gel and ligated into the correspondent vector.

#### **3.1.8.3. Ligation into an expression vector**

The purified DNA fragments were subjected to ligation according to the following scheme:

T4-Ligase (Fermentas) 1 U, 1x Ligation buffer (Fermentas), insert and vector in 5 to 1 ratio (w/w) for the “sticky-end” and 8 to 1 ratio for the “blunt-end” ligation, HPLC-pure water till the final volume of 10 or 20 µl. As a rule, 25 to 50 ng of vector DNA was used per one ligation reaction (Sambrook J., 1989). The ligation was performed for 2h at 22°C or for 12h at 16°C. The ligated constructs were transfected into the bacteria either by chemical transformation or electroporation.

#### **3.1.8.4 Chemical transformation**

100 µl of house-made chemically competent cells were thawed on ice, mixed with 1-2 µl of the ligation mix, incubated for 20 min on ice, heat-shocked for 90 sec at 42°C, then left for 2 min on ice, followed by the incubation at 37°C for 50 min with 700 µl of LB-medium. Finally, the cells were placed on LB-agar plates with the appropriate selectivity antibiotic. Colonies were grown overnight at 37°C (Mandel and Higa, 1970).

#### **3.1.8.5 Transformation by electroporation**

40 µl of electrocompetent cells were thawed on ice, mixed with 1-2 µl of the ligation mix, transferred into an electroporation cuvette and incubated for 1 min on ice. After application of an electrical pulse of 1.8 kV and 25 µF, the transformation reaction was mixed by pipeting with 0.5 ml of LB-medium, preincubated for 30 min and then plated on LB-agar-plates with the appropriate selectivity antibiotic. Colonies were grown ON at 37°C (Dower et al., 1988).

### 3.1.8.6 Verification of the a DNA fragment integration

To verify the integration of the insert DNA fragment into a vector of interest a PCR with the colony material as a template was used (colony-PCR). The colony-PCR was carried out under the conditions indicated above, with an exception, that 0.1-0.2µl of the bacterial colony were used instead of the NA template. For the detection primers either the vector specific, or inserted specific or the combination of the insert and vector specific primers were used.

### 3.2 RNA methods

In order to avoid the RNA degradation by RNAses, the work with RNA samples was performed exclusively with RNase-free water (Ambion or HPLC-pure).

#### 3.2.1 Total RNA isolation

One *Xenopus laevis* embryo or 20 animal caps were collected and homogenized in 200µl or 100µl of caps lysis buffer, supplemented with Proteinase K (20µl Proteinase K for 1 ml of the buffer) respectively. The homogenate was incubated at 42°C for 30min. Subsequently, 200µl (100µl for animal caps) Phenol/Chloroform/isoamylalcohol were added, and the mixture was vortexed and centrifuged for 3min (16000g). The aqueous top layer, which contains nucleic acids, was transferred to new tube containing: 20µl (10µl for animal caps) 3M sodium acetate, pH5.2; 2µl (1µl for animal caps) Glycogen (20µg/µl); 500µl (250µl for animal caps) ethanol. Nucleic acids were precipitated by centrifugation for 15 min at 16000g, and the pellet was washed with 70% ethanol, dried and resuspended in 15µl H<sub>2</sub>O. To digest genomic DNA 10µl DNase solution, containing 2.5µl 10x DNase buffer, 0.4µl DNase, 1.25µl 20mM DTT, 0.5µl RNaseOut, 5,4µl water, was added and incubated at 37°C for 30 min. Subsequently, 75µl H<sub>2</sub>O and 100µl Phenol/Chlorophorm were added, vortexed and centrifuged at 16000g for 3 min to extract RNA. The aqueous phase was transferred into new tube and mixed with 10µl 3M sodium acetate and 250µl ethanol. RNA was precipitated by centrifugation at 16000g for 15 min, the supernatant was carefully discarded and the pellet was washed with 70% ethanol, dried and resuspended it in 20µl water (10µl for animal caps).

#### 3.2.2 Reverse transcription and RT-PCR

20µl RNA (10µl for animal caps) was mixed with 2µl of random hexamers (1µl for animal caps), incubated at 65°C for 4 min. and cooled on ice. In parallel, an RT-Mix, containing 4µl 5x Colorless Dream(Go)Taq buffer, 1µl 20mM DTT, 0.5µl RNaseOut, 1µl 10 mM dNTP, 1,5µl water and 1µl MuLV RT (added after the –RT is pipetted), was prepared. 11µl of RNA with hexameres was pipeted in a tube labeled “-RT” and supplemented with 8µl RT-Mix and 1µl of water. Subsequently 1µl MuLV per reaction was added to the remaining RT-Mix and 9µl of the RT-Mix was mixed with 11µl of the sample. The mixture was incubated at 42°C for 30min to

synthesize the cDNA. The PCR reaction was set up according to the standard protocol (described above) in the volume of 25µl, with 1µl of the prepared cDNA per reaction.

### **3.2.3 *In vitro* transcription**

#### **3.2.3.1. *In vitro* transcription of the digoxigenin-labelled antisense RNA for the whole mount in situ hybridization (WISH)**

For the synthesis of a digoxigenin-labelled antisense WISH RNA probe the following reaction mixture was set up:

- 5 µl of a 5x transcription buffer
- 1 µl each 10 mM rATP, rCTP, rGTP 0.64 µl 10 mM rUTP
- 0.36 µl digoxigenin-rUTP (Boehringer)
- 1 µl 0.75 M DTT
- 0.5 µl RNaseOut,
- 200 ng linearized plasmid (the DNA template)
- 1 µl corresponding polymerase (T3, T7 or Sp6)
- RNase-free water to the final volume of 25 µl

The reaction was carried out for 2h at 37°C, and then the DNA template was destroyed by incubation with 1µl of the DNase for 15min at 37°C. The obtained WISH probe was purified from the reaction mixture with RNeasy Mini Kit (Quiagen) according to manufacturer's instructions.

#### **3.2.3.2. *In vitro* transcription of the capped-mRNA for microinjections**

The synthesis of mRNA for microinjections was done with Sp6, T7 or T3 mMACHINE Kits (Ambion) according to manufacturer's instructions. The reaction was set up in a volume of 20µl and 0.5-1µg of the linear DNA was used for 1 reaction. The *in vitro* transcription was carried out for 2h at 37°C, and subsequently the template was destroyed by 15 min DNase treatment. The mRNA was purified with RNeasy Mini Kit (Qiagene).

### **3.2.4 RNA analysis and concentration measurement**

The RNA samples, both DIG-labelled and capped-mRNA, were analyzed on the 1% agarose gel supplemented with 0.5% ethidium bromide.

The concentration of the total RNA and capped-mRNA was measured on the NanoDrop, by using the following ratio: OD<sub>260</sub>=1 corresponds to 40µg of the RNA. Similar to DNA, the RNA purity was analyzed by measurement of OD<sub>260</sub>/OD<sub>280</sub> and OD<sub>260</sub>/OD<sub>230</sub> ratios. At the same time, the amount of DIG-labeled RNA was estimated visually on an agarose gel.

### 3.3. Protein methods

#### 3.3.1 Protein electrophoresis under the denaturing conditions (SDS-PAGE)

The proteins of different sizes were separated and analyzed by SDS polyacrylamid gel electrophoresis (Laemmli, 1970). Gels of the different acrylamide percentages (%AA) were applied for analysis of the proteins, with distinct molecular weights, according to the Table 3.1

**Table 3.1. The correlation between protein sizes and percentage of the correspondent acrylamide gel**

Protein size, kDa	%AA
36-205	5%
24-205	7.5%
14-205	10%
14-66	12.5%
10-45	15%

The gels were poured as indicated in Table 3.2 and 3.3

**Table 3.2 Separating gel**

For 10 ml	5%	7.5%	10%	12.5%	15%
AA 30%	1.67ml	2.5 ml	3.33ml	4.16 ml	5ml
H <sub>2</sub> O	4.38ml	3.55 ml	2.72ml	1.89 ml	1.05ml
	Final concentration	Stock		For 10 ml	
Tris-HCl pH 8.8	375 mM	1M		3.75ml	
SDS	0.1%	10%		100µl	
TEMED	0.08%	100%		8µl	
Ammonium persulfate	0.1%	10%		100µl	

**Table 3.3 Stacking gel**

Substance	Final concentration	Stock	For 5 ml
H <sub>2</sub> O			3.4 ml
AA	5%	30%	0.83 ml
Tris-HCl pH6.8	130 mM	1M	0.63 ml
SDS	0.1%	10%	50µl
TEMED	0.1%	100%	5µl
Ammonium persulfate	0.1%	10%	50µl

The protein samples were diluted 1:3 with 4x Laemmli loading buffer, boiled for 5 min at 95°C and applied on the gel. The gel run was performed in the BioRad gel chambers in 1X Laemmli running buffer. At the level of the concentrating gels the voltage of 50V was applied, and once the bromphenol-blue front reaches the separating gel, the voltage was changed to 150V.

### 3.3.2 Western blotting

Proteins were separated by SDS-PAGE of the appropriate percentage (Laemmli, 1970) and transferred to a nitrocellulose membrane (0.45 µm, Schleicher & Schuell) in the BioRad Transfer chamber using the wet blotting method (Sambrook J., 1989). The wet blotting was carried out in ice-cold WB buffer for 60.70 min at 100-110V.

After the transfer, the membrane was blocked with a PBS solution supplied with 3% NDM, 0.1% Tween 20. Subsequently incubation with an appropriate primary antibody was carried out overnight at 4°C in the same solution. Next morning the membrane was washed 3 times for 5-7 min each with PBS/0.1% Tween 20 and the secondary antibodies were applied for 1-2 h at the room temperature. Then, the membrane was washed again with PBS/0.1% Tween 20 3 times for 10 min and the correspondent proteins were detected with the help of ECL Kit Super Signal Dura West Kit (Pierce) and X-ray detection film (Amersham).

### 3.3.3 *In vitro* transcription-translation assay

To investigate protein-protein interaction studies as well as the effects of morpholino blocking oligonucleotides, selected constructs were expressed *in vitro* via TNT® Coupled Reticulocyte Lysate System (Promega) according to the manufacturer's user manual (12.5-25 µl reactions). The proteins were subsequently separated by a standard 12% SDS-PAGE and analyzed by western blotting or autoradiography on the phosphoimager (Amersham Biosciences).

### 3.3.4 Co-Immunoprecipitation

Protein-protein interactions were analyzed by co-immunoprecipitation (Co-IP), performed either in *Xenopus* lysates or after the *in vitro* translation (TNT).

The Co-IP from the *Xenopus* lysates was performed as follows:

50 embryos were homogenized with a pipet tip and, subsequently, with a syringe in 500µl of NOP-buffer, supplemented with protease inhibitors (Roche), 1mM NaF and 1mM β-glycerolphosphate. The homogenate was centrifuged at 16000g for 20 min in a cooling centrifuge and the supernatant (Co-IP SN) without yolk was taken to perform an immunoprecipitation. All further C-IP steps were done at 4°C. The supernatant was incubated for 1.5 h with the relevant antibody and subsequently 1h with 20µl protein A sepharose beads (Amersham). Alternatively, 10-15µl of the α-myc-coupled agarose beads can be used instead of antibody-protein-sepharose step. The beads were then precipitated by the low-speed

centrifugation (2000g), washed 4-6 times with NOP buffer, dissolved in 10µl Laemmli loading buffer and analyzed by SDS-PAGE.

The Co-IP from TNT lysate was performed according to the same protocol with an exception that Co-IP SN was obtained by direct dilution of 1 volume of the TNT reaction with 9 volumes of the NOP-buffer, supplemented with the protease inhibitors.

The amounts of the constructs used for the Co-IP were as follows:

Fz7-Dsh-PTK Co-IP from *Xenopus* lysates (amount of the RNA injected): Fz7-MT 100 pg, Dsh-MT 100 pg, PTK7-HA 500 pg; co-IP with  $\alpha$ -myc antibodies or  $\alpha$ -myc-coupled beads (Sigma).

PTK7-RACK1 Co-IP from *Xenopus* lysates (RNA injected):  $\Delta$ EPTK7-MT 500pg, RACK1-HA 300pg; Co-IP with  $\alpha$ -HA antibodies

PTK7-RACK1 Co-IP from TNT (DNA amount per reaction): PTK7-MT 1µg, RACK1-HA 1µg; Co-IP with  $\alpha$ -myc-coupled beads.

### 3.3.5 Investigation of the PTK7-dsh complex by glycerol gradient density centrifugation

For glycerol gradient density centrifugation 20 stage 10.5-11 *Xenopus* embryos, injected with 500 pg MT-PTK7 and 100pg MT-Dsh, were homogenized in 200 µl hypotonic lyses buffer, containing 5% glycerol, 50 mM Tris pH 8, 50 mM KCl, 0.1 mM EDTA and protease inhibitor cocktail (Roche) supplemented with 0.1 mM PMSF. The homogenate was centrifuged two times for 7 min and 200 µl of the supernatant was loaded on a 5-60% glycerol gradient established in a 2 ml tube. The samples were centrifuged in TLS 55 rotor (Beckmann) at a speed of 50,000 rpm (214,200 g) for 4 hours at 4°C and split into ten 200 µl fractions. The proteins were precipitated with 1 ml ice cold acetone overnight at -20°C and then centrifuged for 20 min at 13000 rpm at 4°C. The pellets were washed with 70% ethanol, dissolved in SDS-gel loading buffer (50 mM Tris pH 6.8, 100 mM DTT, 2% SDS, 10% Glycerol and 0,1% bromphenol blue) and analyzed using an SDS polyacrylamid gel.

### 3.3.6 Identification of PTK7-binding partners by tandem mass-spectrometry

500 pg myc-tagged full length *PTK7* RNA or 300 pg RNA coding for the kinase deletion mutant of PTK7 ( $\Delta kPTK7$ ) were injected into the animal pole of one-cell stage embryos. Uninjected embryos were used as a control. At stage 16, 50 embryos were lyzed in 500µl NOP buffer (20 mM Tris pH 7.5, 150 mM NaCl, 0.5% NP40, supplemented with protease inhibitors (Roche), 1 mM beta-glycerol phosphate and 1 mM NaF). All steps were performed at 4°C. Lysates were centrifuged 2 times for 10 min at 16000 g to remove yolk proteins. Supernatants were incubated with anti-myc antibodies (Sigma, 9E10, concentration 1:500) for 1,5 hours and subsequently with Protein A sepharose beads (Ammersham) for 1h. Sepharose beads were washed five times with NOP buffer, diluted with 15 µl 4x Laemmli buffer (Invitrogen) supplemented with DTT. For mass spectrometric analysis of PTK7-associated proteins, precipitated proteins were



separated by SDS-PAGE using a precast 10-15% gradient gel (Invitrogen) and stained with Coomassie Blue. Single lanes were cut into 23 pieces of similar size, and subjected to in-gel tryptic cleavage (Shevchenko et al., 1996). The extracted proteins were analyzed by HPLC-coupled ESI-MS/MS, carried out under standard conditions on a linear ion trap mass spectrometer (4000 Qtrap; Applied Biosystems) coupled to an Agilent 1100 nanochromatography system. Peptide fragment spectra were searched against the NCBI *Xenopus* data base using MASCOT as a search engine. After generation of the protein list, identified in the pull-down, the proteins found in the control lane were subtracted from the proteins found in PTK7-containing lane. Only the protein hits with a score above 20 were considered as real.

### **3.4 *Xenopus laevis* embryos injections and manipulations**

#### **3.4.1 Preparation of *Xenopus laevis* testis**

The testis was taken out from a narcotized decapitated male frog, washed with and stored in the 1x MBSH buffer at 4°C

#### **3.4.2 Embryo injections and culture**

Embryos were obtained from *Xenopus laevis* female frogs by HCG induced egg-laying (800 - 1000 U HCG approximately 12 hours before egg-laying). Spawns were *in vitro* fertilized with minced testis in 0.1 X MBS, dejellied with 1.5-2 % cysteine hydrochloride, pH 8.2 and cultured in 0.1 X MBS at 12.5-18°C. Albino embryos were stained with Nile Blue for 10 min prior to injections to distinguish better between animal and vegetal poles, as well as different stages of development. Injections were performed in the injection buffer on a cold plate (13.5°C). The mRNA and morpholino oligonucleotides were injected animally to the prospective ectodermal tissues. For the different purposes 1-, 2-, 4- or 8-cell injections were done. The injection volume varies from 5 to 10nl. Injected embryos were kept for at least 1 hour in the injection buffer at 18°C and then transferred into 0.1x MBSH. The staging of embryos was done according to Nieukoop and Faber (1956). In order to analyze how the neural crest migration is affected in the whole embryo, the embryos were injected animally into one blastomere at 2-cell stage together with 100 ng  $\beta$ -galactosidase or GFP as a lineage tracer. To observe the neural tube defects the embryos were injected animally at 1-cell stage or in the animally into the dorsal blastomere at 8-cell stage, with GFP as a lineage tracer

The following constructs and MO were used for the WISH analysis and NT defect observation:

#### **3.4.3 Animal cap assay**

For the investigation of intracellular localization of the selected proteins the animal cap assay was employed (Wallingford and Harland, 2001). The RNA encoding the tagged protein constructs or morpholino blocking oligonucleotides was injected animally at one-cell stage. The embryos were grown till stage 8-9 and ectodermal explants (animal caps) were prepared as

described by Wallingford and Harland (Wallingford and Harland, 2001) with the modification that caps were cultured in 0.8 x MBS. At stage 10.5-14 animal caps were fixed using MEMFA and processed for immunostaining.

#### **3.4.4 Cranial neural crest (CNC) explants**

The neural crest explants were done as described previously (Borchers, 2001). In brief, the embryos were grown till the neurula (stage 16-17). Then with a help of forceps the vitellin membrane as well as the epithelial tissue covering the area of the CNC were removed and with a help of an eyebrow-knife the neural crest cells were removed and placed on the fibronectin dish with a mesodermal side at the bottom in DFA medium. The neural crest migration was observed for the next 6h on the Imager M1 Zeiss microscope. Alternatively, the NC explants were fixed, immunostained (see below) and analyze by LSM confocal imaging. The fibronectin dishes were made as follows: frozen bovine fibronectin (Sigma) in the concentration of 1 mg/ml was thawed at 30°C and diluted till 10µg/ml with freshly made 1X PBS. The fibronectin solution was applied on the plastic Petry dishes (Falcon 35 1008) for 1-2h at 37°C. Finally, the fibronectin solution was replaced with DFA and the dishes can be used for the CNC explantation.

### **3.5. Immunostaining and Whole-mount in situ hybridization (WISH)**

#### **3.5.1 Immunostaining of the animal caps (AC)**

Upon the MEMFA fixation the AC were washed 3 times with PBS containing 0.1% Tween20 (PTw) and stained according to the following protocol:

Blocking with 10% fetal calf serum (FCS, Difco) in PTw – 1h at room temperature

Rinse with PTw – 1 time

Application of the primary antibodies ( $\alpha$ -GFP,  $\alpha$ -HA,  $\alpha$ -pJNK,  $\alpha$ - $\beta$ 1integrin), diluted in PTw – for 2-3h at room temperature or at 4°C overnight

Wash with PTw – 7 min, 3 times

Application of the secondary antibodies ( $\alpha$ -myc-Cy3,  $\alpha$ -rabbit-FIC,  $\alpha$ -mouse-Alexa488,  $\alpha$ -mouse-Cy5)

Wash with PTw – 7 min, 3 times

DAPI stain – optional: for the DAPI stain the AC should be rinsed with PBS and incubated in 1µg/ml DAPI PBS solution for 7-10 min, and washed 2 times with PBS.

Upon the immunostaining protein localization was analyzed by laser scanning microscopy on LSM 510Meta, Zeiss.

In addition, the immunostaining with  $\alpha$ -pJNK antibodies the PTw should be substituted by TBST (20mM Tris-HCl, pH 7.5, 150 mM NaCl, 0.1% Tween 20), and the incubation with the primary antibodies should be done in PTw with 10% FCS

### 3.5.2 Immunostaining of the gelatin-albumin sections

**Vibratome sectioning** (Holleman et al., 1999): embryos were embedded in gelatin-albumin (GA), which was polymerized by mixing 2 ml of GA with 125  $\mu$ l of 25% glutaraldehyde. 50  $\mu$ m vibratome sections were made using a Leica VT1000S Vibratome. Sectioned tissue samples were immunostained according to the same procedure as animal caps. GA and mowiol were made as follows: **Gelatin/albumin:** 4.88 mg/ml gelatin, 0.3 g/ml bovine serum albumin, 0.2 mg/ml sucrose in PBS. The gelatin was dissolved by heating the solution to 60°C. Albumin and sucrose were added, filtered with a 0.45  $\mu$ m filter (Satorius) and stored at -20°C. **Mowiol:** 5 g Mowiol was stirred overnight in 20 ml PBS. After addition of 10 ml glycerol, the solution was stirred again overnight. Not dissolved Mowiol was collected by centrifugation for 30 min at 20,000 g. The supernatant was pH adjusted to pH~7.0 (using pH stripes) and stored at -20°C.

### 3.5.3 Whole mount *in situ* hybridization (WISH)

To determine the expression pattern of the selected genes, whole mount *in situ* hybridization was employed. By this method the gene specific RNA can be visualized by the hybridization with the labeled antisense probe, which could be recognized by specific antibody, coupled with alkaline phosphatase.

In the cases, when a change of gene expression needs to be observed, the injected side was labeled with  $\beta$ -galactosidase and the X-gal staining was performed prior to the *in situ*.

#### **Embryo fixation and X-gal staining**

To be directly analyzed by WISH the embryos were fixed in 1x MEMFA solution for 1 h at room temperature and stored in 100% ethanol. In cases, when X-gal stain was required, the following protocol was used:

MEMFA fixation: 20 min at room temperature

Wash with PBS: 3x, 10 min

Application of the X-gal staining solution: 20-30 min at room temperature

Wash with PBS: 3x, 5 min

MEMFA fixation: 40 min at room temperature

Store embryos in 100% ethanol

#### **Rehydration of embryos**

Prior to *in situ* embryos were rehydrated, as it is described in the Table 3.4

**Table 3.4. Rehydration of embryos**

Solution	Incubation time
100% ethanol	5min
75% ethanol in water	5min
50% ethanol in water	5min
25% ethanol in PTw	5min
PTw	5min

**Proteinase K treatment**

To make embryos accessible for RNA probes, they were treated with proteinase K (10µg/ml) in PTw. And the proteinase K incubation time was chosen depending on the embryo stage (Table 3.5).

**Table 3.5 Proteinase K treatment**

Stage	Incubation time (min)	Temperature
9-10.5	6-8	RT
14-16	8-10	RT
20-25	15-18	RT
36	22-25	RT
40	17-20	37°C
42-43	27-30	37°C
46	32-35	37°C

**Acetylation and refixation**

Following the proteinase K treatment the embryos undergo acetylation (Table 3.6) and refixation.

**Table 3.6 Acetylation**

Buffer	Incubation time
1M Triethanol amine HCl (TEA), pH 7.0	2x 5min
1M TEA with 0.3% acetic anhydride	5 min
1M TEA with 0.6% acetic anhydride	5 min
PTw	5 min

Upon the acetylation, embryos were fixed for 20 min in 4% formaldehyde in PTW and washed 5 times with PTw subsequently after the fixation

### Hybridization

After the last washing step, 1ml PTw was left in the tubes and 250  $\mu$ l Hyb-Mix were added. The solution was replaced immediately by 500  $\mu$ l fresh Hyb-Mix and incubated for 10 minutes at 60°C. Hyb-Mix was exchanged again (1ml Hyb-Mix was added) and embryos were incubated 4-5h at 60°C. After incubation, the Hyb-Mix was replaced with the desired RNA probe, diluted in Hyb-Mix solution. The hybridization took place overnight at 60°C and mild shaking.

### Washing

To remove unspecific bound RNA probes, the samples were washed and digested with RNase A (10  $\mu$ g/ml) and RNase T1 (10 U/ml) (Table 3.7).

**Table 3.7 Washing and RNase treatment**

Solution	Incubation temperature (°C)	Incubation time (min)
Hyb Mix	60	10
2x SSC	60	3x 15
RNases solution in 2x SSC	37	60
2x SSC	RT	5
0.2x SSC	60	2x 30
MAB	RT	2x 15

### Antibody incubation

Prior to incubation with the Sheep AP-coupled anti-Dig antibody (sigma), embryos were incubated in blocking solution, containing MAB, BMB and horse serum to block unspecific binding sites according to the scheme, indicated in Table 3.8.

**Table 3.8 Blocking and antibody incubation**

Solution	Incubation temperature (°C)	Incubation time (min)
MAB/2%BMB	RT	10
MAB/2%BMB/20% serum	Horse RT	30
MAB/2%BMB/20% serum 1:5000 $\alpha$ -DIG antibodies	Horse RT	240
MAB	RT	3x 10
MAB	4	overnight

**Staining reaction and bleaching**

**Alkaline phosphatase**, coupled to antibodies, performs a reaction, in which its substrates BCIP (5-Bromo-4-chloro-3-indolyl phosphate) and NBT (Nitro blue tetrazolium chloride) were oxidized to a blue precipitate, gives a strong staining specifically in the regions, where the RNA probe is present. The staining reaction was performed as follows (Table 3.9).

**Table 3.9. Coloring reaction**

<b>Solution</b>	<b>Incubation time (min)</b>
MAB	5x 5 min
APB	3x 5min
APB with NBT/BCIP	Up to three days (until stained)

Upon the staining embryos were fixed in MEMFA, washed with PTw, documented and stored in 100% ethanol. Pigmented embryos undergo bleaching procedure (Table 3.10)

**Table 3.10. Bleaching of embryos**

<b>Solution</b>	<b>Incubation time (min)</b>
2xSSC	3x 5 min
2xSSC with 50% formamide, 1% H <sub>2</sub> O <sub>2</sub> , On the light	30min – until bleached, the solution should be replaced each 15 min
MEMFA	30 min
PTw	3x 5 min

## 4. Results

### 4.1 PTK7 functions in PCP signaling by recruiting dsh to the plasma membrane

PTK7 was identified as a regulator of planar cell polarity, necessary for proper neural tube closure and establishment of inner ear hair cell polarity. The genetic interaction with Vangl2 suggests that PTK7 is an integral part of the PCP signaling cascade (Lu et al., 2004). However, it is not clear how PTK7 intersects with PCP signaling. One possibility could be that PTK7 signals via dsh, a main PCP regulator, which similarly to PTK7 regulates neural convergent extension and inner ear hair cell polarity (Wallingford and Habas, 2005).

#### 4.1.1 PTK7 recruits dsh to the plasma membrane via its kinase homology domain

A prerequisite for the PTK7-dsh interaction is the co-localization of both proteins at the plasma membrane. To analyze whether this is the case, the *Xenopus* animal cap assay was employed. Animal caps are ectodermal explants of blastula stage *Xenopus* embryos that allow to analyze the intracellular localization of overexpressed tagged proteins. Previously, the animal cap assay was used to demonstrate the interaction and co-localization of dsh with fz7 at the plasma membrane (Medina and Steinbeisser, 2000). The animal cap assay shows, that GFP-tagged dsh is predominantly localized in the cytoplasm of animal cap cells (Fig. 4.1 A, G), but is translocated to the plasma membrane if myc-tagged fz7 is co-expressed (Fig. 4.1 C, G). To examine whether PTK7 translocates dsh to the plasma membrane, myc-tagged PTK7 was co-expressed with GFP-tagged dsh. Like fz7, PTK7 can recruit dsh-GFP from the cytoplasm to the membrane (Fig. 4.1 E, G). Interestingly, the deletion mutant of PTK7 (PTK7 $\Delta$ k), lacking the kinase homology domain, was not able to recruit dsh to the plasma membrane (Fig. 4.1F). To estimate the efficiency of the PTK7-dependend dsh membrane recruitment, the experiment was repeated several times (6 times for PTK7 and dsh and 4 times for PTK7 $\Delta$ k and dsh) and the number of cells, which demonstrate PTK7-dsh co-localization at the plasma membrane, was estimated (Fig. 4.1 G). Frizzled 7 recruits dsh to the membrane in 94% of cells, PTK7 co-localizes with dsh on the plasma membrane in 70% of cells, while the membrane recruitment of dsh by PTK7 $\Delta$ k is observed only in 6% of the animal cap cells. Thus, PTK7 can recruit dsh to the plasma membrane and requires the kinase homology domain for this function.

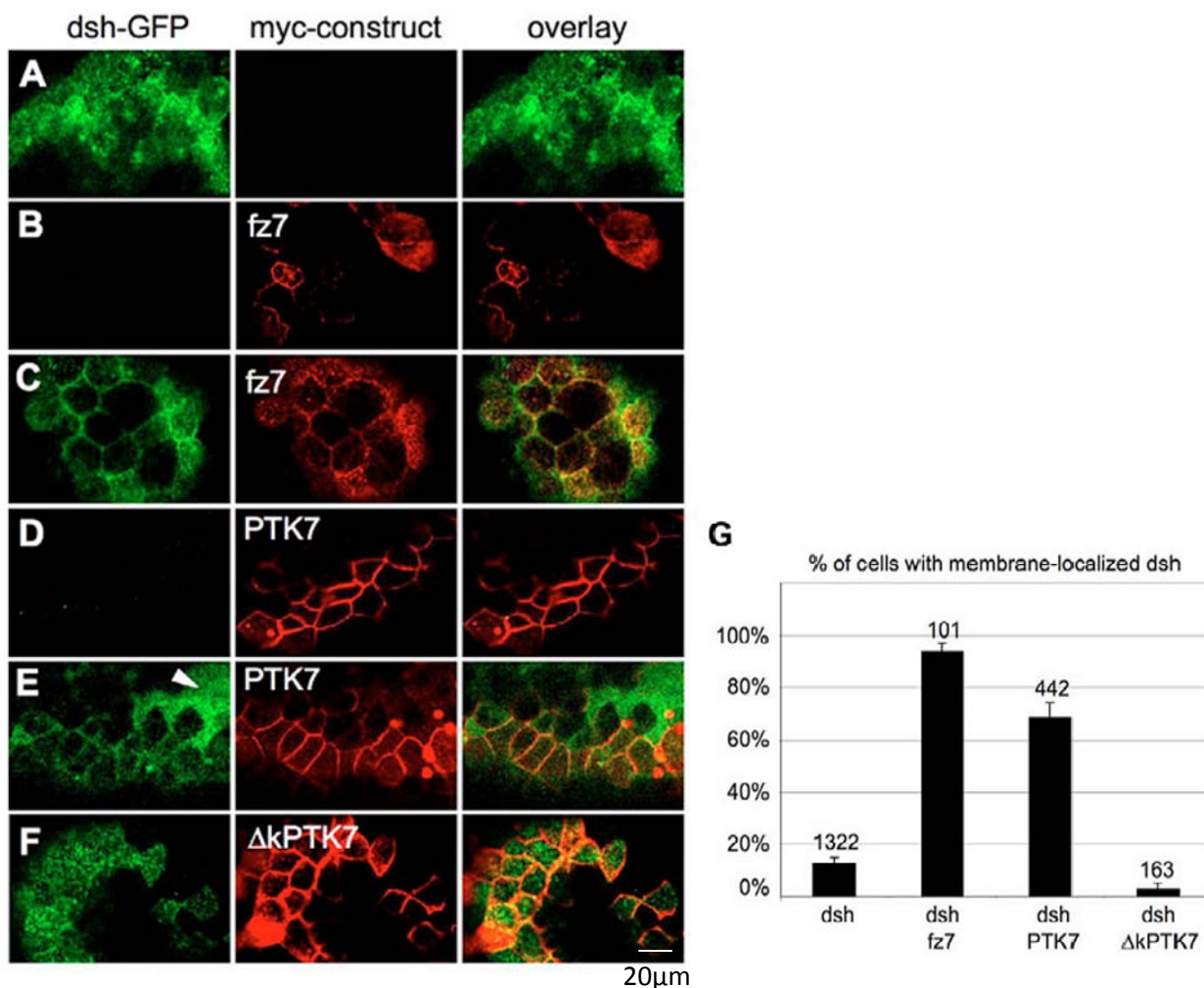


**Figure 4.1. PTK7 recruits dsh to the plasma membrane.** GFP-tagged dsh (green, left), co-expressed myc-tagged protein (red, middle) and merged pictures (right) are shown. (A) GFP-tagged dsh is localized to the cytoplasm of animal caps injected with 100 pg dsh-GFP RNA. (B) Myc-tagged fz7 is predominantly membrane localized in animal caps injected with 100 pg fz7-myc RNA. (C) Co-injection of 100 pg dsh-GFP and 100 pg fz7-myc RNA leads to membrane recruitment of dsh. (D) PTK7 is membrane localized in animal caps injected with 500 pg myc-tagged PTK7 RNA. (E) Animal caps co-injected with 100 pg dsh-GFP RNA and 500 pg PTK7-myc RNA show membrane-recruitment of dsh. (F) Animal caps injected with 250 pg RNA coding for a PTK7 mutant lacking the conserved kinase domain ( $\Delta$ kPTK7) and 100 pg dsh-GFP RNA do not show membrane localization of dsh. (G) Graph summarizing the percentage of cells with membrane-localized dsh. For the co-localization assays using PTK7 or fz7, only cells in which these proteins were membrane localized were analyzed. To determine the number of cells with dsh localized in the cytoplasm, DAPI co-staining was used. The total number of cells is indicated above each column.

To further confirm the complex formation between PTK7 and dsh in a biochemical assay, we used glycerol gradient density centrifugation (Fig. 4.2). This method allows proteins separation according to their molecular weight and protein complex formation can be detected as a shift to higher molecular weight fractions. Indeed, the dsh protein tailed into higher density fractions in the presence of full length PTK7, but not the kinase deletion mutant (Fig. 4.2). Thus, both animal



cap assay and glycerol gradient density centrifugation indicate a complex formation between dsh and PTK7.

#### 4.1.2 PDZ domain of dsh is required for the co-localization with PTK7

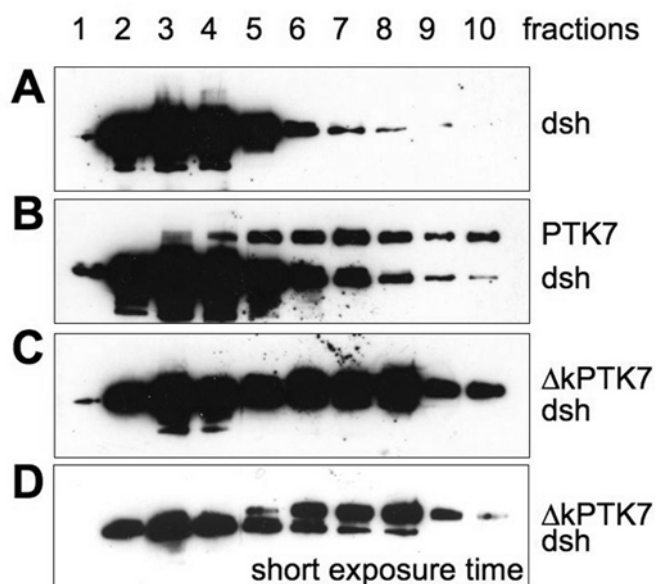


**Figure 4.2. PTK7 and dsh co-localization is detected by glycerol-gradient centrifugation.** The figure represents one of three independent experiments, showing the same result. Dsh (A) shifts to higher molecular weight fractions (9,10) if PTK7 is co-expressed (B), indicating complex formation. By contrast,  $\Delta$ kPTK7 fails to shift dsh (C, D). The image in (D) represents the same western blot as in (C), but taken at a lower exposure time, to distinguish between  $\Delta$ kPTK7 and dsh protein bands. For the glycerol gradient ultracentrifugation 100 pg of myc-tagged dsh, 500 pg of myc-tagged PTK7 and 250 pg of  $\Delta$ kPTK7 were injected anally at the one cell stage.

To identify which dsh domains are necessary for the interaction with PTK7, its deletion mutants were tested for co-localization in ectodermal explants. Dsh contains three different functional domains, namely the DIX, PDZ and DEP domains, involved in the regulation of canonical and non-canonical Wnt signaling (Fig. 4.3 A) (Sokol, 1996). To identify which of these domains are necessary for the PTK7-dependent dsh-translocation, we expressed GFP-tagged deletion mutants of the DIX, the PDZ and the DEP domain of dsh in animal caps. All mutant dsh proteins were mainly localized in the cytoplasm, when expressed alone (Fig. 4.3 B, D, F, and H). But upon co-expression with PTK7  $\Delta$ DIX- as well as  $\Delta$ DEP-dsh were transferred to the plasma membrane (Fig. 4.3 C, G, and H). However, in the case of the membrane localization of the  $\Delta$ DIX-dsh was slightly inhibited, resulting in a residual cytoplasmic staining in the animal cap cells that was not observed in  $\Delta$ DEP-dsh injected caps. Contrary,  $\Delta$ PDZ-dsh was not translocated to the plasma membrane in the presence of PTK7 (Fig. 4.3 E, H), indicating that the PDZ domain is required for complex formation. Similarly, to the previous experiment, the efficiency of PTK7-dependent

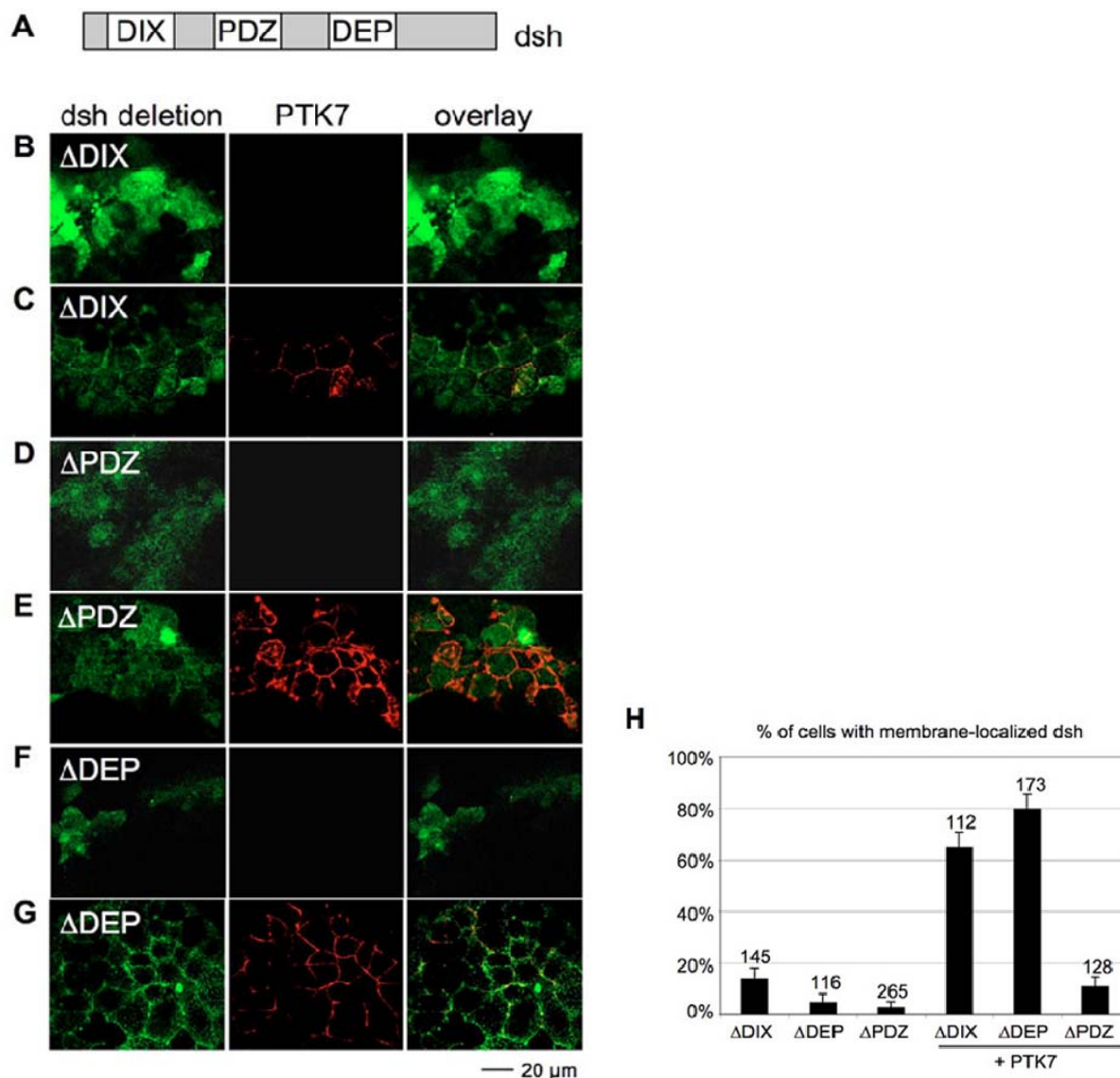


**Figure 4.3. The PDZ domain is necessary for PTK7-dependent membrane translocation of dsh.** (A) Dsh protein structure indicating the DIX, PDZ and DEP domain. (B) Animal cap injected with 100 pg  $\Delta$ DIX-GFP RNA showing cytoplasmic protein localization. (C) Co-injection of 500 pg PTK7-myc RNA results in the translocation of  $\Delta$ DIX-dsh-GFP to the membrane. (D) Animal caps injected with 100 pg  $\Delta$ PDZ-GFP RNA show only cytoplasmic localization of the protein. (E) No significant change in the localization of  $\Delta$ PDZ-dsh-GFP is observed upon the co-expression with PTK7-myc RNA. (F) Animal caps injected with 100 pg  $\Delta$ DEP-GFP RNA express the protein in the cytoplasm, whereas co-injection of 100 pg PTK7-myc RNA leads to its membrane recruitment (G). (H) Graph summarizing the percentage of cells with membrane-localized dsh. Only the cells with membrane expression of PTK7 were analyzed for dsh localization in 4 independent experiments. The total number of cells is indicated on each column.

membrane recruitment of dsh deletion mutants was estimated by counting the number of cells, showing the co-localization of both proteins at the plasma membrane (Fig. 4.3 H). Thus, these data indicate that the PDZ domain of dsh is required for the PTK7-mediated dsh localization.

#### 4.1.3 PTK7 is a part of a fz7/dsh complex

The ability of PTK7 to recruit dsh to the plasma membrane suggests an interaction between the two proteins. Therefore, the binding of PTK7 and dsh was analyzed by co-immunoprecipitation experiments in both *in vitro* transcription system and *Xenopus* embryo lysates. Differently tagged constructs, namely GFP-dsh, myc-dsh, PTK7-HA, PTK7-MT and PTK7 kinase domain (CtPTK7-HA) were immunoprecipitated with either  $\alpha$ -HA or  $\alpha$ -myc antibodies. However, independent of the strategy, no significant binding between PTK7 and dsh was detected in any of the experiments (data not shown). Therefore, it was suspected, that additional molecules should be required to mediate the PTK7-dsh interaction. Frizzled 7, which is a PCP signaling molecule, able to recruit dsh to the plasma membrane, can serve as a likely candidate to mediate the PTK7-

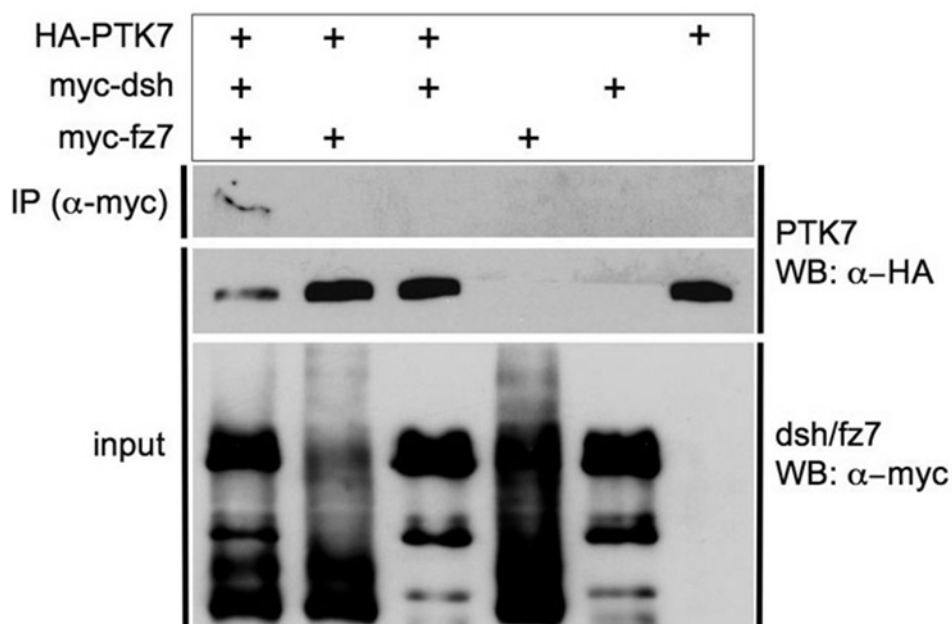


**Figure 4.4. Fz7 and dsh are both required to co-precipitate PTK7.** Embryos were injected with 1ng PTK7-HA, 0.2ng dsh-myc and 0.2 ng fz7-myc RNA and their combinations. Protein complexes were precipitated using  $\alpha$ -myc antibodies (IP). Immunoprecipitated HA-tagged PTK7 protein was detected by western blotting using  $\alpha$ -HA antibody (upper panel). The middle panel shows the PTK7 input detected by western blotting (WB) using anti-HA antibodies. The lower panel shows the dsh/fz7 inputs detected by anti-myc antibodies.

dsh interaction. To test whether PTK7 forms a complex with dsh and fz7, co-immunoprecipitation from the *Xenopus* embryo lysates expressing HA-tagged PTK7 with either myc-tagged dsh or myc-tagged fz7, or a combination of the two was performed (Fig. 4.4). HA-tagged PTK7 was co-precipitated with myc tagged Fz7 together with dsh, indicating that PTK7 is part of fz7-dsh complex. Interestingly, in cell culture experiments Frizzled 7 alone was sufficient for the precipitation of PTK7. Moreover, pull-down experiments using human  $\Delta$ kPTK7 and

*Xenopus* Fz7 expressed in MCF7 cell lysates show that the extracellular domain of PTK7 is required for complex formation with fz7 (Martina Podleschny, unpublished data).

#### 4.1.4 PTK7 loss of function affects fz7-mediated dsh membrane recruitment and hyperphosphorylation

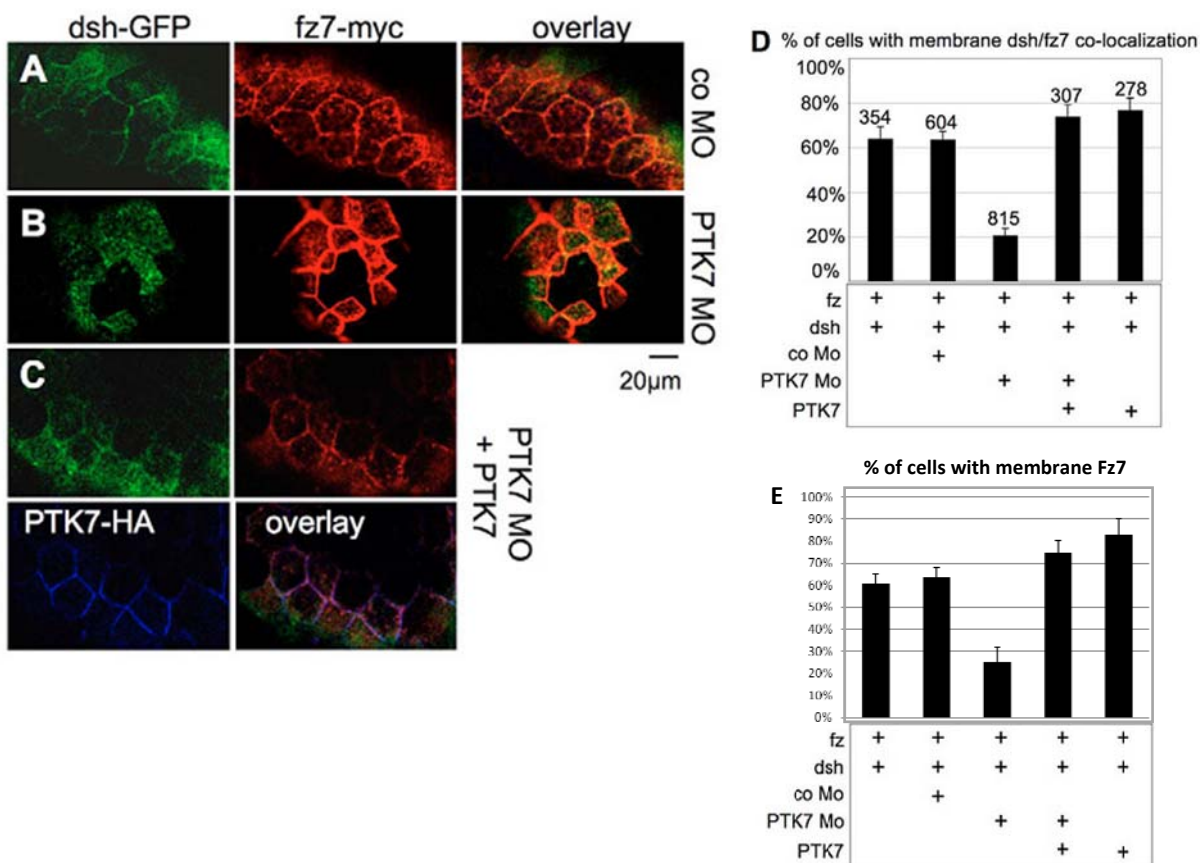


**Figure 4.5. PTK7 is required for fz7-mediated dsh membrane recruitment.** GFP-tagged dsh is shown in green, myc-tagged fz7 in red, HA-tagged PTK7 in blue. (A) GFP-tagged dsh is localized at the plasma membrane in animal cap cells, injected with 100 pg dsh-GFP RNA, 100 pg fz7-myc RNA and 20 ng control MO. (B) GFP-tagged dsh is not recruited to the plasma membrane in animal caps injected with 100 pg dsh-GFP and 100 pg fz7-myc RNA and 20 ng PTK7 MO. (C) Co-injection of 100 pg wild-type PTK7 RNA lacking the MO binding site rescues dsh-localization of animal caps injected with 100 pg dsh-GFP RNA, 100 pg fz7-myc RNA and 20 ng PTK7 MO. (D-E) Graphs summarizing the percentage of cells with simultaneously membrane-localized dsh and fz7 and fz7 alone. The total number of cells is indicated on each column and equal for the both experiments

If PTK7 complexes with fz7, it could have an influence on the fz7-mediated dsh membrane recruitment. To test whether this is the case, we analyzed how loss of PTK7 function affects fz7-dsh co-localization in animal caps, which endogenously express PTK7 (Fig. 4.7 A). As demonstrated before, in the presence of control morpholino oligonucleotides (MOs), fz7 recruits GFP-tagged dsh to the plasma membrane (Fig. 4.5 A, D). At the same time, loss of PTK7 function inhibits fz7-dsh co-localization at the plasma membrane (Fig. 4.5 B, D). This effect could be rescued by co-expression of PTK7-HA lacking the MO binding site (Fig. 4.5 C, D). The

effect of PTK7 loss of function was estimated in 10 independent experiments by counting the number of the cells, showing Fz7-Dsh co-localization at the plasma membrane (Fig. 4.5 D). Since fz7 did not localize to the plasma membrane in all analyzed cells, the percentage of cells, showing membrane localization of fz7 was analyzed. Interestingly, in addition to the disturbance of fz7-dependend dsh membrane recruitment PTK7 loss of function has also an effect on Frizzled7 membrane localization itself (Fig. 4.5 E), indicating that it functions by stabilizing fz7-dsh complex at the plasma membrane.

Since it was previously shown that fz7-mediated dsh membrane translocation correlates with dsh hyperphosphorylation (Rothbacher et al., 2000), we examined whether PTK7 loss of function affects dsh phosphorylation. The expression of either myc-tagged dsh or myc-tagged dsh with PTK7 in *Xenopus* ectodermal explants shows a single band in western blots using  $\alpha$ -myc antibodies. An additional high molecular weight band representing hyperphosphorylated dsh was detected only in lysates with dsh, fz7 and control MO (Fig. 4.6). Interestingly, this fz7-mediated hyperphosphorylation of dsh is inhibited by the PTK7 MO, indicating an emerging role of PTK7 in this process. Thus, PTK7 is a part of the fz7-dsh complex, which is required for its stabilization at the plasma membrane and fz7-mediated dsh hyperphosphorylation.

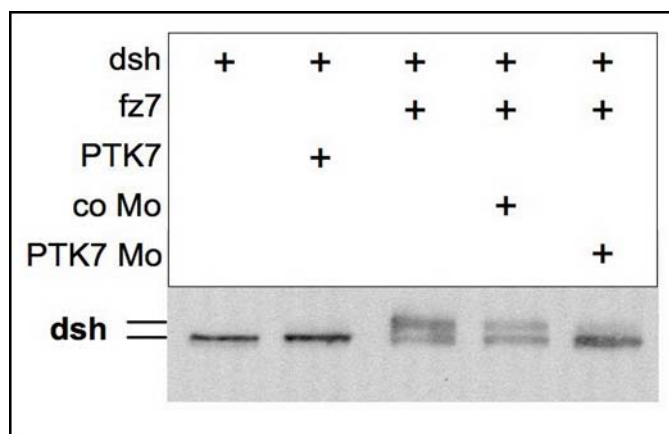


**Figure 4.6. PTK7 is required for fz7-mediated dsh hyperphosphorylation.** MT-dsh was overexpressed in animal caps and detected with  $\alpha$ -myc antibodies. Dsh-MT shows a single band (indicated as a lower band), when overexpressed alone or in combination with PTK7. Co-expression with Fz7 results in the appearance of the second higher molecular weight band (indicated as a higher band), which corresponds to dsh hyperphosphorylation. The co-injection of 20 ng control MO does not significantly affect dsh phosphorylation, while 20 ng PTK7 MO blocks it. For the experiment *Xenopus* embryos were injected animally at the one cell stage with 100 pg myc-tagged dsh, 100 pg Fz7 and 500 pg PTK7 RNA. At the blastula stage the ectodermal explants were excised and cultivated till stage 11. The hyperphosphorylation of dsh was analyzed by western blot with  $\alpha$ -myc antibodies.

**4.1.5 Fz7 loss of function does not affect the PTK7-mediated dsh membrane recruitment**

Since PTK7 is a part of the Fz7-dsh complex, it would be interesting to test, whether loss of Fz7 function affects PTK7-dependent dsh membrane recruitment. Similar to PTK7, endogenous Fz7 is expressed in animal caps (Fig. 4.7 A). To knock down the Fz7 function, two morpholinos directed against known Fz7 isoforms (Fz7a and Fz7b) were used (Djiane et al., 2000; Winklbauer et al., 2001). However, the analysis of animal caps expressing MT-PTK7 together with GFP-Dsh in the presence of both morpholinos in high amounts (40ng) does not show any significant differences in PTK7-dsh membrane co-localization (Fig. 4.7 B, D) in comparison with control samples (Fig. 4.7 C, D). Thus, these data indicate that PTK7-dsh interaction is not mediated exclusively via frizzled 7. Since two other frizzled family molecules, namely frizzled 4 and 8, are expressed in animal cap cells (Fig. 4.7 A), they could also stabilize the PTK7-dsh complex at the plasma membrane. Alternatively, PTK7-mediated dsh recruitment may be mediated by additional mechanisms. Therefore, in the further work we attempted to identify novel PTK7-binding proteins, which could facilitate PTK7-dsh interaction.

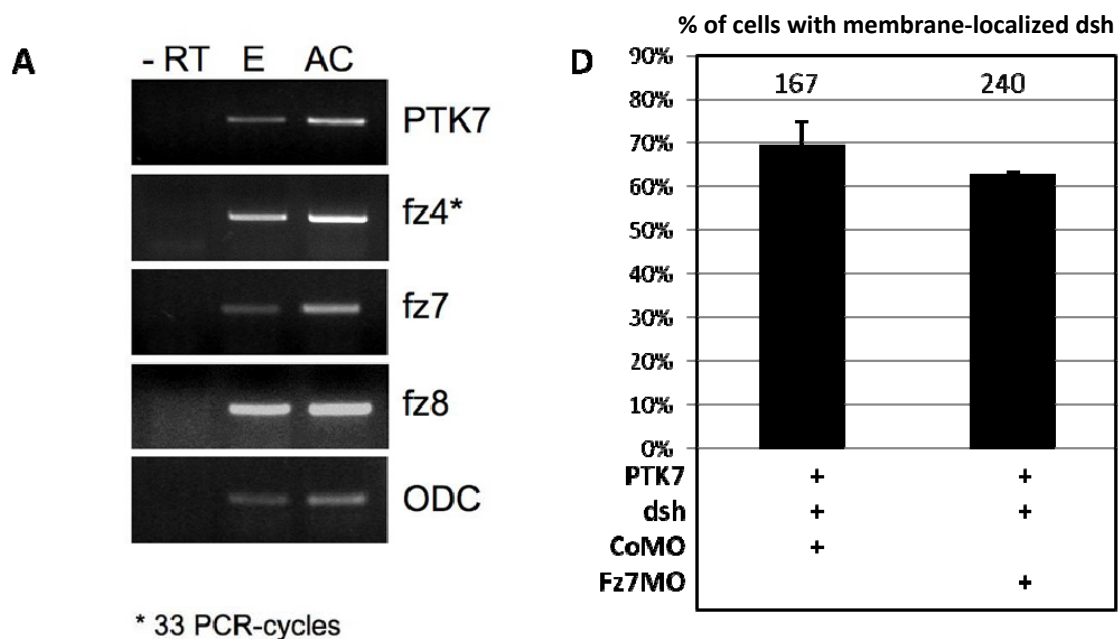


**Figure 4.7. Loss of fz7 function does not affect the PTK7-dsh co-localization.** (A) Animal caps express PTK7 as well as several members of frizzled the family: fz4, fz8 and fz7; AC - RT-PCR of the animal caps, E – of the whole embryo at the corresponding stage. (B) Animal cap cells, showing the PTK7-dsh co-localization in the presence of the control MO and (C) the combination of fz7aMO and fz7bMO. (D) Summary of three independent experiments, demonstrating the percentage of cells, where PTK7 recruits dsh to the plasma membrane.

#### 4.1.6 RACK1 is a novel PTK7-binding partner, identified by tandem mass-spectrometry

To identify new PTK7 binding partners tandem mass-spectrometry analysis was employed. For this purpose myc-tagged PTK7 together with its binding partners was precipitated from *Xenopus* embryos at the stage 16, when neural crest cells start to migrate. The proteins were separated by SDS-PAGE, which was cut in 23 slices and the content of the each slice was analyzed by tandem mass-spectrometry. In parallel, a pull-down from control embryos was performed, and the proteins identified in the control lane were subtracted from the list of potential PTK7-interacting partners. Finally, to select proteins, which could interact with PTK7 with higher probability, the threshold score of 20 was applied to the protein hits. Among 32 potential binding partners (data not shown), we found receptor of activated PKC 1 (RACK1), which has a score of 203.

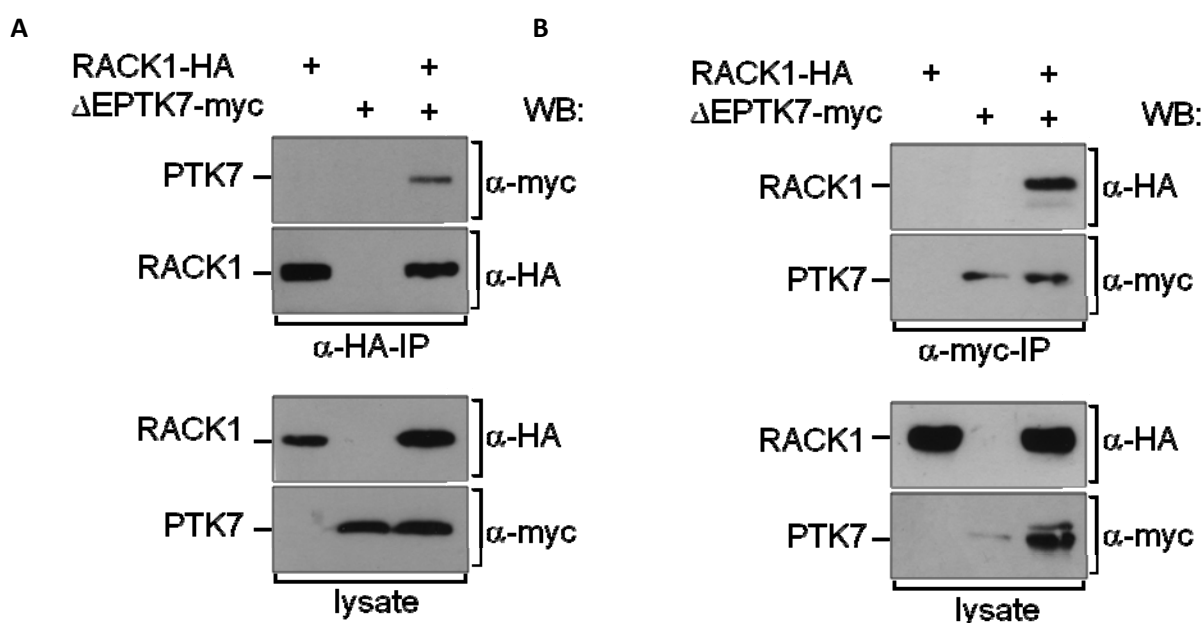


**Figure 4.8. RACK1 interacts with PTK7.** (A) RACK1 co-precipitates a deletion mutant of PTK7 lacking the extracellular domain ( $\Delta$ EPTK7) from *Xenopus* embryo lysates. IP: immunoprecipitation, WB: Western blot. (B) *In vitro* translated myc-tagged  $\Delta$ EPTK7 protein precipitates HA-tagged RACK1 protein.

RACK1 is a conserved scaffold protein, which consists of 7 tryptophane-aspartate domains (WD40-domains). It is involved in variety of cellular processes, including adhesion, migration, cell survival and protein translation (McCahill et al., 2002; Nilsson et al., 2004; Sklan et al., 2006). The RACK1 protein was originally identified by its ability to bind PKC and facilitate its interaction with downstream signaling components (Mochly-Rosen et al., 1991). Since the proteins of the PKC family have been implicated in the regulation of PCP signaling and, particularly, dsh membrane recruitment (Kinoshita et al., 2003), RACK1 was further analyzed to investigate whether it acts as a potential mediator of the PTK7-dsh interaction.



To verify PTK7-RACK1 interaction, HA-tagged RACK1 and myc-tagged PTK7, lacking the extracellular part ( $\Delta$ EPTK7-MT), were overexpressed both *in vitro* and in *Xenopus* embryos and co-immunoprecipitation experiments were performed. In *Xenopus* lysates, HA-tagged RACK1 precipitates  $\Delta$ EPTK7-MT if the immunoprecipitation is performed with  $\alpha$ -HA antibodies (Fig. 4.8 A). Furthermore, *in vitro* translated  $\Delta$ EPTK7-MT precipitates *in vitro* translated RACK1-HA, if precipitated with  $\alpha$ -myc-coupled agarose beads (Fig. 4.8 B). The fact that co-precipitation was demonstrated with *in vitro* translated proteins suggests direct interaction between RACK1 and PTK7.

#### **4.1.7 Similar to PTK7, RACK1 regulates neural tube closure**

If the RACK1-PTK7 interaction has a biological relevance than both molecules should regulate similar developmental processes. So far the role of RACK1 in development has not been characterized. However, the expression pattern of RACK1 in *Xenopus* embryo was published and it shows overlap with the one of PTK7 (Kwon et al., 2001; Lu et al., 2004). In particular, both proteins are expressed in the area of the neural tube and PTK7 was already shown to regulate neural tube closure (Lu et al., 2004). To test whether RACK1 has a function in neural tube closure two translation blocking morpholino oligonucleotides were designed (Fig. 4.9 A). The morpholinos efficiencies were tested in the *in vitro* translation system (Fig. 4.9 B) as well as in *Xenopus* embryo lysates (Fig. 4.9 C). MO1 binds at the beginning of the RACK1 coding sequence and thus, can be rescued with a human homolog of RACK1, while MO2 targets the 5'-UTR and the rescue can be performed with a *Xenopus* RACK1 construct, lacking the MO binding site (Fig. 4.9).

A

RACK1 5'-UTR and CDS

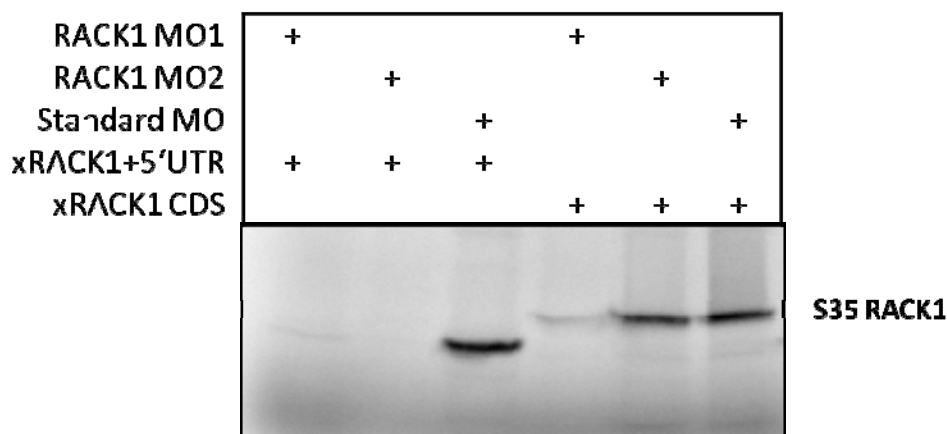
RACK1 MO2

5'-CTTCAGGCCTTGTGTCAGCCATCTGCCTCCATCCTTAGTCGGTGGAGCGGTTTCAG-3'  
 3'-AGGAATCAGCCACCTCGCCAAAGTC-5'

GCTCATCACAGCC(ATG)ACTGAGCAAATGACACTTCGGGGGACCC-3'  
 3'-TACTGACTCGTTTACTGTGAAGCCC-5'

B

RACK1MO1



C

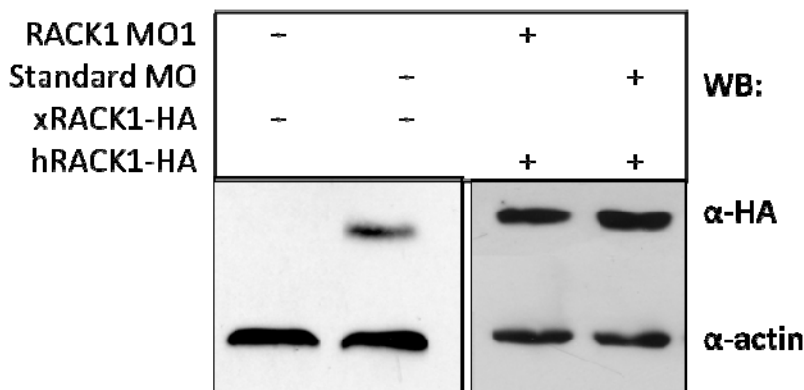


**Figure 4.9. RACK1 morpholino oligonucleotides.** (A) The RACK1 MO1 targets the ATG (highlighted in blue) and RACK1 MO2 the 5'UTR (highlighted in green) of the *Xenopus RACK1* gene (Gene bank accession number BC041541). (B) Both MO inhibited *in vitro* translation of full length RACK1 containing the 5'UTR (xRACK1), the translation of an HA-tagged RACK1 construct lacking the 5' UTR (xRACK1-HA) is inhibited by MO1, but not MO2, the translation of hRACK1 remains unaffected and standard MO does not influence protein translation. The radioactive translated RACK1 proteins ( $S^{35}$  RACK1) are shown. (C) RACK1 MO1 inhibits the translation of x-RACK-HA, but not hRACK1-HA in *Xenopus* lysates

The animal injections of either MO1 or MO2 result in neural tube closure defects, resembling PTK7 loss of function phenotype (Fig. 4.10 A-C). The effects of both morpholinos can be effectively rescued by co-injection of RACK1 constructs, lacking morpholino binding sites (Fig. 4.10 B and C).

To exclude the mesodermal influence on the neural tube closure, animal injections at 8-cell stage were performed. During this type of injections the constructs are targeted primarily to the neural tissues. Subsequently, the injection of RACK MO1 together with GFP as a lineage tracer also results in neural tube closure defects (Fig. 4.11).

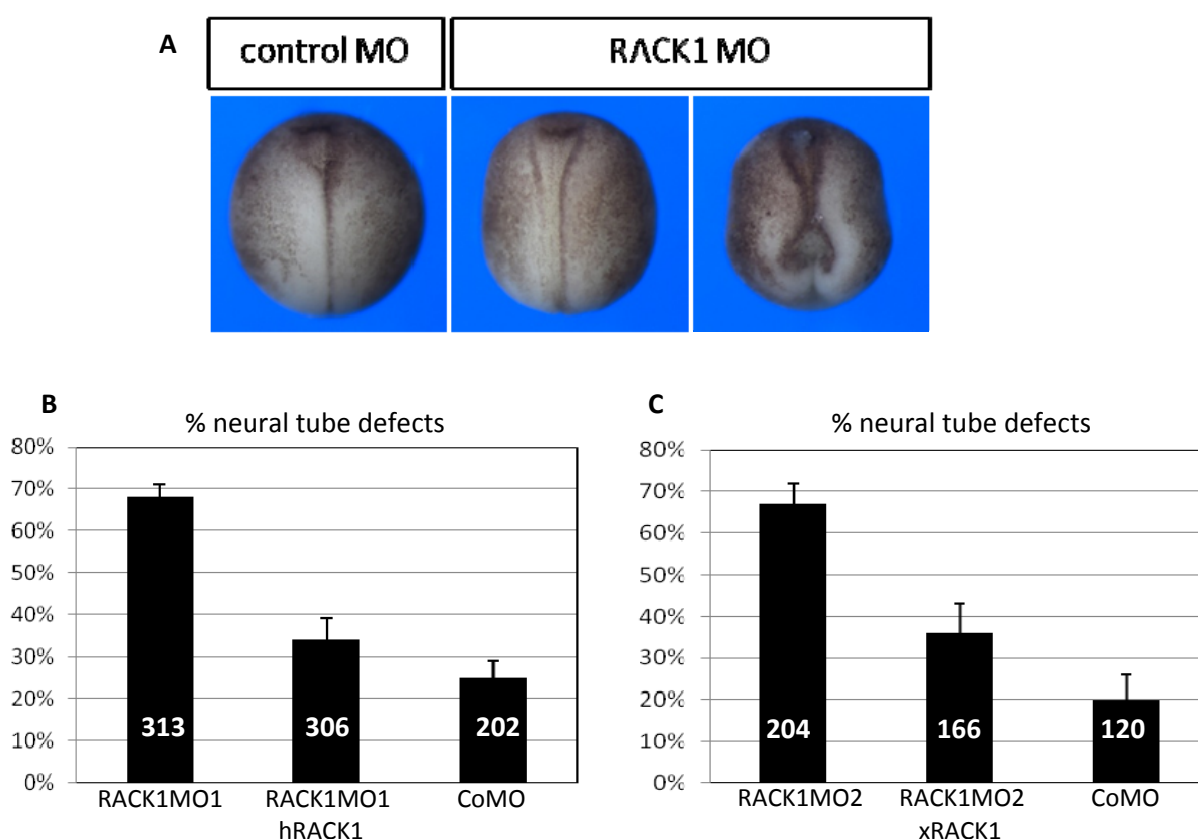


**Figure 4.10. RACK1 loss of function phenotype.** (A) The injection of either 20ng of RACK1 MO1 or 20 ng of MO2 results in neural tube closure defects, while embryos injected with 20 ng control MO (CoMO) display closed neural tubes. (B) Graph summarizing the percentage of neural tube closure defects in three independent experiments. The embryos were injected animally with 20 ng RACK1 MO1, 20 ng RACK1 MO1 plus 300pg of hRACK1 or 20ng control MO at neurula stages (st. 16-17) neural tube closure defects were analyzed. (C) Graph, summarizing three independent experiments, where the neural tube defects caused by the injection of RACK1 MO2. 20ng RACK1 MO2 was injected and its effect was rescued by co-injection of 300 pg *Xenopus* RACK1. The injection of control MO did not cause major neural tube closure defects. The third repetition of the RACK1 MO2 injections was done by Peter Werner.

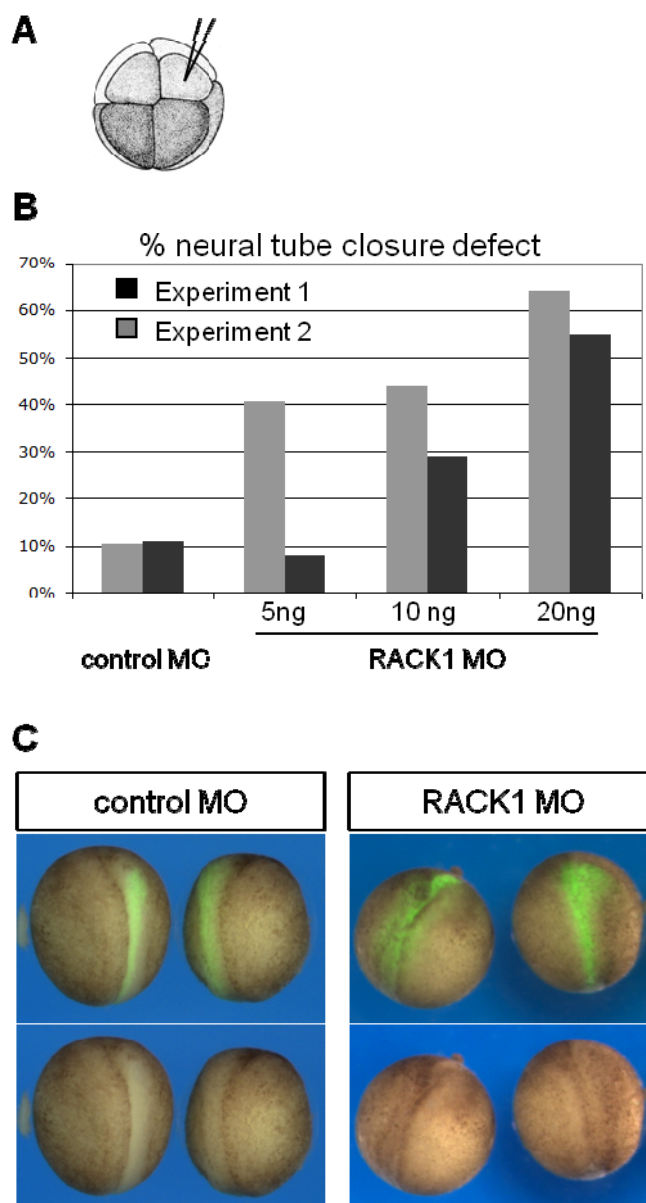


**Figure 4.11. Targeted injection of RACK1 MO1 also results in neural tube closure defects.** (A) The RNA injections were performed at the 8-cell stage into the dorsal animal blastomere, which result in the targeting to prospective neural tissues. (B) Two independent experiments, demonstrating the effect of RACK1 MO1 injected in different concentrations. (C) RACK1 MO1 was co-injected with GFP as a lineage tracer and causes NT closure defects, while control Mo injected embryos did not display any significant neural tube closure abnormalities.

To test whether RACK1 gain of function influences NT closure, animal injections at the one-cell stage (P.Werner, unpublished) as well as targeted injections at 8-cell stage were performed. Indeed, RACK1 overexpression also results in the certain amount of NT closure defects, however the results have high variations between five tested batches of embryos (data not shown).

#### 4.1.8 PTK7 recruits RACK1 to the plasma membrane in animal cap cells

As PTK7 and RACK1 demonstrate physical interaction and both have a function in NT closure, RACK1 may mediate the PTK7-dependent dsh membrane recruitment. If this hypothesis is correct, then, similarly to dsh, RACK1 should co-localize with PTK7 at the plasma membrane. Therefore PTK7-RACK1 co-localization was analyzed by confocal microscopy in ectodermal explants (animal caps) of blastula stage *Xenopus* embryos. HA-tagged RACK1 is expressed in the cytoplasm of animal caps (Fig. 4.12 A), but is recruited to the plasma membrane upon co-expression of GFP-tagged PTK7 (Fig. 4.12 B, D). Subsequently, a kinase deletion mutant of PTK7 ( $\Delta$ kPTK7), which does not recruit dsh, failed to translocate RACK1 to the plasma membrane (Fig. 4.12 C, D). Thus, these data show that PTK7 recruits RACK1 to the plasma membrane and that the kinase homology domain of PTK7 is necessary for this function. Furthermore, this supports the hypothesis that RACK1 functions in the PTK7-mediated membrane localization of dsh.

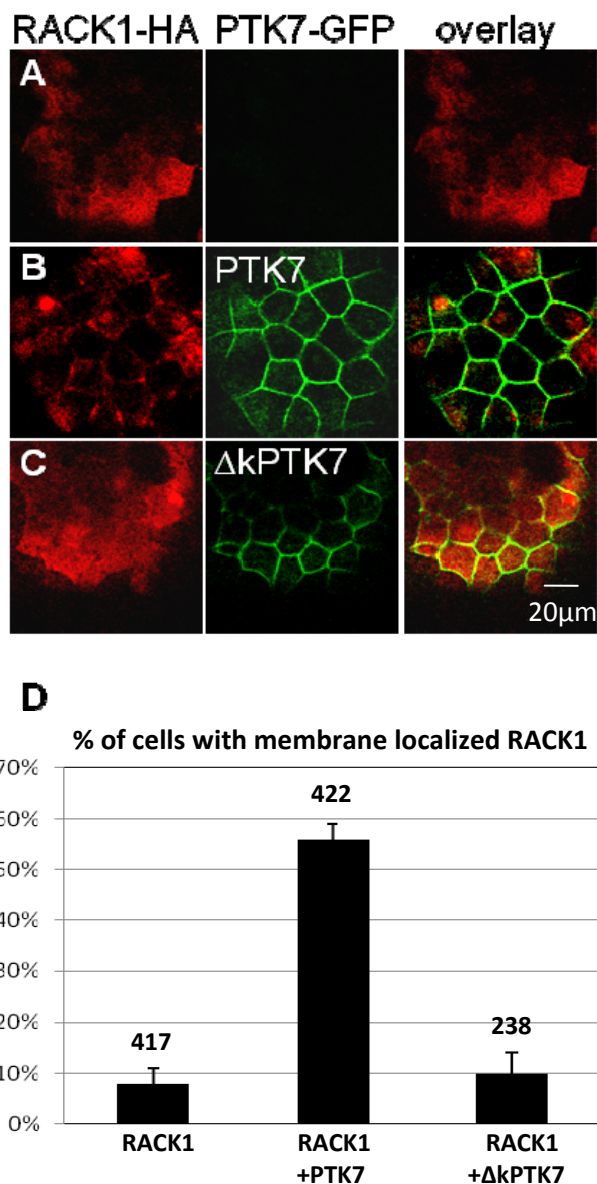


**Figure 4.12. PTK7 recruits RACK1 to the plasma membrane.** Animal caps expressing tagged proteins were analyzed by confocal microscopy. HA-tagged RACK1 (red) is shown on the left, the GFP-tagged PTK7 constructs (green) in the middle and the overlay on the right. **(A)** RACK1 is localized in the cytoplasm of animal caps injected with 250 pg RACK1-HA RNA. **(B)** Co-expression of 500 pg PTK7-GFP recruits RACK1 to the plasma membrane. **(C)** Deletion of the kinase domain abolishes membrane recruitment of RACK1. Embryos were co-injected with 250 pg RACK1-HA RNA and 500 pg  $\Delta$ kPTK7-GFP. **(D)** Graph summarizing the percentage of cells with membrane-localized RACK1. The number of cells analyzed from 10 independent experiments is indicated for each column. The p-value of RACK1 recruitment to the membrane by PTK7 in Student's t-test is less than 0.001.

#### 4.1.9 RACK1 is required for PTK7-mediated dsh membrane recruitment

To further prove the hypothesis that RACK1 mediates the PTK7-dsh interaction, it was investigated how the loss of RACK1 function affects the PTK7-dsh co-localization. This was analyzed in animal cap cells, which endogenously express RACK1 as confirmed by RT-PCR (data not shown) as well as RACK1 expression pattern (Kwon et al., 2001). In animal cap cells cytoplasmically localized GFP-tagged dsh (Fig. 4.13 A) is recruited to the plasma membrane in the presence of PTK7 and control MO (Fig. 4.13 B, E). In contrast, co-injection of the RACK1 MO significantly inhibit PTK7-mediated dsh membrane recruitment (Fig. 4.13 C, E), indicating that RACK1 is required for this process. Identical results are observed for the RACK1 MO1, the RACK1 MO2 and the combination of these MOs (Fig. 4.13 E). Moreover, this effect is considered to be specific to the loss of RACK1 function, since PTK7-dsh membrane co-localization can be rescued by RACK1 constructs lacking the MO binding site (Fig. 4.13 D, E). Thus, RACK1 is required for the PTK7-mediated dsh membrane recruitment. However, dsh does not demonstrate any binding to RACK1 in the co-immunoprecipitation experiments of the *in vitro* translated proteins (data not shown). Therefore, other proteins could be required to mediate RACK1 dsh interaction.

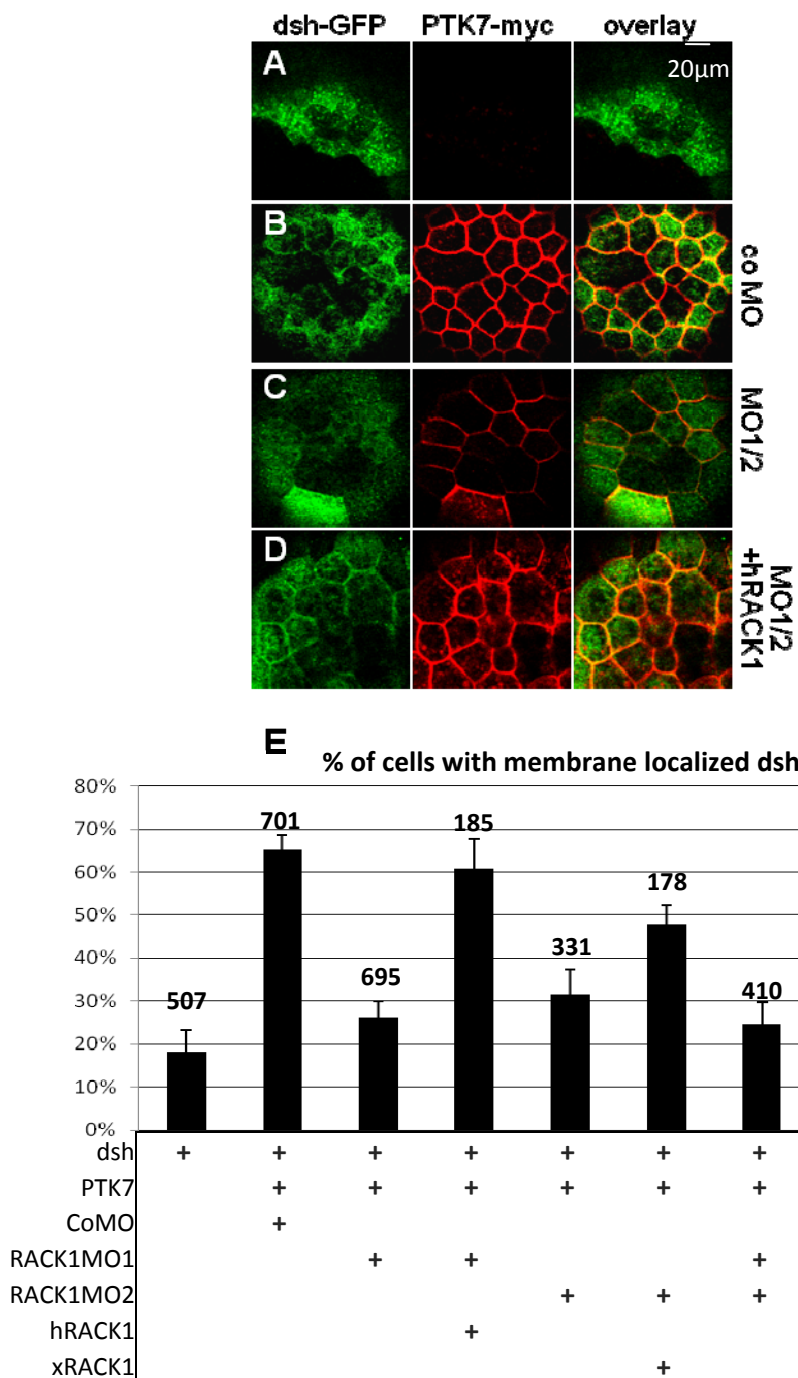


**Figure 4.13. RACK1 is required for the PTK7-mediated dsh membrane localization.** (A) Animal caps injected with 100 pg dsh-GFP RNA express dsh mainly in the cytoplasm. (B) PTK7 translocates dsh to the plasma membrane in animal caps co-injected with 20 ng control MO and 500 pg PTK7 RNA. (C) Co-injection of 20 ng RACK1 MO1 abolishes membrane localization of dsh in caps injected with 100 pg dsh-GFP and 500 pg PTK7, which can be rescued by co-injection of 300 pg hRACK1. (E) Graph summarizing the percentage of cells with membrane-localized dsh. The number of cells analyzed in a total of 13 independent experiments is indicated for each column. The p-value for the RACK1 morpholino injections vs standard were estimated in homoscedastic t-test as lower than 0.01, for the rescue experiments – lower than 0.05



#### 4.1.10 RACK1 is required for the interaction between PTK7 and PKC $\delta$ 1

In human tissue culture RACK1 was shown to bind PKC $\delta$  (Lopez-Bergami et al., 2005). Subsequently, in *Xenopus* PKC $\delta$  directly binds dsh and is essential for dsh function in a non-canonical Wnt signaling pathways and regulation of convergent extension movements (Kinoshita et al., 2003). Thus, RACK1 can link PTK7 to dsh via PKC $\delta$ . The interaction between RACK1 and PKC $\delta$ 1 in *Xenopus* embryo lysates was additionally verified by the co-immunoprecipitation of HA-tagged RACK1 and GFP-tagged PKC $\delta$ 1 (Fig. 4.14 A). In the result, RACK1 was shown to bind PKC $\delta$ 1, supporting the hypothesis that PKC $\delta$  may be necessary for the regulation of the dsh membrane localization by PTK7. However, if this is true, than PKC $\delta$ 1 should, similar to dsh, co-localize with PTK7 at the plasma membrane in a RACK1-dependent manner. The PTK7-dependent PKC $\delta$ 1 membrane recruitment as well as the requirement of RACK1 for this process was tested in animal caps. GFP-tagged PKC $\delta$  is expressed in the cytoplasm of animal caps, and is recruited to the plasma membrane by co-expression of myc-tagged PTK7 in the presence of standard MO (Fig. 4.14 B, C, and F). However, co-injection of the RACK1 MO abolishes PKC $\delta$ 1 membrane translocation in the presence of PTK7 (Fig. 4.14 D, F). In accordance with the previous experiments, similar effects were observed for the injection of MO1, MO2 and their combination (Fig. 4.14 F). Additionally, to prove the RACK1-specificity of the observed effects, rescue experiments with both human and *Xenopus* RACK1 constructs were performed (Fig. 4.14 E, F).

Finally, to prove that RACK1 mediates the PTK7-dsh interaction via PKC $\delta$ , we tested how PKC $\delta$ 1 loss of function affects the co-localization of PTK7 and dsh in the animal cap assay. Similarly to previous experiments, in the presence of control MO PTK7 recruits dsh to the plasma membrane, while membrane localization of dsh significantly decreases in the presence of PKC $\delta$ 1 MO (Fig. 4.15).

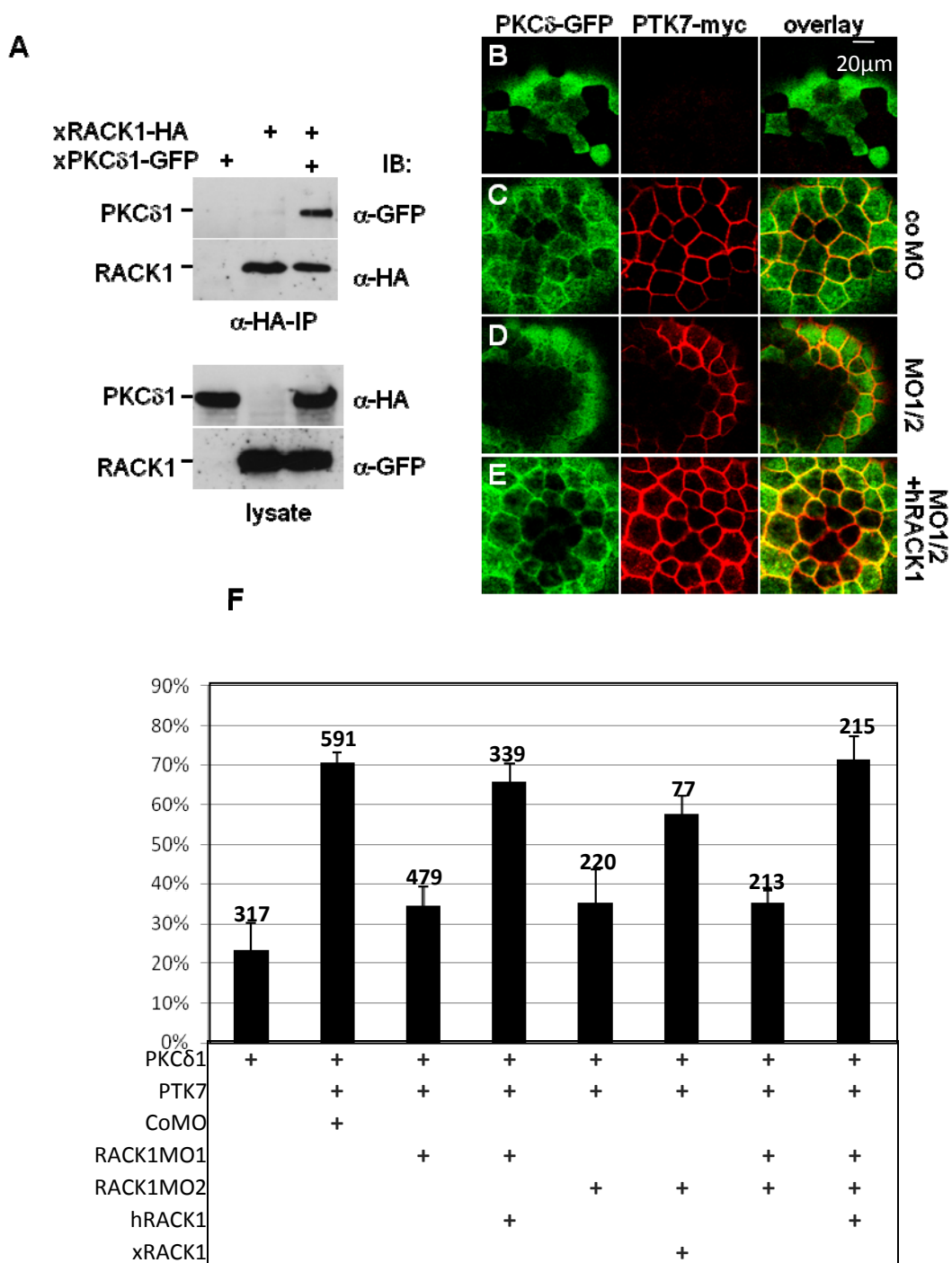


**Figure 4.14. PKC $\delta$ 1 is recruited to the plasma membrane by PTK7 via RACK1.** (A) HA-tagged RACK1 precipitates myc-tagged PKC $\delta$ 1 from Xenopus lysates injected with 300 pg RACK1-HA RNA and 500 pg PKC $\delta$ 1-GFP RNA. (B-E) Animal cap localization assay showing co-localization of PTK7 with PKC $\delta$ . GFP-tagged PKC $\delta$ 1 (green) is shown on the left, myc-tagged PTK7 (red) in the middle and the overlay on the right. (B) GFP-tagged PKC $\delta$ 1 is localized in the cytoplasm of animal caps injected with 250 pg PKC $\delta$ 1-GFP RNA. (C) Co-expression of myc-tagged PTK7 recruits GFP-tagged PKC $\delta$ 1 to the plasma membrane in animal caps injected with 700 pg PTK7-myc and 250 pg PKC $\delta$ 1-GFP RNA and 20 ng of control MO. (E) Co-injection of either 20ng RACK1 MO1, or MO2 or their combination affects the PTK7-mediated PKC $\delta$  membrane recruitment. (F) Graph summarizing the percentage of membrane-recruited PKC $\delta$ 1 from 12 independent experiments. The p-value between control MO and RACK1 MOs injections was lower, than 0.001 in Student's t-test, while in the rescue experiments the p-value did not exceed 0.05.

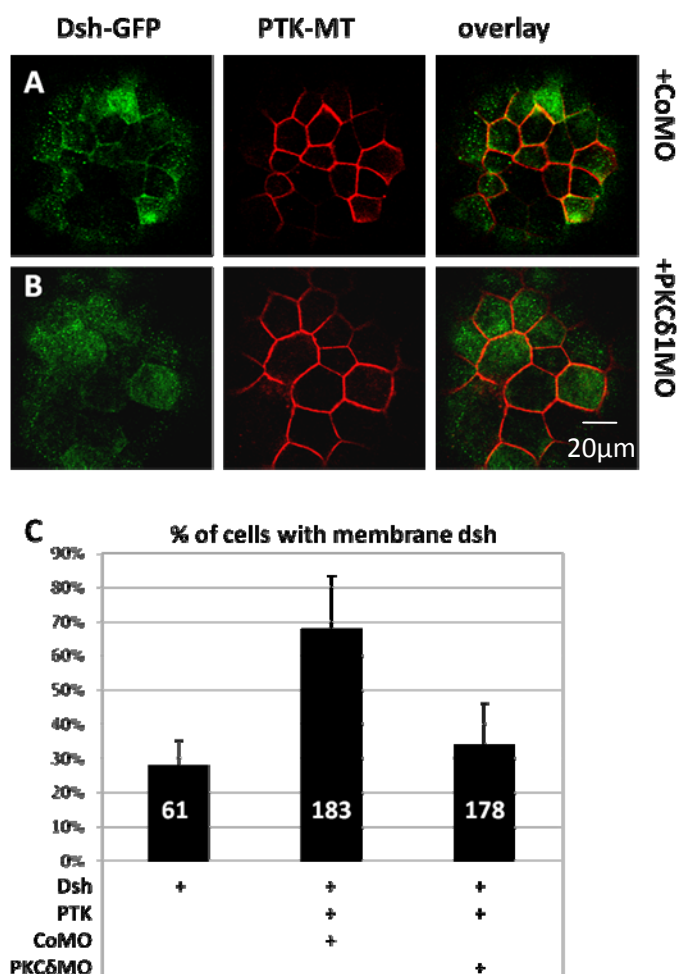


**Figure 4.15. PKC $\delta$ 1 is required for PTK7-dsh co-localization.** (A) Upon co-expression with PTK7 (500 pg mRNA) dsh-GFP (100 pg mRNA) translocates to the plasma membrane in the presence of 20 ng control MO. (B) The co-injection of 20 ng PKC $\delta$ 1 MO inhibits PTK7-mediated dsh membrane recruitment. (C) Graph demonstrating the percentage of membrane localized dsh from one experiment. Error bars show the standard deviation between 12 evaluated pictures, the p-value for CoMO vs PKC MO is lower than 0.001 in the Student's t-test.

#### 4.1.11 RACK1 is not required for the fz7-mediated dsh localization

Since dsh can be recruited to the membrane by members of the frizzled receptor family, particularly frizzled 7, we analyzed if the fz7-mediated dsh localization is also affected by RACK1. Protein localization in animal caps demonstrates that myc-tagged fz7 recruits GFP-tagged dsh to the plasma membrane in the presence of a control MO (Fig. 4.16 A). But RACK1 is not required for the fz7-mediated dsh localization, because neither RACK1 MO1 nor RACK1 MO2 nor the combination of MO1 and 2 (Fig. 4.16 B, C) disturb the recruitment of dsh by fz7. Conversely, RACK1 loss of function does not have any effect on the fz7-dependent hyperphosphorylation of dsh. Upon the expression in both animal caps and embryos, myc-tagged

dsh is detected as a single band in Western blots using  $\alpha$ -myc-antibodies, while co-injection of fz7 leads to the formation of a second high molecular weight band, which corresponds to hyperphosphorylated dsh. Co-injection of either RACK1 MO1 or the combination of the MOs does not affect the dsh phosphorylation status. The same effects were observed in the whole embryo, where co expression of dsh and fz7 results in a triple band, corresponding to

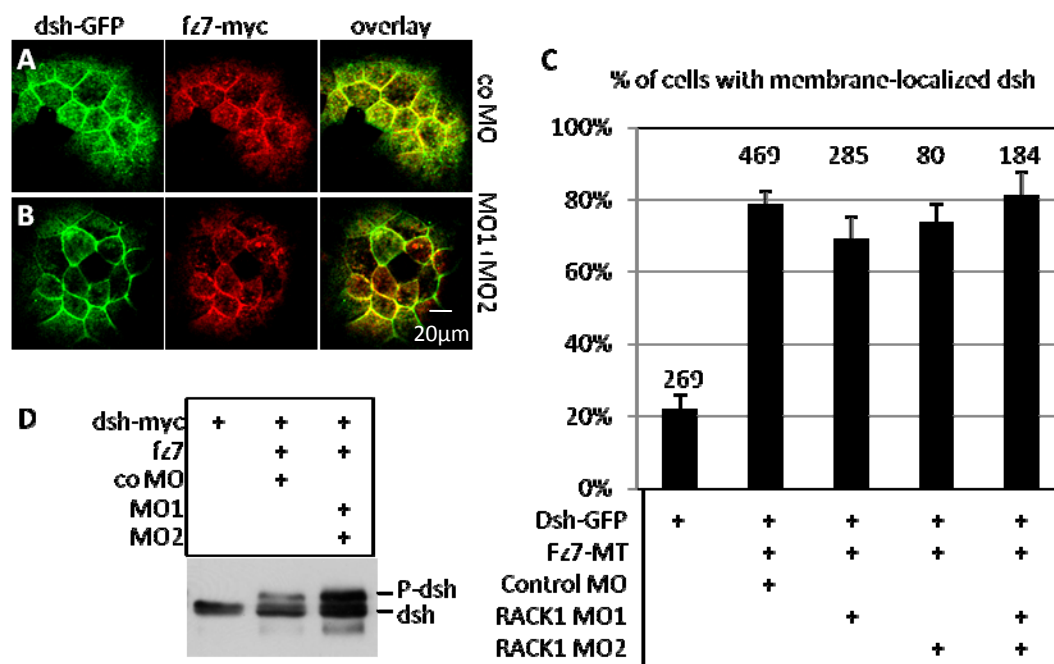


**Figure 4.16. RACK1 does not affect the fz7-dependent dsh membrane recruitment and phosphorylation.** (A) Co-expression of fz7 (100 pg) and dsh (100 pg) leads to dsh membrane recruitment in the presence of control MO, as well as in the presence of RACK1 MO1, MO2 and the combination of the MOs (B). (C) Graph summarizing the percentage of cells with membrane-localized dsh. (D) Upon the co-expression with fz7, myc-tagged dsh forms a higher molecular weight band, which corresponds to hyperphosphorylated dsh in the presence of the control MO or the RACK1 MO.

phosphorylated dsh (Fig. 4.16 D). Thus, fz7-mediated membrane localization and hyperphosphorylation of dsh are not RACK1-dependent.

#### 4.1.12 Both PTK7 and RACK1 can activate JNK phosphorylation

To test whether PTK7 and RACK1 can affect downstream PCP signaling events, we tested how the phosphorylation of c-Jun N-terminal kinases (JNK) is influenced by these molecules in animal caps. Previous work demonstrated that JNKs can be phosphorylated and translocated to the nucleus during the activation of PCP signaling (Tahinci et al., 2007; Yamanaka et al., 2002). And the overexpression of several PCP regulators, including dsh, can induce JNK phosphorylation. The activation of JNK was analyzed in the animal caps stained with  $\alpha$ -phospho-JNK antibodies and DAPI to mark the nucleus. The increase in JNK activity was estimated by

counting the cells, where  $\alpha$ -phospho-JNK stain co-localizes with DAPI (Fig. 4.17, A-B, and E). Similarly to dsh, overexpression of either RACK1 or PTK7 in animal caps increases JNK phosphorylation. (Fig. 25 C-E). Moreover, PTK7 loss of function inhibits JNK phosphorylation, induced by dsh, which indicates that dsh should form a complex with PTK7 to activate JNK. (Fig. 25 E). Subsequently, loss of RACK1 function inhibits JNK phosphorylation, caused by PTK7-dsh co expression (Fig. 25 E), supporting the hypothesis of RACK1 mediating PTK7-dsh signaling.

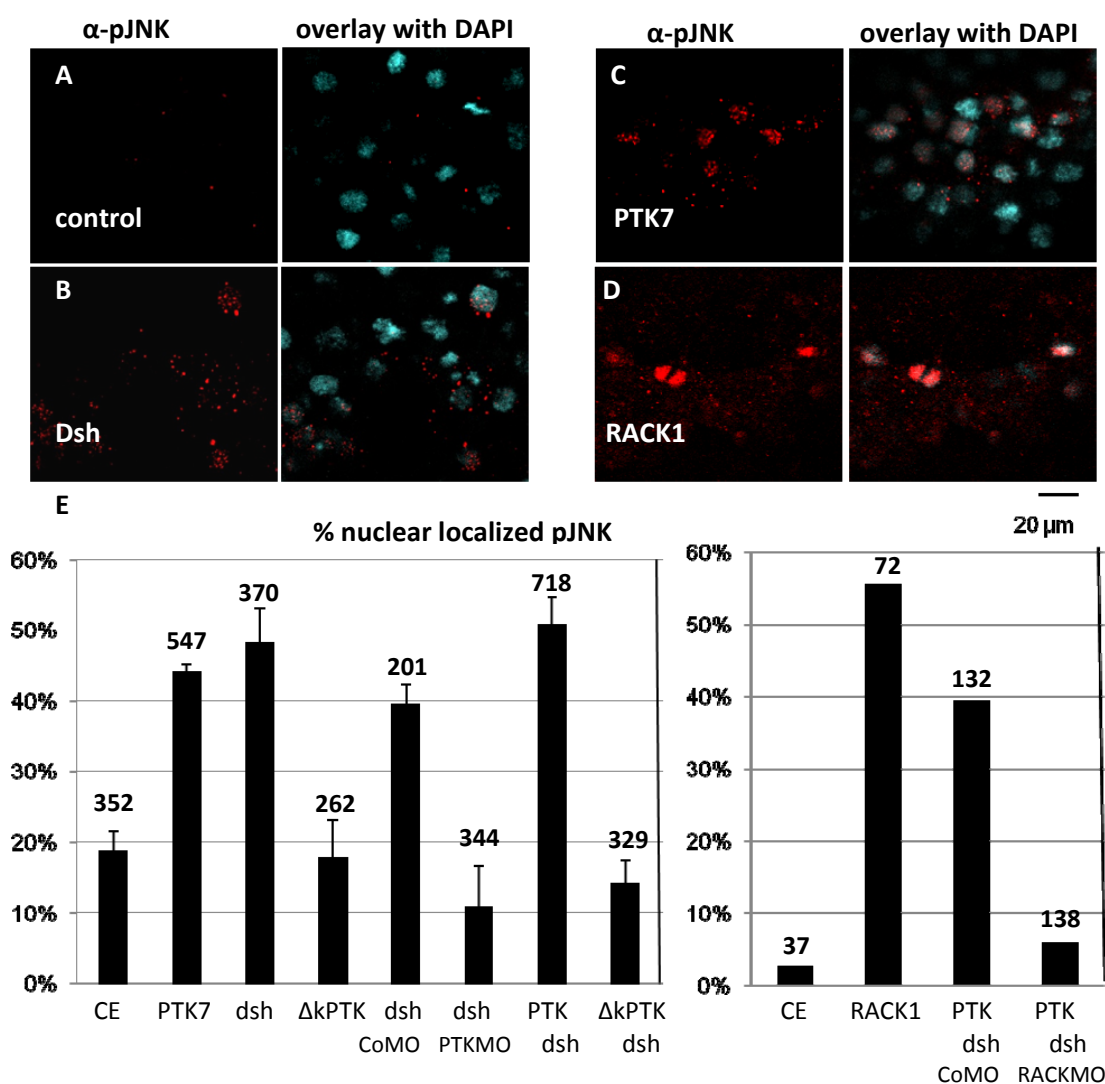


**Figure 4.17. Both RACK1 and PTK7 act upstream of dsh to activate JNK phosphorylation.** A-D Animal caps, stained with  $\alpha$ -phospho-JNK antibodies. (A) Control caps do not demonstrate high levels of JNK phosphorylation. Overexpression of dsh (B), PTK7 (C) or RACK1 (D) leads to phosphorylation of JNK. (E) Graph summarizing the percentage of cells with pJNK detected in the nucleus: overexpression of  $\Delta$ kPTK7 or co-injection of either PTK7-MO or RACK1-MO inhibits dsh-dependent JNK-activation. The graph on the left summarizes the results of three independent experiments. The graph on the right shows one out of two independent experiments.

## 4.2. The function of PTK7 in neural crest migration

### 4.2.1 PTK7 is expressed in the area of the pre-migratory and migratory neural crest cells

To further elucidate the *in vivo* function of PTK7 whole mount *in situ* hybridization (WISH) analysis of *Xenopus laevis* embryos was performed at different developmental stages. In addition to the neural tube, where it has been already shown to have a function (Lu et al., 2004), PTK7 is expressed in the area of the neural fold, pre-migratory and migrating neural crest cells (Fig. 4.18 A, B,C respectively, the mentioned areas are indicated with white arrow). Since recent data demonstrate an emerging role of PCP signaling in neural crest migration, the function of PTK7 in the NC migration was further addressed in the current work.

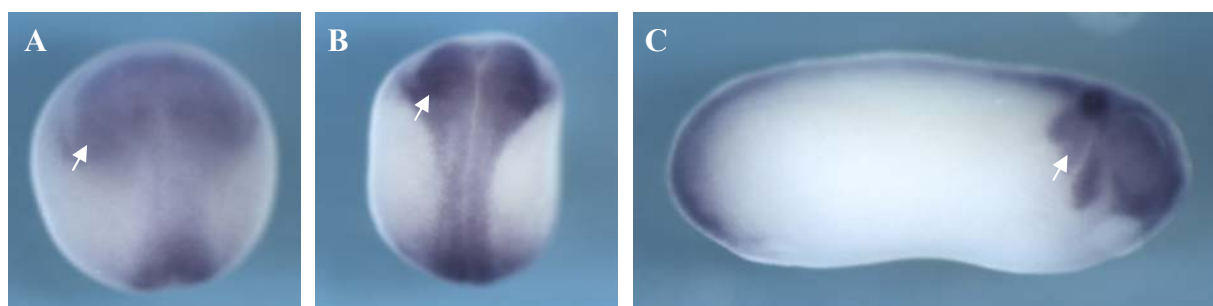


**Figure 4.18.** In *Xenopus laevis* embryo PTK7 is expressed in the area of pre-migratory and migrating neural crest. (A) At early neurula stages PTK7 is detected in the neural tube and prospective neural crest area. At late neurula (B) and tadpole stages (C) PTK7 is expressed in the neural tube and the neural crest. White arrows indicate the neural crest area.

### 4.2.2 PTK7 loss of function, but not the overexpression leads to defects in neural crest migration.

To investigate whether PTK7 has a function in neural crest development, its loss of function phenotype was analyzed. For this purpose *Xenopus laevis* embryos were injected with PTK7 MO and *GFP* RNA or  $\beta$ -galactosidase RNA as a lineage tracer into one blastomere at the two-cell stage and neural crest migration was analyzed by WISH at both neurula and tadpole stages with different NC-specific markers. The injection of the PTK7 MO inhibited neural crest migration both at neurula and tadpole stages. The WISH analysis of the PTK7MO-injected embryos showed, that *twist*-positive neural crest cells are induced, however they fail to migrate (Fig. 4.19 A). At the same time the induction and migration of *twist*-positive cells in the coMO-injected embryos was <sup>normal</sup> in (Fig. 4.19 B). At tadpole stages, a few migrating neural crest cells are observed in the embryos injected with PTK7 MO, however, their number and migration distance are reduced compared to the control (Fig. 4.19 C, D). Similar migration defects were also seen with other neural crest markers such as AP-2 and Sox10 (shown by Annette Borchers), whereas

the expression of the midbrain-hindbrain marker engrailed is not affected at the same MO concentrations (Fig. 4.19 D, right embryo). Thus, the PTK7 MO seems to specifically affect neural crest migration, without causing additional morphological changes.

To verify the specificity of PTK7 loss-of function rescue experiments were performed. For this purpose, embryos were injected with PTK7 MO in combination with either 100 pg or 1 ng wild-type PTK7 RNA lacking the MO-binding site. The injection was done in one blastomere at the two-cell stage using lacZ or GFP RNA as a lineage tracer. Subsequently, the neural crest migration was analyzed by WISH using twist probe both at neurula and tadpole stages. A total of three injection experiments, showing a concentration-dependent rescue effect of the PTK7 MO phenotype by wild-type *PTK7* RNA, is summarized on Figure 4.19, I.

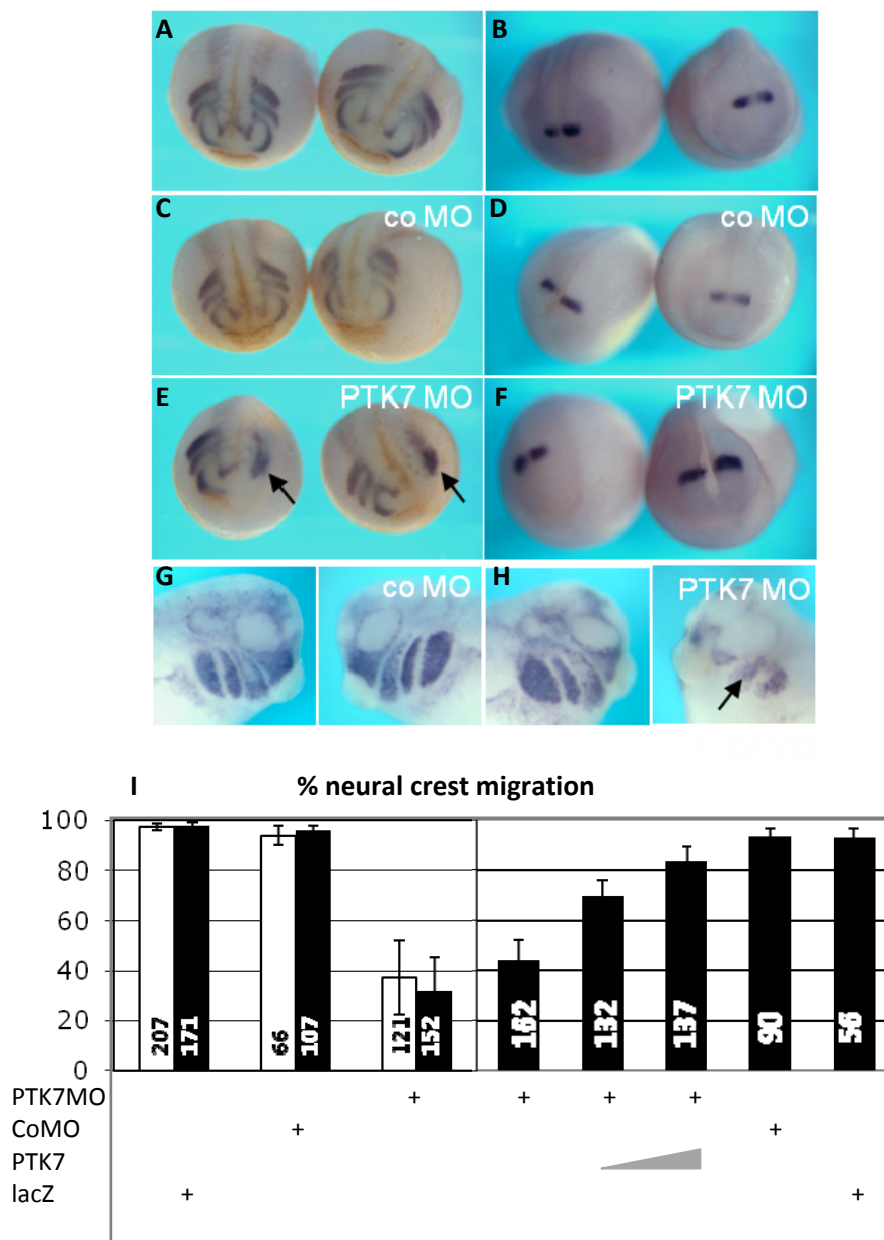


**Figure 4.19. Loss of PTK7 function causes neural crest migration defects.** (A-B) Control embryos, co-injected with a lineage tracer stained for neural crest marker Twist (A) or engrailed (B). Co-injection of control MO does not cause any effects on neural crest migration both at neurula (C,I) and tadpole stage (G,I). (D) The *engrailed*-specific staining did not reveal any major defects in neural tube development. The injection of PTK7-MO leads to neural crest migration defects on both neurula (E, injected side is marked with arrow) and tadpole (H, injected side marked with arrow) stages. At the same time neural tube development remains unaffected, which was verified by *engrailed*-specific staining (F). (I) Graph, summarizing the percentage of the neural crest defects in three independent experiments, as well as the rescue of PTK7 loss of function (also three independent experiments)

To further investigate the PTK7 function during the neural crest development, different concentrations of myc-tagged and untagged PTK7 RNA were injected in one blastomere at the two-cell stage and neural crest migration was analyzed at neurula and tadpole stages. In contrast to loss of PTK7 function, neither neural crest induction nor neural crest migration were affected by overexpression of PTK7 (Fig. 4.20 A-D). To verify the expression of the protein in



*Xenopus* embryo, a myc-tagged version of PTK7 was used and its expression was detected by western blot and immunostaining (Fig. 4.20 E, F). Thus, PTK7 is required for neural crest migration; however, an excess of the protein seems not to disturb neural crest development. Although the loss of PTK7 function affects primarily neural crest migration, it is difficult to exclude the possibility, that PTK7 can have an indirect influence on neural crest development, for instance by affecting neural tube closure. To prove that PTK7 harbors a specific function in the migration of neural crest cells further investigations were performed. The role of PTK7 in the neural crest migration is further tested by three different approaches: neural-crest-specific overexpression of PTK7 and its dominant negative construct, *in vitro* migration of explanted neural crest cells as well as neural crest transplantation experiments (NC transplantations were done by A. Borchers).

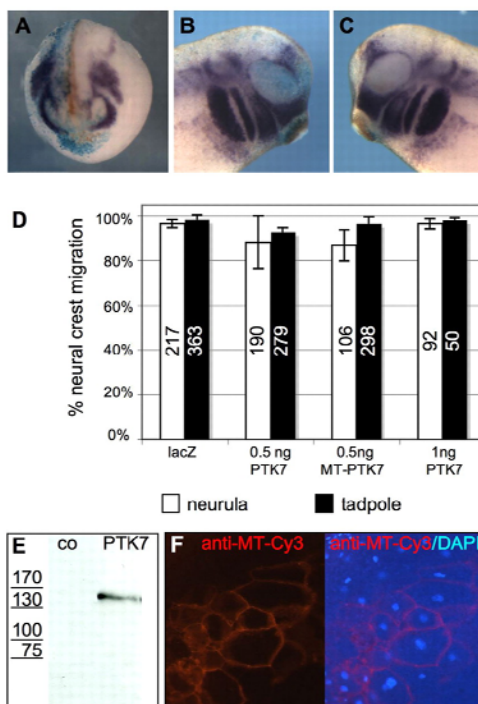


**Figure 4.20. PTK7 overexpression does not affect neural crest migration.** (A-C) Embryos were injected with 1 ng *PTK7* RNA and 50 pg *lacZ* RNA in one blastomere at the two-cell stage and analyzed for *twist* expression by in situ hybridization at neurula (A) and tadpole stages (B,C). Light blue *lacZ* staining marks the injected side. *Twist*-positive neural crest cells show normal migration at neurula (A) and tadpole stages (B,C). (B) Injected side of a tadpole stage embryo. (C) Uninjected side. (D) Graph summarizing the percentage of *twist*-expressing embryos injected with 50 pg *lacZ* RNA, 0.5 ng *PTK7* RNA, 0.5 ng myc-tagged *PTK7* RNA or 1 ng *PTK7* RNA at neurula and tadpole stages. Numbers on the columns indicate the number of injected embryos. (E) Confirmation of *PTK7* expression using western blotting (co, uninjected controls) or (F) immunostaining on transverse sections of neurula stage embryos injected with 0.5 ng myc-tagged *PTK7* RNA. In (F), membrane localization can be detected with a Cy3-coupled myc antibody (left panel). Right panel shows an overlay with the DAPI staining.

#### 4.2.3 Neural crest specific expression of $\Delta k$ PTK7 inhibits migration

In order to study the function of *PTK7* in neural crest migration independently from earlier developmental defects, and, particularly, neural tube closure; we targeted the expression of *PTK7* to neural crest cells. For this purpose, *PTK7* constructs, namely full length *PTK7* (Fig. 4.21 C, D) and its kinase deletion mutant ( $\Delta k$ PTK7) (Fig. 4.2 E,F), were expressed under the control of the neural crest-specific *slug* promoter, so that only cells, already specified to become neural crest, are affected. The  $\Delta k$ PTK7 was used as an antimorph, since it mimics *PTK7* loss of function phenotype (injection of 50 pg  $\Delta k$ PTK7 RNA caused 44% neural crest migration defects,  $n=122$ ) and fails to recruit *dsh* to the plasma membrane (Fig. 4.1 F). In the microinjection the plasmid DNA, containing the correspondent constructs, was used. This approach results in the neural

crest specific expression of selected molecules. However, DNA injection leads to mosaic expression of proteins, resulting in milder effects on NC migration. Therefore, a large numbers of embryos (around 200-300) was injected for one experiment and the 20-30% of migration defects were considered as a significant phenotype. The construct, containing GFP under the control of the *Slug*-promoter was used as a toxicity control. Plasmids were injected together with *lacZ* RNA as a lineage tracer in one blastomere at the two-cell stage and embryos were analyzed for twist expression at tadpole stages. The results demonstrate that the neural crest-specific expression of  $\Delta$ kPTK7 significantly inhibited the migration of twist-expressing neural crest cells (Fig. 4.21 E, F), whereas the expression of GFP or full-length PTK7 rarely affects neural crest migration (Fig. 4.21 A-D, G).

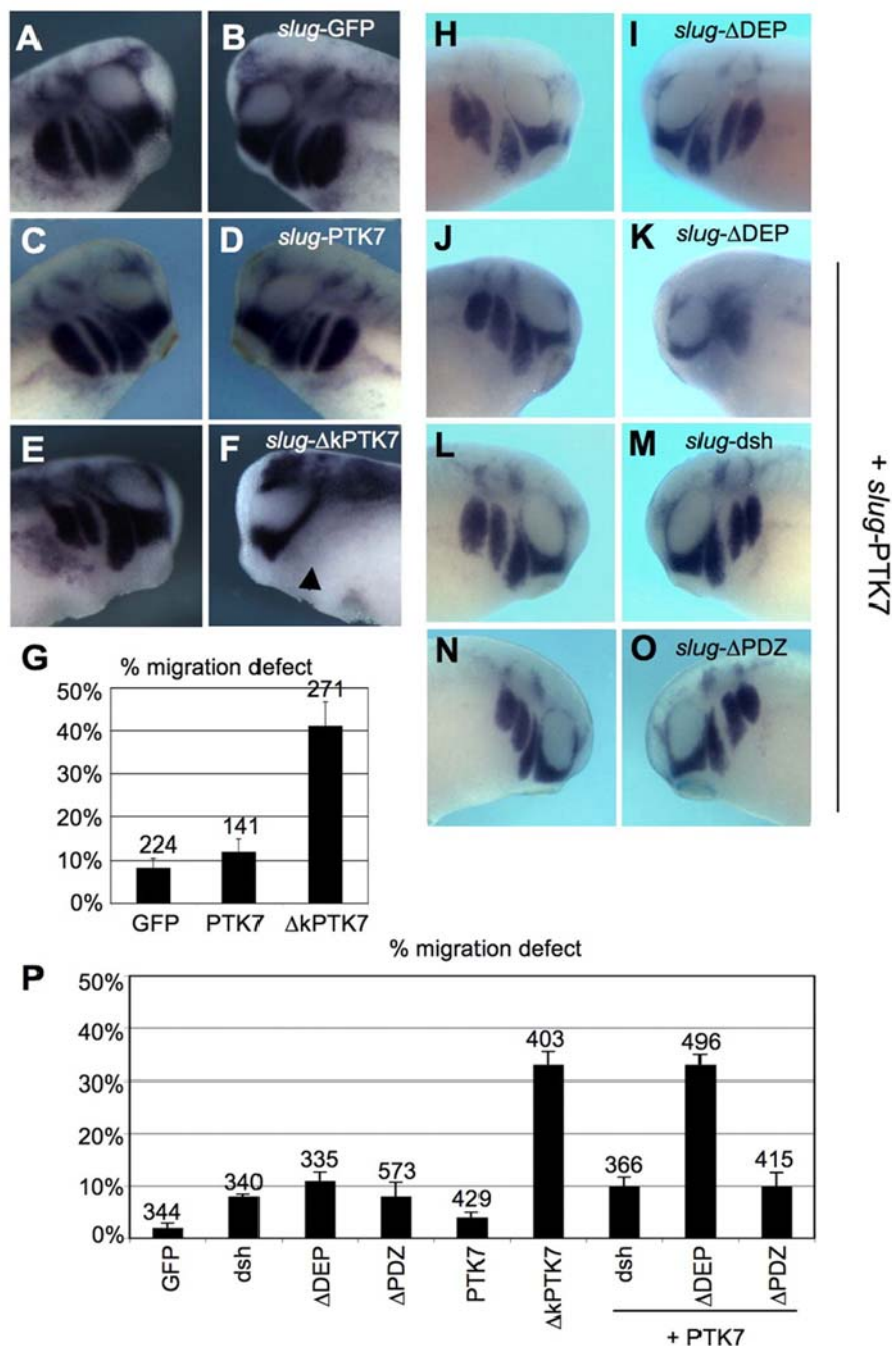


**Figure 4.21. Neural-crest-specific expression of PTK7 and dsh constructs.** Two-cell stage embryos were injected in one blastomere with plasmids containing a minimal *slug* promoter driving the expression of GFP (A,B), wild-type PTK7 (C,D) or  $\Delta$ kPTK7 (E,F) to NC. (A-F) Tadpole stage embryos analyzed by *twist* in situ hybridization. The injected side is presented in the right panel (B,D,F). (A,B) Embryo injected with 100 pg *slug*-GFP plasmid. (C,D) Embryo injected with 100 pg *slug*-PTK7 plasmid. (E,F) Embryo injected with 100 pg *slug*- $\Delta$ kPTK7. Arrowhead in F indicates the inhibition of neural crest migration. (G) Graph summarizing the percentage of neural crest migration defects in five independent injection experiments. The number of injected embryos is indicated on each column. (H,I) Embryo injected with 50 pg *slug*- $\Delta$ DEP. (J-O) Embryo injected with 50 pg *slug*-PTK7 together with 50 pg *slug*- $\Delta$ DEP (J,K) or 50 pg *slug*-dsh (L,M) or 50 pg *slug*- $\Delta$ PDZ (N,O). (P) Graph summarizing three dsh and PTK7 co-injection experiments. The number of analyzed embryos is indicated on each column.

#### 4.2.4 Recruitment of dsh DEP domain by PTK7 is required for neural crest migration

Since the neural crest specific overexpression of  $\Delta k$ PTK7 has an effect on NC migration, we decided to characterize the genetic interaction of PTK7 and dsh in migrating neural crest cells. For this purpose the expression of PTK7, as well as of different dsh mutants was targeted to neural crest cells using the same *slug* promoter system. To equilibrate the expression levels during the injection of single constructs, *slug*-GFP was co-injected.

First, it was analyzed, whether the expression of dsh,  $\Delta$ PDZ dsh or  $\Delta$ DEP dsh under the control of *Slug*-promoter affects neural crest migration. The  $\Delta$ PDZ dsh, was chosen because it cannot be recruited to the plasma membrane by PTK7, and  $\Delta$ DEP dsh, because it acts as a dominant negative dsh towards the PCP activity and affects neural crest migration (De Calisto et al., 2005; Park et al., 2005). However, single injections of all dsh constructs result in very mild neural crest migration defects (Fig. 4.21 H, I, P). The same holds true for the neural crest specific co-expression of PTK7 together with full length dsh or  $\Delta$ PDZ dsh (Fig. 4.21 L-P). However, the combination of *slug*-PTK7 with *slug*- $\Delta$ DEP constructs results in the inhibition of neural crest migration, comparable to the effect of *slug*- $\Delta k$ PTK7 (Fig. 4.21 J,K,P), which fails to recruit dsh to the plasma membrane. Thus, although  $\Delta$ DEP dsh can be recruited by PTK7, its lack of PCP activity inhibits neural crest migration.

#### 4.2.5 PTK7 is necessary for the migration of explanted neural crest cells

To further prove that PTK7 specifically affects the migration of NC cells, an *in vitro* neural crest migration assay was employed. GFP-tagged PTK7,  $\Delta k$ PTK7 or PTK7-MO together with mRFP were injected into one blastomere at the two cell stage. The embryos were grown to stage 16-17 and then the cranial neural crest was excised from an embryo with a cat-whisker knife and explanted on a fibronectin coated dish. During the first 30 min neural crest cells start to migrate out of the graft, and their migration was analyzed by time-lapse imaging during the next 3-6 hours. The usage of fluorescently tagged constructs allows to observe the migratory behavior of only those cells, which were targeted by microinjection. The results of the time-lapse series demonstrate, that NC cells expressing GFP-PTK7 show active migration on fibronectin (Fig. 4.22 A), while the expression of  $\Delta k$ PTK7 as well as the injection of PTK7 MO strongly inhibits neural crest migration (Fig. 4.22 B, C). Interestingly,  $\Delta k$ PTK7 expressing cells were still able to form lamellipodia and start to migrate (Fig. 4.22 B), while PTK7 MO targeted cells show a round shape and form stress fibers (Fig. 4.22 C).

In addition, the fluorescent imaging of PTK7-GFP expressing neural crest cells reveal the asymmetric distribution of PTK7 within a cell. Neural crest cells are polarized and start their migration as a group. The cells, which start migrating first, form big lamellipodia at the leading

edge and remain in contact with other cells at the trailing part. The analysis of PTK7-GFP distribution within NC cells demonstrate, that PTK7 is enriched on the membrane at cell-cell contacts and shows weak diffuse staining in lamellipodia (Fig. 4.22 D, white arrowhead). To further investigate PTK7 redistribution within migrating neural crest cells we used laser scanning microscopy.

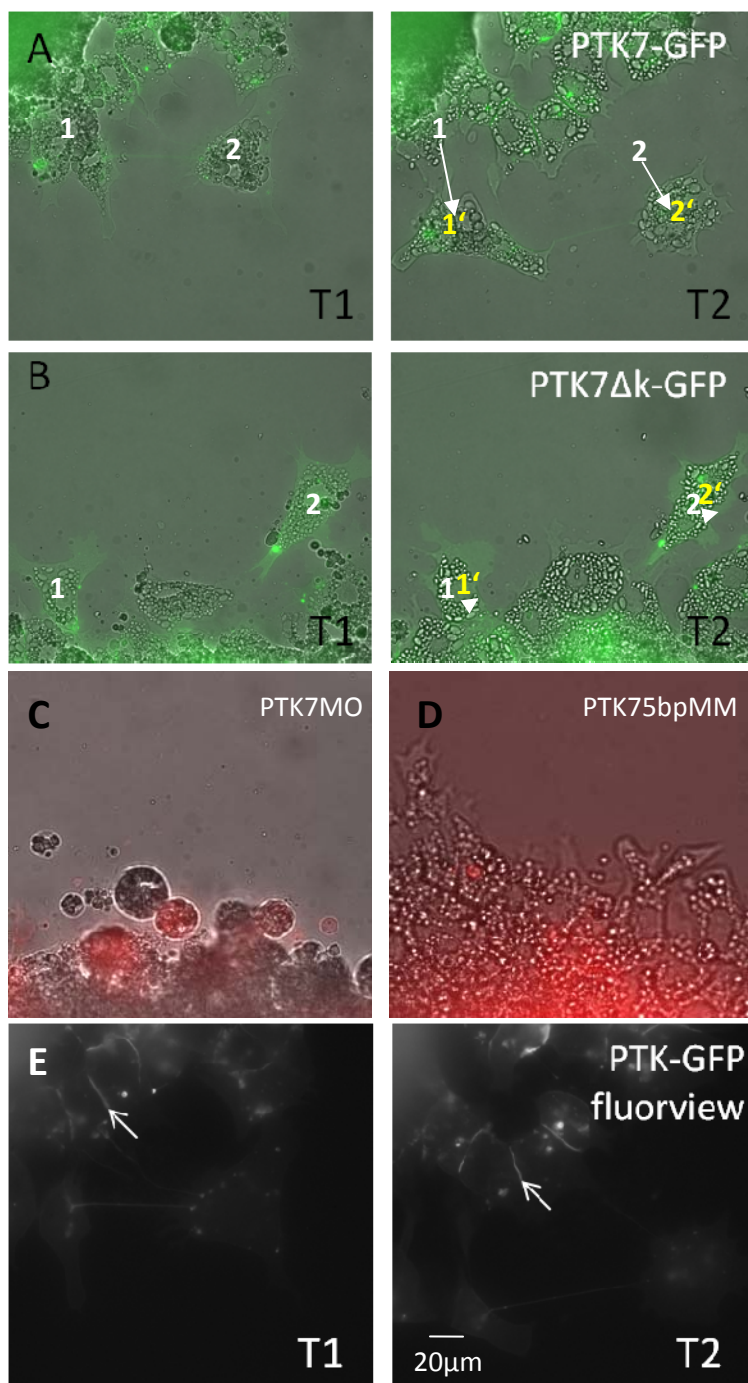


**Figure 4.22. PTX7 is required for *in vitro* neural crest migration.** (A) Overexpression of GFP-tagged PTX7 (500 pg of the RNA) did not inhibit the migration of neural crest cells on fibronectin. T1 and T2 – points of the time lapse, approximately 1h in difference. The numbers 1 and 2 indicate the position of the two selected cells at the beginning of the time-lapse, 1' and 2' indicate the position of the same cells 1h later, white arrows show the straight distance, covered by the cells. (B) The kinase deletion mutant of PTX7 inhibits neural crest migration. Similar to (A) 1 and 2 indicates the position of selected cells and white arrows show their migration distance. During the period of 1h no significant migration was observed, however the cells do form lamellipodia. (C) The injection of 10ng PTX7-MO blocks neural crest migration. The image of PTX7MO explants 2,5h after the explantation, the cells injected with PTX7-MO and RFP as a lineage tracer display predominantly round shape. (D) The explants, injected with PTX7MM and RFP as a lineage tracer show migration 2,5h after the explantation. (E) The fluorescent image of PTX7-GFP timelapse (A), the arrowheads indicate PTX7 enrichment in cell contacts

#### 4.2.6 PTK7 localizes at cell-cell contacts and possesses homophilic binding

The confocal analysis of fixed immunostained explants also shows, that PTK7 is enriched on the plasma membrane at cell-cell contacts (Fig. 4.23 A, red arrows). Interestingly, PTK7 localizes to the membrane not only at initial contacts between cells, but also restored the membrane localization in newly formed contacts.

**$\alpha$ -MT-PTK7 immunostaining overlaid with the explant DIC image**

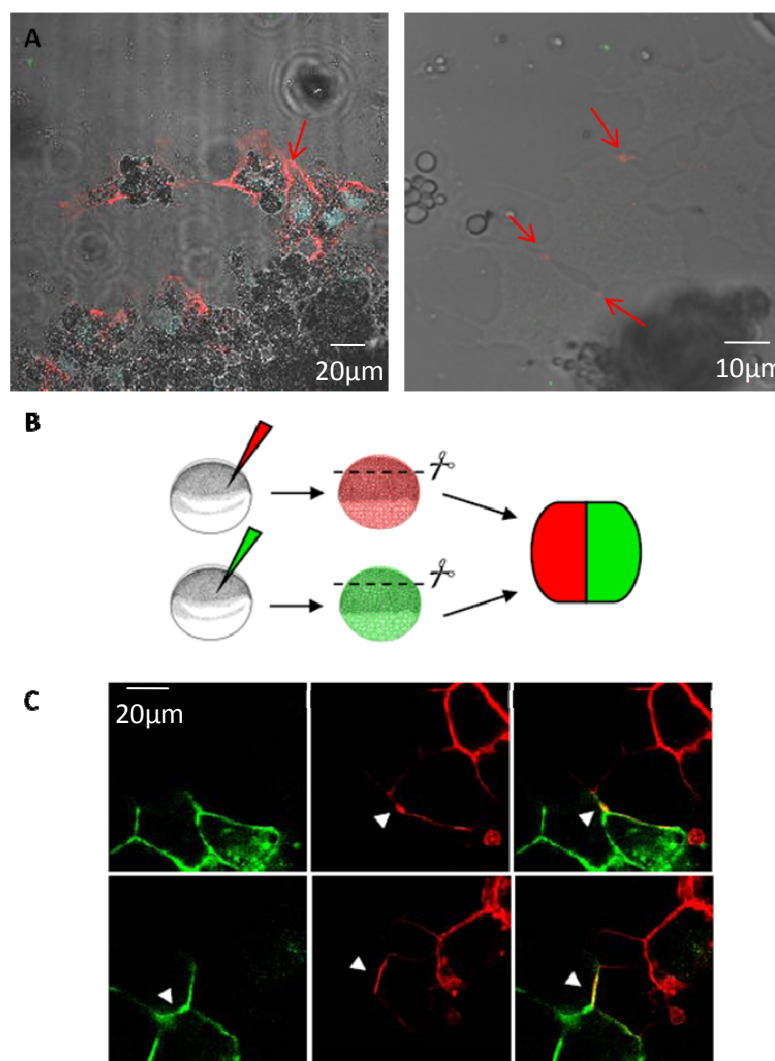


**Figure 4.23. PTK7 is enriched at the area of cell-cell contacts.** (A) PTK7 is localized to the cell contacts in migrating NC cells (red arrows). The localization of myc-tagged PTK7 was analyzed by the laser scanning microscope after immunostain with  $\alpha$ -myc antibodies. (B) Experimental set-up to monitor the co-localization of the differently tagged PTK7 versions in the ectodermal explants: animal caps expressing either myc-tagged (red) or HA-tagged (green) versions of PTK7 were cut and fused together. The fusion area was visualized by LSM (C). PTK7 demonstrates the enrichment from the both sides of the contact (white arrowheads).

In addition, PTK7 enrichment in cell-cell contacts was further analyzed in animal cap cells. For this purpose differently tagged versions of PTK7, PTK7-MT and PTK7-HA, were injected anally into embryos. At blastula stages the ectodermal explants were cut and then PTK-HA



explants were fused with PTK7-MT explants immediately upon the cutting and stained with correspondent antibodies (Fig. 4.23 B). The explants fusion area was analyzed by confocal microscopy, which demonstrates, that PTK7 also increases at the plasma membrane in the regions, where both PTK7 expressing cells contact each other (marked with white arrow), compared to regions, where they contact non-expressing cells (Fig 4.23 C).

Structurally, the extracellular part of PTK7 consists of seven immunoglobulin-like domains, which can also be found in several homophilic binding molecules, like cadherins. To test, whether PTK7 possesses homophilic binding, co-immunoprecipitation from *Xenopus* lysates was performed. MT-PTK7 was co-precipitated with its HA-tagged version, proving a homophilic binding (Fig. 4.24). The obtained results were refined by co-immunoprecipitation between different PTK7 deletion mutants. This further demonstrates that the extracellular piece of PTK7 possesses homophilic binding properties (Martina Podleschny, unpublished data). Thus, by interacting with each other through the extracellular part, PTK7 molecules may cluster at the points, where two PTK-expressing cells form a contact.

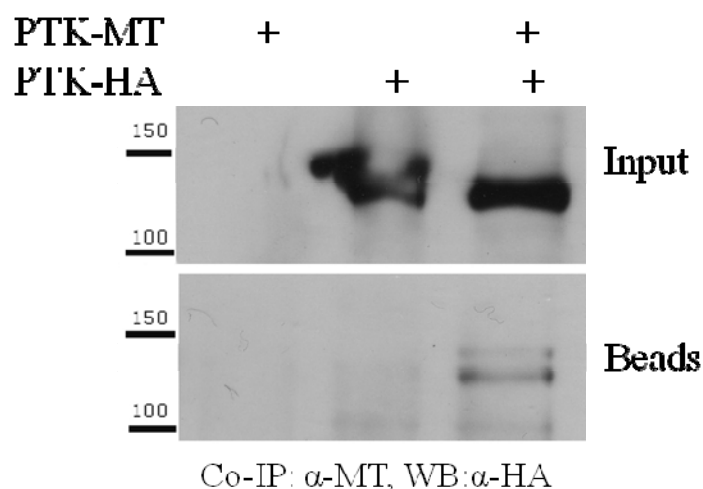


**Figure 4.24. PTK7 possess homophilic binding.** Differently tagged versions of PTK7, PTK7-MT and PTK7-HA, were overexpressed in *Xenopus* embryo (500pg of each RNA was injected at 1-cell-stage). At gastrula stages the co-immunoprecipitation was performed with  $\alpha$ -myc antibodies. HA-tagged PTK7 was detected in the lysate, when expressed alone and together with MT-PTK7 (Input, upper line). However, upon the co-immunoprecipitation the HA-tagged PTK7 was only detected in the lane, where the myc-tagged version is present (Beads, lower lane), which indicates the interaction

#### 4.2.7 PTK7, but not its kinase deletion mutant co-localizes with dsh in migrating neural crest cells

Since PTK7 forms a complex with dsh and both proteins have a function in neural crest migration, they should co-localize in migrating neural crest cells. To test whether this is true, RNAs encoding for MT-PTK7, MT $\Delta$ kPTK7 and GFP-dsh were injected animally in the one-cell stage embryos and at stage 16-17 the neural crest cells were explanted and upon three hours of

migration fixed, immunostained and analyzed by confocal microscopy. In parallel, stage 16-17 embryos were embedded in gelatin-albumin, sectioned and immunostained to observe, whether dsh co-localizes with PTK7 *in vivo*. In the sections neural crest cells were marked with  $\alpha$ - $\beta$ 1-integrin antibodies.

The imaging of explanted NC demonstrated, that PTK7 co-localizes with dsh at the area of cell contacts, additionally dsh demonstrate a cytoplasmic enrichment in newly formed lamellipodia (Fig. 4.25 A, lamellipodia are marked with blue arrows, cell contacts – with white arrows). Surprisingly, a weak signal of MT-PTK7 was also detected in lamellipodia, which may indicate that PTK7 is also required for dsh signaling there. However, the specificity of the obtained signal should be further verified (Fig. 4.25 B, lamellipodia are marked with blue arrows, cell contacts – with white arrows). As the neural crest explants expressing  $\Delta$ kPTK7 together with dsh are inhibited in their migration, the confocal imaging is not shown for these explants. On sections of the whole embryo dsh displays membrane localization as well as co-localization with PTK7 in the neural crest area (Fig. 4.23 C, D). In accordance with the animal caps data, co-expression of dsh and  $\Delta$ kPTK7, as well as dsh with PTK7MO, results in dsh dislocalization from the plasma membrane (Fig. 4.23 D, E). Thus the kinase homology domain of PTK7 is necessary to recruit dsh to the plasma membrane *in vivo* in migrating neural crest cells.

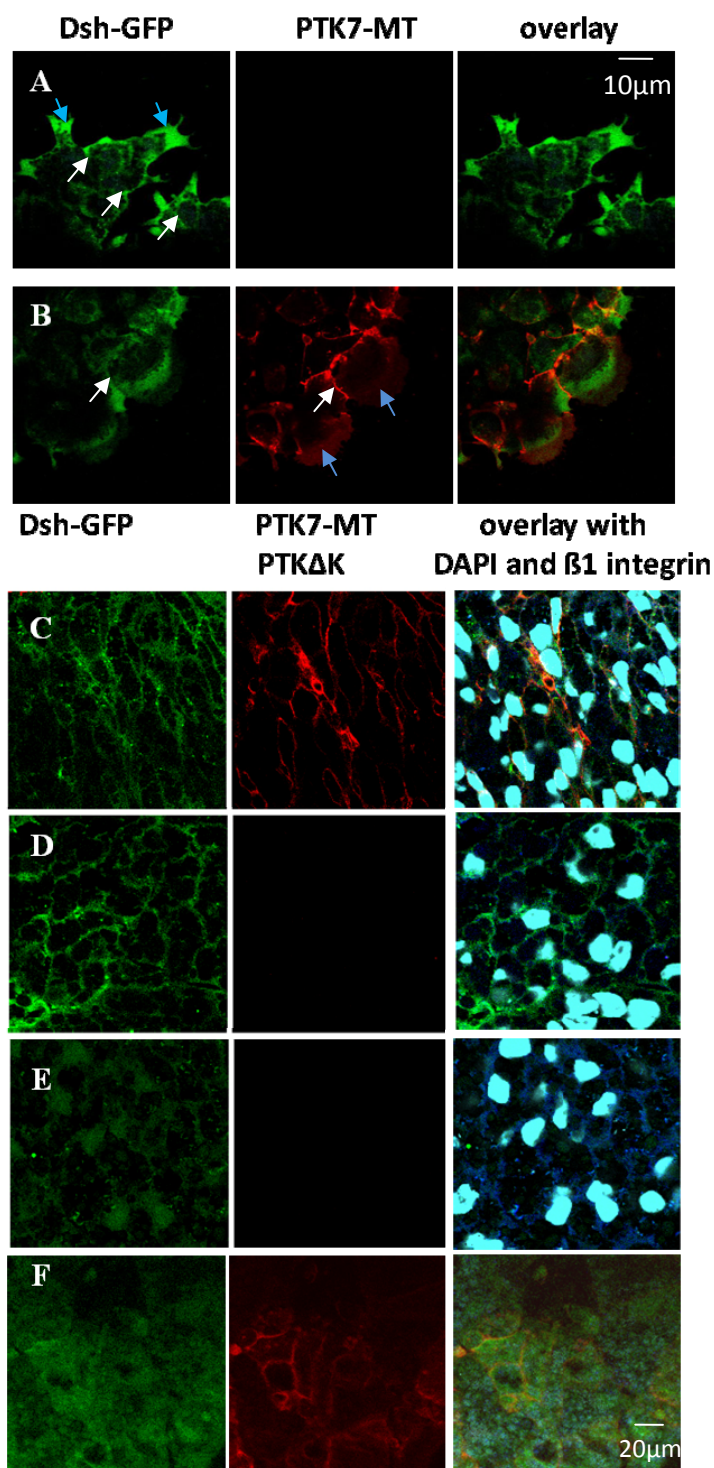


**Figure 4.25. PTK7 co-localizes with dsh in migrating neural crest.** (A-B) Migrating neural crest explants, which overexpress either dsh-GFP or dsh-GFP together with PTK7-MT (100 pg and 500 pg mRNA respectively) were immunostained and analyzed by confocal microscopy. The dsh protein localizes to cell contacts (white arrow) and lamellipodia (blue arrow) (A), PTK7 co-localizes with dsh in cell contacts (white arrow), weak staining for PTK7 was also detected in lamellipodia (blue arrow) (B). (C-F) Sections through the neural crest are stained for dsh-gfp, PTK7-MT, DAPI and  $\beta$ 1-integrin to label the neural crest cells. Dsh shows primarily membrane localization, when overexpressed alone (D) or with PTK7-MT (C). The co-injection of PTK7-MO (E) or  $\Delta$ kPTK7-MT (F) inhibits dsh translocation to the plasma membrane.

#### 4.2.8 PTK7 may be required for contact inhibition of locomotion

It was recently shown, that migrating neural crest cells possess contact inhibition of locomotion, which is regulated by dsh recruitment to cell contacts and subsequent activation of Rho-GTPase (Carmona-Fontaine et al., 2008). Since PTK7 is a homophilic binding molecule, which localizes to cell contacts in migrating neural crest cells and recruits dsh to the plasma membrane, it was tested, whether PTK7 is also necessary for contact inhibition of locomotion. For this purpose a NC explants confrontation assay was employed. The explants from either PTK7MO or control MO injected embryos were placed in front of control explants and the interaction of migrating NC cells was observed during the period of several hours. The results demonstrate, that upon contact with control MO explants, migrating neural crest cells change the direction of migration (Fig 4.26 A, blue arrows indicate direction of migration before the contact, red arrows – after the contact). In contrast upon the contact with PTK7 MO cells, the contacting control cell migrates further on top of the PTK7 MO explants without any changes in the direction of movement (Fig. 34 B). This effect with PTK7 MO explants was observed in three independent experiments. In addition, the neural crest fate of PTK7 MO explants was verified by WISH using  $\alpha$ -Slug probe, demonstrating that the injection of PTK7MO does not change NC fate (data not shown).

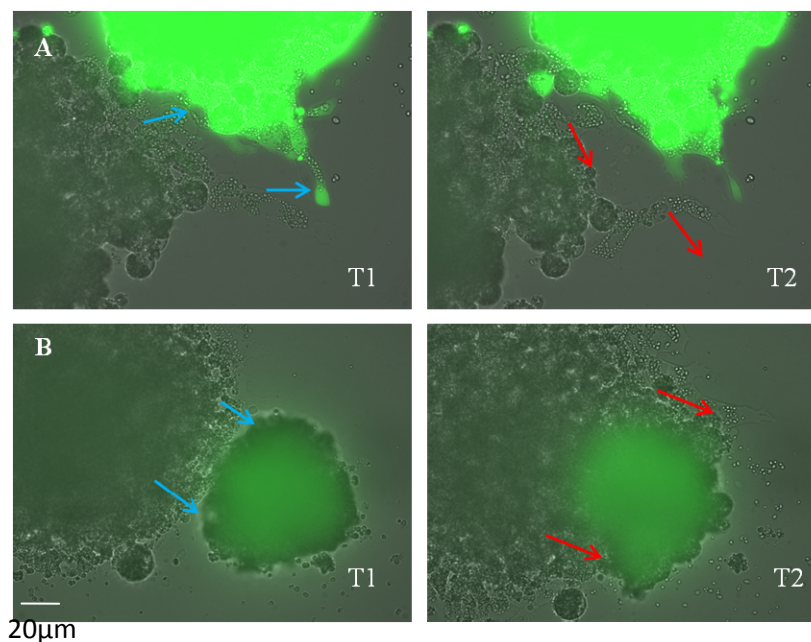


**Figure 4.26. PTK7 mediates contact inhibition of locomotion.** (A) The explants injected with control MO and GFP as a lineage tracer demonstrate contact inhibition of locomotion in the confrontation assay with uninjected explants. T1 and T2 are different frames of the time-lapse movie. At T1 CoMO explants is in contact with control explants, however at T2 NC cells start migrating in different direction. (B) The confrontation assay between PTK7-MO explants (green) and control explants. At the T1 explants are in contact, however, the direction of migration does not change over time (T2). Blue arrows indicate the direction of lamellopodia formation/migration before the contact, red arrows – after the contact.

#### 4.2.9 RACK1 can also regulate neural crest migration

RACK1 was shown to interact and signal downstream of PTK7. At the same time, both proteins are expressed in the area of pre-migratory and migrating neural crest (Kwon et al., 2001). Since loss of PTK7 function affects neural crest migration, the depletion of RACK1 should result in similar effects. However, the injection of RACK1 MO1 does not demonstrate severe neural crest migration defects. Furthermore, the presence of either RACK1 MO1 or MO2 in the explanted neural crest does not show significant inhibition of cell migration. However, preliminary data shows that the injection of RACK1 MO1 and MO2 combination affects the migration of explanted neural crest (Figure 4.27), indicating that IRACK1 may function during neural crest migration.

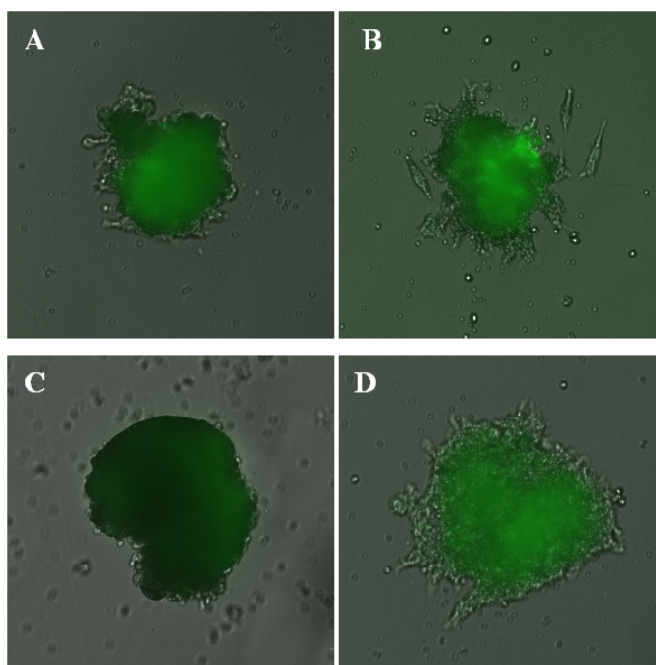


**Figure 4.27. RACK1 loss of function affects the migration of explanted neural crest cells.** Explants, injected with 20 ng RACK1 MO1, MO2 or their combination and GFP as a lineage tracer were cultured on fibronectin, where their migration was observed for 2h. RACK1 MO1 (A) as well as RACK1 MO2 (B) explants migrate in the most of cases, while the combination of both morpholinos (C) inhibits neural crest migration. The control MO explants (D) demonstrate no migration defects. The experiment was done once with 10 explants analyzed for each injection. In the result 90% of control explants, as well as 80% of MO1 or MO2 injected explants migrate normally, while in the case of the explants with the MO1 and MO2 combination the migration was observed in 20% of cases.

Finally, NC explants expressing GFP-tagged PTK7 together with HA-tagged RACK1 were analyzed by confocal imaging to observe the co-localization of both proteins. GFP-tagged PTK7 was localized in cell contacts, while RACK1-HA was found in the cytoplasm as well as at the cell contacts, where it co-localizes with PTK7 (Fig. 4.28, white arrows). Interestingly, similar to dsh, RACK1 was also accumulated in lamellipodia, where these proteins can act together (Fig. 4.28, blue arrows).

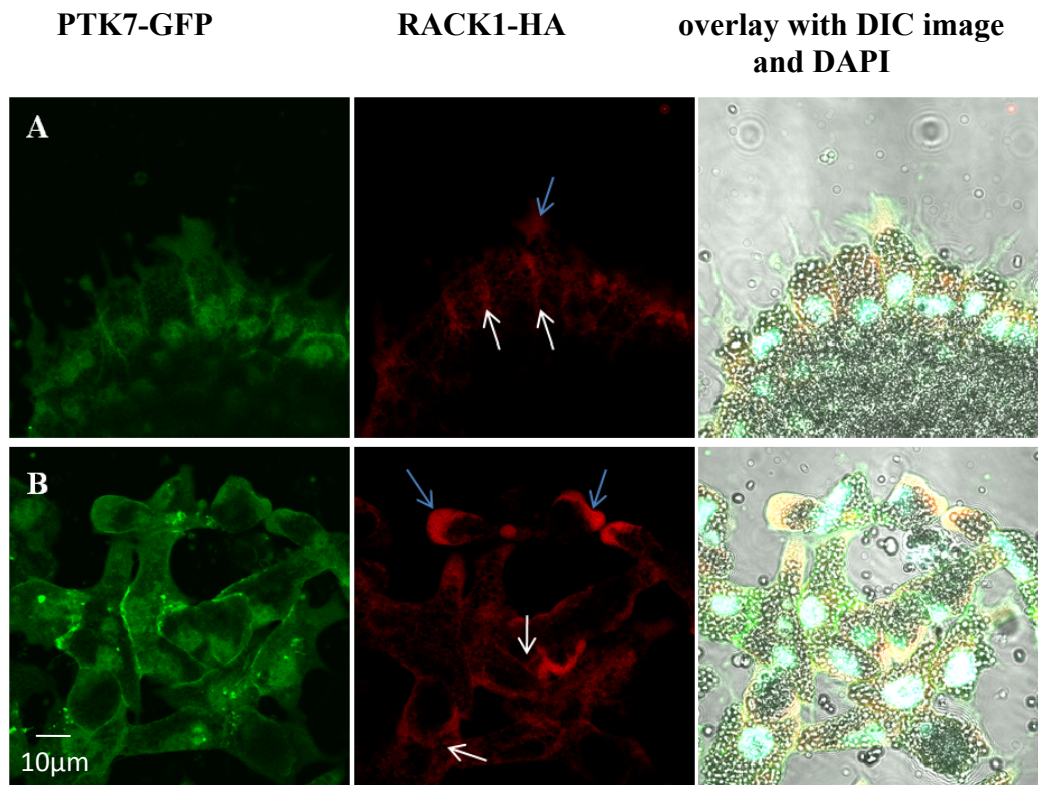


**Figure 4.28. RACK1 co-localizes with PTK7 at cell contacts.** (A-B) The NC explants with RACK1-HA (250 pg of mRNA injected) and PTK7-GFP (500 pg). (A) and (B) corresponds to different time points of migration: in (A) the cells are migrating as a branch, while in (B) – they migrate rather as single cells. PTK7-GFP is enriched at cell contacts and RACK1-HA co-localizes with PTK7 at these points (white arrows). Additionally RACK1 is enriched in lamellipodia (blue arrows)

## 5. Discussion

The aim of this project was to characterize the signaling function of PTK7 in neural crest migration. PTK7 was identified as a regulator of the planar cell polarity signaling, necessary for neural convergent extension and the establishment of stereocilia orientation (Lu et al., 2004). Planar cell polarity signaling is a branch of Wnt signaling, which is involved in the regulation of complex morphogenetic movements in vertebrates (Simons and Mlodzik, 2008). The studies on the knockout mice showed that PTK7 interacts genetically with Vangl1, which points to its emerging role in the regulation of the PCP signaling (Lu et al., 2004). However, it was not entirely clear, where exactly PTK7 intersects with PCP signaling cascade. Using a candidate approach it was demonstrated that PTK7 acts by recruiting dsh to the plasma membrane. And the screening for the novel PTK7 binding partners revealed that PTK7-dsh interaction is mediated via the RACK1 and PKC $\delta$ . Moreover, PTK7 is a component of the fz7-dsh complex, which is necessary for the fz7-mediated dsh membrane recruitment and phosphorylation. The analysis of PTK7 expression pattern during *Xenopus laevis* embryogenesis revealed that, in addition to the neural tube area, PTK7 is expressed in the pre-migratory and migrating neural crest. Since it has been already shown, that several PCP components are required for neural crest migration (Bekman and Henrique, 2002; De Calisto et al., 2005; Goto and Keller, 2002; Nakaya et al., 2004), the second part of the work was dedicated to analyze the PTK7 function during this process. The analysis of the PTK7 gain- and loss-of function phenotypes revealed, that PTK7 is required for the neural crest migration. Moreover, the neural crest specific co-expression of PTK7 with dsh deletion mutant show, that PTK7-mediated membrane recruitment of the DEP-domain of dsh is crucial for NC migration.

### 5.1 PTK7 functions in PCP signaling

Dsh is a key regulator of Wnt signaling, which, probably, serves as a branching point between canonical and PCP signaling pathways. The dsh protein is known to interact with more than 30 proteins and the majority of these interactions depend on the activation of distinct Wnt-signaling pathways. For instance, during the activation of canonical Wnt signaling dsh forms a complex with axin, while during PCP signaling it interacts with DAAM and activates RhoA etc (Wallingford and Habas, 2005). In addition, the intracellular localization of dsh shows a correlation between the activation of different Wnt signaling branches. Thus, during the PCP activity dsh demonstrates primarily membrane recruitment, while during  $\beta$ -catenin pathway it locates to the cytoplasm and could be translocated to the nucleus (Itoh et al., 2005; Rothbacher et al., 2000; Sokol, 1996). Upon the co-expression with PTK7 in animal cap cells, cytoplasmically localized dsh is recruited to the plasma membrane (Fig. 4.1), thus indicating an interaction

between these two proteins and, possibly, activation of the PCP signaling. In addition, the complex formation between PTK7 and dsh was also supported by glycerol gradient density ultracentrifugation, where dsh tails to the higher fractions in the presence of PTK7 (Fig. 4.2). However, co-immunoprecipitation experiments did not reveal any PTK7-dsh binding, which suggests that other molecules are required for PTK7-dsh interaction.

*Xenopus* Frizzled 7 is another PCP regulator, shown to bind dsh and recruit it to the membrane (Medina and Steinbeisser, 2000). Since both fz7 and PTK7 were shown to regulate CE movements and recruit dsh to the membrane, they could interact to regulate PCP signaling (Axelrod et al., 1998; Medina and Steinbeisser, 2000). Consistently, our immunoprecipitation experiments have demonstrated that PTK7 can be co-precipitated together with both Fz7 and dsh in *Xenopus* lysates, which proves complex formation of these proteins (Fig. 4.4). Interestingly, in MCF7 cells PTK7 as well as its kinase deletion mutant can be pulled down by Frizzled7 alone (M. Podleschny, unpublished data), which could be explained by a relatively high amount of endogenous dsh, which is not engaged in any of the signaling cascades, and can therefore stabilize PTK7-Fz7 interaction. Alternatively, since PTK7 was shown bind Wnt molecules (Hanna Peradziryi, unpublished data), the stability of PTK7-fz7-dsh complex may depend on the presence of appropriate Wnt proteins. Finally, the Fz7-dsh-PTK7 complex could be stabilized by additional interaction between PTK7 and dsh, mediated via other downstream components, which will be discussed below.

Since PTK7 was found to interact with fz7-dsh, we tested how the formation of Fz7-PTK7-dsh complex is affected by loss of function of either PTK7 or fz7. The injection of PTK7 MO significantly inhibits FZ7-dsh co-localization on the plasma membrane. Moreover, PTK7 leads to inhibition of Fz7-dependent dsh hyperphosphorylation (Fig. 4.5 and 4.6), which associates with dsh membrane recruitment and Wnt signaling activation (Rothbacher et al., 2000). Interestingly, loss of PTK7 function also affects fz7 membrane localization and this effect can be rescued by co-injection of PTK7 RNA, lacking the MO binding site (Fig. 4.5, E). Thus, PTK7 may stabilize fz7 at the plasma membrane in the proper conformation to recruit dsh. Contrary to PTK7 loss of function, the injection of fz7 morpholinos does not significantly affect PTK7-dsh co-localization at the plasma membrane. This phenomenon could be explained by the fact, that other molecules of the frizzled family can stabilize the PTK7-dsh complex. In fact, two other frizzleds, fz4 and fz8, are expressed in animal cap cells (Fig. 4.7 A). And, indeed, PTK7 was shown to bind Fz8 in MCF7 cells and mediate Fz8-dependent dsh recruitment and phosphorylation (Hanno Sjuits, unpublished data). Interestingly, the PDZ domain of dsh is crucial for its PTK7-mediated membrane recruitment, while the localization of  $\Delta$ DEP-dsh and  $\Delta$ DIX-dsh did not show significant differences (Fig. 4.3). These data are controversial to the fz7-mediated dsh membrane



recruitment, since it was already demonstrated that deletion of the DEP domain is required for fz7-dependent dsh localization (Axelrod et al., 1998; Pan et al., 2004). This suggests that PTK7 has additional mechanisms to recruit dsh to the plasma membrane. Since the kinase homology domain of PTK7 is required for dsh recruitment, it could dimerise and be phosphorylated by other kinases, which link dsh to it. The *in silico* analysis of PTK7 C-terminal with a ProSite online tool revealed high probability PKC-phosphorylation sites. And since PKC $\delta$  has a function in the regulation of PCP signaling and fz7-mediated dsh membrane recruitment, it seemed to be a likely candidate to link dsh to PTK7. However, the co-immunoprecipitation experiments did not prove direct binding between PTK7 and PKC $\delta$ . Therefore a mass-spectrometry analysis was employed to identify PTK7 binding partners, which could mediate dsh membrane recruitment.

### **5.2 RACK1 is a novel PTK7 binding partner, which mediates its dsh membrane recruitment**

Among several putative PTK7 interacting proteins we identified the receptor of activated PKC 1 (RACK1). RACK1 is a scaffold protein, which consists of seven tryptophane-aspartate domains (WD40 domains) forming a  $\beta$ -propeller-like structure. RACK1 was originally identified as a protein, which mediates the interaction of the activated PKC with its downstream targets. It is involved in variety of cell biological processes including the regulation of protein translation, proliferation as well as cell migration (McCahill et al., 2002; Nilsson et al., 2004; Sklan et al., 2006). The function of RACK1 during development was not elucidated. However, the expression pattern of RACK1 *Xenopus* ortholog was published elsewhere and exhibits almost complete overlap with PTK7 expression pattern (Kwon et al., 2001). In human tissue culture, RACK1 was shown to bind PKC $\delta$  and mediate PKC-dependent JNK phosphorylation (Lopez-Bergami et al., 2005). PKC $\delta$  belongs to the PKC superfamily and has two homologues, PKC $\delta$ 1 and PKC $\delta$ 2, in *Xenopus*. Both of the homologues are implicated in the regulation of PCP signaling via the interaction with dsh and regulation of its Fz7-dependent recruitment and phosphorylation (Kinoshita et al., 2003). Since RACK1 interacts with PKC $\delta$ , which in turn binds dsh, RACK1 is a likely candidate to link PTK7 with dsh.

Immunoprecipitation experiments with both *in vitro* translated proteins and *Xenopus* embryo lysates confirm the direct nature of the PTK7-RACK1 interaction. Moreover, RACK1 also co-localizes with PTK7 in animal cap cells, where it may mediate dsh recruitment. Conversely, the PTK7 kinase deletion mutant, which fails to recruit dsh to the plasma membrane, does not co-localize with RACK1 in the animal cap assay (Fig. 4.8 and 4.12). The experiments in animal cap cells indeed demonstrate that loss of RACK1 function affects PTK7-dsh co-localization. Thus RACK1 serves as a scaffold protein, possibly, mediating the PTK7-dsh interaction (Fig. 4.13).

Surprisingly, the co-immunoprecipitation experiments of *in vitro* translated proteins do not show RACK1-dsh binding. Since RACK1 was known to directly bind human PKC $\delta$  (Lopez-Bergami et al., 2005), and this interaction is conserved in *Xenopus* (Fig. 4.14, A), it is likely that PKC $\delta$  binds dsh and provides a link between dsh and RACK1/PTK7 (Kinoshita et al., 2003). Furthermore, PKC $\delta$  is also recruited to the membrane by PTK7 in a RACK1-dependent manner (Fig. 4.14) and, subsequently, loss of PKC $\delta$ 1 function affects PTK7-dsh co-localization in animal cap cells (Fig. 4.15). In conclusion, the PTK7-RACK1-dsh interaction is dependent on PKC $\delta$  and thus the PTK7 intersection with PCP signaling components may be illustrated by the model indicated on the Figure 5.1. Here, PTK7 interacts with RACK1, which in turn recruits PKC $\delta$  and dsh to the plasma membrane. The extracellular part of PTK7 interacts with fz7, stabilizes it on the membrane and enables dsh recruitment. It could be speculated, that the formation of the Fz7-dsh-PTK7 complex depends on Wnt activity and PTK7 serves here as a molecule, which stabilizes it and channels dsh towards the activation of PCP signaling.

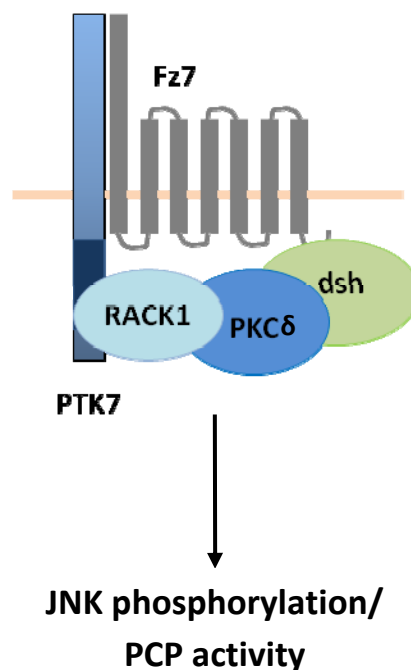


**Figure 5.1. The model of PTK7 intersection with PCP signaling.** Via its extracellular part PTK7 recruits frizzled 7 and stabilizes it on the membrane in a proper conformation to recruit dsh and cause its hyperphosphorylation. Via its intracellular part, PTK7 additionally recruits dsh via RACK1 and PKC $\delta$  to channel it towards the activation of PCP signaling.

### 5.3 The role of PTK7 and RACK1 in the regulation of PCP downstream effects.

To address how PTK7 and RACK1 affect PCP downstream effectors several approaches could be applied. First, the activity of small GTPases, like Rho and Rac needs to be elucidated. This could be done by the use of Rho/Rac FRET biosensors or by western blotting analysis with a use of specific proteins, recognizing activated GTPases. Alternatively, activation of PCP signaling causes an increase of JNK phosphorylation and their nuclear translocation (Tahinci et al., 2007; Yamanaka et al., 2002). Finally, the effects of RACK1/PTK7 overexpression and knockdown on the convergent extension movements need to be analyzed. Overexpression of either PTK7, RACK1 or dsh results in an increase of JNK phosphorylation, indicating activation of PCP signaling (Fig. 4.17, A-D). Conversely, co-expression of PTK7 together with dsh or RACK1 also results in JNK phosphorylation. At the same time co-injection of either  $\Delta$ kPTK7 or PTK7 MO inhibits dsh-mediated JNK activation (Fig. 4.17, E). Therefore, PTK7 is likely acting upstream of dsh during PCP-signaling activation. Moreover, co-injection of the RACK1-MO inhibits PTK7/dsh-mediated JNK activation, which supports the hypothesis that RACK1 serves as a scaffolding protein mediating the PTK7-dsh interaction.

Thus, PTK7 is a novel activator of PCP signaling, which acts by recruiting dsh to the plasma membrane and, most probably, channels dsh to the activation of the PCP pathway. The function of PTK7 in the activation of PCP, but not canonical, Wnt signaling is supported by the number of facts. First, PTK7 recruits dsh to the plasma membrane via RACK1 and PKC $\delta$ . And it was shown, that membrane associated dsh is rather observed during the activation of PCP, than  $\beta$ -catenin signaling (Axelrod et al., 1998; Park et al., 2005; Wallingford et al., 2000). Also, PTK7 forms a complex with fz7 and dsh to stabilize it at the plasma membrane. Fz7 is the first *Xenopus* frizzled, implicated in the activation of the PCP signaling. The co-localization of Fz7-dsh on the plasma membrane is a pre-requisite of the PCP activation (Medina et al., 2000; Medina and Steinbeisser, 2000; Park et al., 2005; Rothbacher et al., 2000). Interestingly, PTK7 recruits dsh via its PDZ domain, which is implicated in the majority of dsh protein interactions (Wallingford and Habas, 2005). Thus, PTK7-mediated activation of PCP signaling may be achieved simply by competition with the other  $\beta$ -catenin activating molecules for dsh binding. Similar to other PCP molecules, PTK7 activates JNK phosphorylation and regulates convergent extension movements, reviewed in Simons and Mlodzik, 2008. Interestingly, dsh cannot activate JNK in the absence of PTK7. Thus, as already mentioned above, PTK7 is crucial for dsh dependent activation of PCP signaling. Finally, overexpression of PTK7 did not activate canonical Wnt signaling either in the luciferase or in the double axis assay. Moreover, it efficiently inhibits Wnt-mediated activation of the  $\beta$ -catenin pathway in both of assays (Hanna Peradziryi, unpublished data), which also supports that PTK7 has a function rather in the activation of PCP than  $\beta$ -catenin signaling.

The function of PTK7 in PCP signaling is mediated via RACK1. This is a first indication of RACK1 function in this signaling pathway. Since PTK7 and RACK1 expression patterns overlap, it is entirely possible that RACK1 mediates PTK7 function in several developmental processes. So far it was demonstrated, that similar to PTK7, RACK1 regulates neural convergent extension (Fig. 4.10 and 4.11), which is one of the first indications of RACK1 function in vertebrate embryogenesis. Previously, RACK1 has been only implicated to have a function in the ovary development of *Drosophila* and sword development of the swordtail fish (Kadmas et al., 2007; Offen et al., 2009).

As mentioned before, RACK1 is a scaffold protein with 7 protein-protein interaction domains. Thus, potentially it can mediate an interaction of several proteins with PTK7. In HEK293 cells RACK1 mediates an interaction between PKC $\delta$  and JNK and is necessary for JNK phosphorylation (Lopez-Bergami et al., 2005). It is possible, that the PTK7-dependent activation of JNK occurs via the same mechanism, meaning that RACK1 could recruit not only PKC $\delta$ -dsh to PTK7 but also JNK. Since in the PCP pathway the activation of JNK is thought to occur via Rac1, this small GTPase can also be a component of the PTK7-RACK1 multiprotein complex (Wallingford and Habas, 2005). Thus, PTK7 together with RACK1 may form a “scaffolding platform” for other PCP signaling components, like PKC $\delta$ , Rac, dsh and JNK, as well as Fz7, which activates the PCP branch of Wnt signaling. Obviously, to prove this hypothesis a number of questions should be further clarified. In particular, it is necessary to examine, whether *Xenopus* PKC $\delta$ -dependent JNKs phosphorylation requires RACK1. Next, the influences of RACK1/PTK7 on the activity of Rac1/Rho/CDC42 small GTPases as well as cytoskeletal rearrangements need to be investigated. This could be done by using GTPases FRET biosensors (Itoh et al., 2002; Pertz et al., 2006). Alternatively, the lysates of either *Xenopus* embryos or cells with overexpressed or knock-down PTK7 and RACK1 can be analyzed for the levels of active GTPases as described previously. Finally, it would be interesting to observe how PTK7-RACK1-dsh are co-localized with cytoskeletal components in tissues, undergoing convergent extension.

#### **5.4 The role of PTK7 and RACK1 in dsh hyperphosphorylation.**

Another question, which remains to be further investigated, is the hyperphosphorylation of dsh. To mediate downstream signaling in both canonical and PCP pathways dsh needs to be “activated” by phosphorylation. The phosphorylated dsh can be detected as a higher molecular weight band on the SDS-PAGE and it occurs, when dsh is co expressed with frizzled and Wnt proteins (Lee et al., 1999; Rothbacher et al., 2000; Takada et al., 2005; Yanagawa et al., 1995). As already mentioned, several kinases, namely casein kinase  $\epsilon$  and PAR1 can cause dsh phosphorylation. Surprisingly, PKC $\delta$  does not lead to dsh phosphorylation, but, at the same time, it is required for the fz7-mediated dsh phosphorylation (Cong et al., 2004; Kinoshita et al., 2003; Ossipova et al., 2005;

Sun et al., 2001; Willert et al., 1997). Similar effect was demonstrated for PTK7, which could serve as an additional argument that both proteins act together in this process. However, loss of RACK1 function does not influence either dsh hyperphosphorylation or its Fz7-dependent membrane recruitment. At a first glance this may be explained by the fact that the RACK1 MO did not result in a complete inhibition of the protein expression. And if the expression level of the protein remains high, the amount of RACK1 may still be sufficient for its function. In addition, the function of RACK1 in this process could be fulfilled by other homologous proteins. But since the same amounts of RACK1 MO inhibit PTK7-dsh as well as PTK7-PKC localization, this can hardly be the right explanation. A better explanation may be that RACK1, PKC $\delta$  and PTK7 have distinct functions in the regulation of dsh hyperphosphorylation. As it was shown, dsh phosphorylation correlates with an activation of the Wnt signaling and thus occurs upon Wnt-frizzled interaction. The hyperphosphorylation of dsh, caused only by co-expression of frizzleds, can be explained by the action of endogenous Wnts. Since PTK7 can bind frizzled 7 and wnt via its extracellular part, it can stabilize the signaling complex the membrane in the proper conformation to recruit dsh and cause its phosphorylation, possibly, via casein kinase  $\epsilon$ . At the same time, RACK1 acts intracellularly by stabilizing the complex between kinase homology domain of PTK7, PKC $\delta$ , dsh, and, probably, several other PCP components. The role of PKC $\delta$  in the dsh phosphorylation remains to be further identified. Since PKC $\delta$  can directly bind dsh (Kinoshita et al., 2003), it could be, that dsh can further be phosphorylated only in the complex with PKC $\delta$ . Alternatively, PKC may be responsible for the “priming” steps in dsh phosphorylation, which cannot be detected as a shift in molecular weight on the SDS-PAGE. Subsequently, this initial phosphorylation of dsh may be required for its membrane recruitment and further fz7-dependent hyperphosphorylation events.

### **5.5 PTK7 functions in neural crest migration**

Recent studies demonstrated an emerging role of PCP signaling in the regulation of neural crest migration (De Calisto et al., 2005). PTK7 is a novel regulator of PCP, which is also expressed in *Xenopus* neural crest. The present work shows that, similarly to dsh, PTK7 is required for neural crest migration. In particular, PTK7 loss of function results in the inhibition of NC migration both in the whole embryo as well as in *in vitro* migration assay.

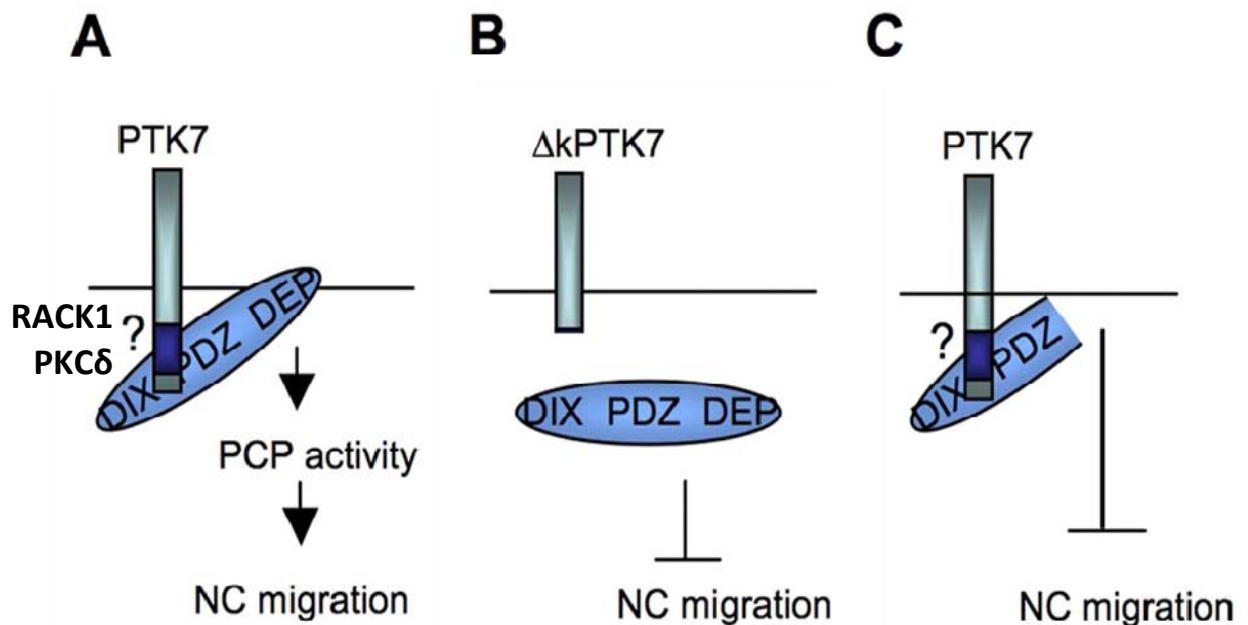


**Fig. 5.2. The model of PTK7 role of in neural crest migration.** (A) PTK7 recruits dsh to the plasma membrane, leading to activation of PCP and enabling neural crest migration. The interaction of PTK7 and dsh may involve RACK1, PKC $\delta$  and fz7 (indicated as?). (B) Deletion of the conserved kinase domain of PTK7, as well as loss of PTK7 function by injection of tzhz specific MOs, inhibits membrane localization of dsh and, thus, neural crest migration. (C)  $\Delta$ DEP dsh can be recruited to the membrane by PTK7, but lacks PCP activity and therefore blocks neural crest migration.

The first question to be addressed is whether the inhibition of neural crest migration is a primary effect of PTK7 loss of function or it is caused by improper neural development in general. PTK7 was previously shown to affect neural tube closure (Lu et al., 2004). And since the induction of neural crest requires proper formation of the neural tube (Mayor et al., 1999), it could entirely be possible, that the influence of PTK7 on the neural crest migration may be indirect. To exclude this, only embryos, which did not display severe neural tube defects, were counted and analyzed by WISH with NC-specific probes. In addition, neural crest induction in PTK7-MO injected embryos has been analyzed and the migratory behavior of explanted as well as transplanted neural crest cells was observed. Finally, overexpression of PTK7 dominant negative version was targeted specifically to the neural crest with a help of the Slug-promoter.

Although, it was difficult to exclude the role of PTK7 in the induction of the neural crest, since the injection of higher PTK7-MO concentrations, indeed, partially affects the NC formation, the use of all above mentioned approaches demonstrate that PTK7 loss of function specifically affects the migration. First, the injection of lower doses of PTK7-MO does not show an effect on the Slug and Twist expression at pre-migratory neural crest, while at later stages the migration of the NC is severely inhibited. Then, the expression of a dominant negative PTK7 version under the control of the Slug promoter affects NC migration at tadpole, but not at neurula stages, supporting a specific role of PTK7 in neural crest migration. Finally, the observation of the explanted and transplanted neural crest allows analyzing the migratory behavior independent from induction events. And,

indeed PTK7 loss of function severely inhibits migration of both explanted and transplanted (shown by A. Borchers) neural crest cells. Therefore, PTK7 has a distinct function in two types of morphogenetic movements, neural convergent extension and neural crest migration.

Since PTK7 functions via dsh recruitment to the plasma membrane in animal cap cells and dsh has a function in neural crest migration (De Calisto et al., 2005), it was assumed, that PTK7 acts through dsh to regulate the migration of NC. Indeed, this was demonstrated by the overexpression of PTK7 with different dsh mutants under the control of the Slug-promoter. First, the overexpression of PTK7 deletion mutant, which is unable to recruit dsh to the plasma membrane,  $\Delta$ kPTK7, results in the inhibition of the neural crest migration (Fig. 4.21 E, F). The dislocalization of dsh from the plasma membrane in neural crest cells upon loss of PTK7 function was additionally verified by immunostaining of NC sections (Fig. 4.25 F). In addition, the co-expression of  $\Delta$ DEP-dsh and PTK7 also results in the same amount of NC defects (Fig. 4.21). This can be explained by the fact that  $\Delta$ DEP-dsh can be efficiently recruited to the plasma membrane by PTK7, where it competes with endogenous dsh. However, since it is unable to activate PCP signaling it results in the same amount of the NC migration defects as  $\Delta$ kPTK7. Surprisingly, the NC-specific overexpression of  $\Delta$ DEP dsh alone results in a minor neural crest defects, which could be explained by primarily cytoplasmic localization of the dominant negative form.  $\Delta$ DEP dsh can be translocated to the plasma membrane only in the presence of PTK7, since its Fz7-dependent translocation is blocked. Upon the co-expression of PTK7, the amount of  $\Delta$ DEP-dsh at the plasma membrane increases, causing thus more efficient inhibition of NC migration. Thus, PTK7 function in neural crest migration can be demonstrated by the following model (Fig. 5.2): PTK7 recruits dsh to the plasma membrane and induce the activation of the PCP signaling via dsh DEP domain (Fig. 5.2 A). The loss of PTK7 function results in the dsh dislocalization from the plasma membrane, inhibition of PCP signaling, which subsequently affects NC migration (Fig. 5.2 B), the recruitment of  $\Delta$ DEP dsh to the plasma membrane also results in the inhibition of PCP signaling and neural crest migration defects.

Another question, which remains to be opened in the proposed model, is whether the mechanisms of dsh membrane recruitment in neural crest cells remain similar to the ones in the animal caps. Although, the functions of fz7, RACK1 and PKC $\delta$  during neural crest migration was not addressed in detail, all these molecules are expressed at the right time and place to have a function in NC migration (Kinoshita et al., 2003; Kwon et al., 2001; Medina et al., 2000). In addition, the loss of RACK1 function inhibits NC migration *in vitro*. Therefore, the role of RACK1 in the PTK7-dependent dsh membrane recruitment may also be relevant for its function in the neural crest. Moreover, the analysis of RACK1 localization in migrating NC explants shows that it is enriched in lamellipodia and cell contacts (Fig. 4.28), where it can facilitate dsh function.

Interestingly, immunostaining the neural crest explants against MT-PTK7 also reveals its presence in lamellipodia. This can occur either when PTK7 is internalized or when its intracellular part is cleaved and has a separate function in the cytoplasm. Thus, fz7, PTK7, RACK1, PKC $\delta$  and dsh may form a PCP signaling complex, which regulates for neural crest migration. However, this assumption requires further investigations.

Recently it was shown, that during neural crest migration dsh facilitates contact inhibition of locomotion via its recruitment to cell contacts (Carmona-Fontaine et al., 2008). The phenomenon of contact inhibition of locomotion was first shown for mouse fibroblasts, migrating *in vitro*. And it has a particular importance for the guidance of cell migration and metastasis processes. Thus, the involvement of PCP signaling in contact inhibition of locomotion of neural crest cells may reveal general cell migration mechanisms. However, the mechanisms, by which dsh localizes to cell contacts, remains to be identified. So far it was only demonstrated that other PCP signaling components, namely Fz7 and Wnt11, co-localize with dsh at cell contacts (Carmona-Fontaine et al., 2008).

PTK7 is a homophilic binding molecule and the analysis of PTK7 localization in neural crest explants demonstrates, that PTK7 is enriched in cell contacts (Fig. 4.22 D, 4.23 A). The mechanisms of PTK7 enrichment at contacts may be explained by clustering of the molecules, caused by homophilic binding. Since PTK7 was shown to recruit dsh to the plasma membrane, it may facilitate dsh-dependent contact inhibition of locomotion. To test whether PTK7 has a role in contact inhibition of locomotion, a neural crest explants confrontation assay was employed. Upon the confrontation of PTK7 MO explants with control explants, control neural crest cells do not change their direction of migration upon the contact with PTK7MO cells. At the same time, upon the contact with PTK7 MM cells the direction of control NC cells migration changes. This, of course, can raise a question regarding the change in the NC specification during loss of PTK7 function. However, as it was shown before, PTK7 did not affect slug expression of pre-migratory NC cells. Additionally, PTK7-MO explants demonstrate the expression of Slug in WISH, which also supports, that their specification is not affected. The role of PTK7 in dsh-dependent contact inhibition of locomotion is also supported by the finding that in migrating NC explants PTK7 co-localizes with dsh at cell contacts (Fig. 4.23 B). Thus, PTK7 may play a key role in the neural crest migration by participating together with dsh in contact inhibition of locomotion.

This hypothesis, clearly, requires further verification. And, first of all, the downstream PTK7 signaling, and particularly, the activation of Rho and Rac GTPases needs to be elucidated. Dsh was shown to activate Rho in cell contacts and Rac – in lamellipodia (Carmona-Fontaine et al., 2008). Therefore, it is extremely important to find, how loss- and gain-of PTK7 function affects the activity of small GTPases. Next, the detailed analysis of NC specification, caused by loss of



PTK7 function, should be performed. Furthermore, it was shown, that NC can invade other types of tissue, particularly mesoderm or endoderm (Carmona-Fontaine et al., 2008). Since, PTK7 expression is not detected in both tissues, it would be interesting to know how PTK7 overexpression in mesoderm affects neural crest invasion behavior. Finally, the direct function of PTK7 in contact inhibition of locomotion has to be verified by analyzing explants migration on fibronectin additionally coated with PTK7 protein.

## 6. Conclusions

The present work analyzed two main questions, namely, how PTK7 intersects with planar cell polarity signaling and whether it has a function during *Xenopus* neural crest migration.

In respect to the interaction with PCP signaling it was demonstrated that PTK7 intersects with PCP signaling at the level of dsh and recruits dsh to the plasma membrane. This function is dependent on the kinase homology domain of PTK7 and the PDZ domain of dsh. However, since direct binding between PTK7 and dsh was not demonstrated, other proteins, which could mediate this interaction, were identified. It was shown, that PTK7 is part of the fz7-dsh complex, required for its stability at the plasma membrane and fz7-dependent dsh phosphorylation. Furthermore, tandem mass-spectrometry analysis identified receptor of activated PKC 1 (RACK1) as a novel PTK7 binding partner. Subsequently, in the animal cap assay RACK1 was shown to be required for the PTK7-dependent dsh membrane translocation. However, RACK1 requires the interaction with PKC $\delta$  to link dsh with PTK7. In addition, dsh, RACK1 and PTK7 were shown to induce JNK phosphorylation, which supports their function in PCP signaling. Thus PTK7 regulates PCP signaling by stabilizing the fz7-dsh complex on the plasma membrane and additionally recruiting dsh via RACK1 and PKC $\delta$ .

Next, the influence of PTK7 on *Xenopus* neural crest migration was shown. The loss of PTK7 function inhibited neural crest migration, while the overexpression did not show any effect. The PTK7 function in neural crest migration was also mediated via dsh membrane recruitment and subsequent PCP activity. This was proven by overexpression of the selected PTK7 and dsh mutant under the control of Slug promoter, as well as by dsh-PTK7 co-localization in neural crest samples upon immunostaining of the tagged proteins. However, the role of fz7, PKC $\delta$  and RACK1 in the formation of the PTK7-dsh complex during the neural crest migration remains to be further addressed.

Finally, it was demonstrated, that the PTK7 molecule possesses homophilic binding properties, which could be crucial for its function during NC migration. Migrating neural crest cells exhibit contact inhibition of locomotion, which is associated with accumulation of dsh and subsequent RhoA activation in cell contacts. Since PTK7 is a homophilic binding molecule, which accumulates in the area of cell contacts, it may facilitate contact inhibition of locomotion by mediating dsh recruitment to this area. This hypothesis was supported by the finding that the PTK7 MO explants did not possess contact inhibition of locomotion during the explants confrontation assay. But the further work should be performed in order to prove the specific role of PTK7 during contact inhibition of locomotion.

## 7. Bibliography

- Aaku-Saraste, E., Hellwig, A., and Huttner, W.B. (1996). Loss of occludin and functional tight junctions, but not ZO-1, during neural tube closure--remodeling of the neuroepithelium prior to neurogenesis. *Dev Biol* **180**, 664-679.
- Abercrombie, M., and Heaysman, J.E. (1953). Observations on the social behaviour of cells in tissue culture. I. Speed of movement of chick heart fibroblasts in relation to their mutual contacts. *Exp Cell Res* **5**, 111-131.
- Abercrombie, M., and Heaysman, J.E. (1954). Observations on the social behaviour of cells in tissue culture. II. Monolayering of fibroblasts. *Exp Cell Res* **6**, 293-306.
- Abu-Elmagd, M., Garcia-Morales, C., and Wheeler, G.N. (2006). Frizzled7 mediates canonical Wnt signaling in neural crest induction. *Dev Biol* **298**, 285-298.
- Adams, R.H., Diella, F., Hennig, S., Helmbacher, F., Deutsch, U., and Klein, R. (2001). The cytoplasmic domain of the ligand ephrinB2 is required for vascular morphogenesis but not cranial neural crest migration. *Cell* **104**, 57-69.
- Adler, P.N. (2002). Planar signaling and morphogenesis in Drosophila. *Dev Cell* **2**, 525-535.
- Adler, P.N., Zhu, C., and Stone, D. (2004). Inturned localizes to the proximal side of wing cells under the instruction of upstream planar polarity proteins. *Curr Biol* **14**, 2046-2051.
- Ahumada, A., Slusarski, D.C., Liu, X., Moon, R.T., Malbon, C.C., and Wang, H.Y. (2002). Signaling of rat Frizzled-2 through phosphodiesterase and cyclic GMP. *Science* **298**, 2006-2010.
- Alfandari, D., Cousin, H., Gaultier, A., Hoffstrom, B.G., and DeSimone, D.W. (2003). Integrin alpha5beta1 supports the migration of Xenopus cranial neural crest on fibronectin. *Dev Biol* **260**, 449-464.
- Alfandari, D., Cousin, H., Gaultier, A., Smith, K., White, J.M., Darribere, T., and DeSimone, D.W. (2001). Xenopus ADAM 13 is a metalloprotease required for cranial neural crest-cell migration. *Curr Biol* **11**, 918-930.
- Anderson, R.B. (2009). Matrix metalloproteinase-2 is involved in the migration and network formation of enteric neural crest-derived cells. *Int J Dev Biol*.
- Angers, S. (2008). Proteomic analyses of protein complexes in the Wnt pathway. *Methods Mol Biol* **468**, 223-230.
- Angers, S., and Moon, R.T. (2009). Proximal events in Wnt signal transduction. *Nat Rev Mol Cell Biol* **10**, 468-477.
- Aoki, Y., Saint-Germain, N., Gyda, M., Magner-Fink, E., Lee, Y.H., Credidio, C., and Saint-Jeannet, J.P. (2003). Sox10 regulates the development of neural crest-derived melanocytes in Xenopus. *Dev Biol* **259**, 19-33.
- Arvanitis, D., and Davy, A. (2008). Eph/ephrin signaling: networks. *Genes Dev* **22**, 416-429.
- Axelrod, J.D. (2001). Unipolar membrane association of Dishevelled mediates Frizzled planar cell polarity signaling. *Genes Dev* **15**, 1182-1187.
- Axelrod, J.D., Miller, J.R., Shulman, J.M., Moon, R.T., and Perrimon, N. (1998). Differential recruitment of Dishevelled provides signaling specificity in the planar cell polarity and Wingless signaling pathways. *Genes Dev* **12**, 2610-2622.
- Aybar, M.J., and Mayor, R. (2002). Early induction of neural crest cells: lessons learned from frog, fish and chick. *Curr Opin Genet Dev* **12**, 452-458.
- Aybar, M.J., Nieto, M.A., and Mayor, R. (2003). Snail precedes slug in the genetic cascade required for the specification and migration of the Xenopus neural crest. *Development* **130**, 483-494.
- Bacallao, R.L., and McNeill, H. (2009). Cystic kidney diseases and planar cell polarity signaling. *Clin Genet* **75**, 107-117.
- Bakal, C., Linding, R., Llense, F., Heffern, E., Martin-Blanco, E., Pawson, T., and Perrimon, N. (2008). Phosphorylation networks regulating JNK activity in diverse genetic backgrounds. *Science* **322**, 453-456.
- Baker, J.C., Beddington, R.S., and Harland, R.M. (1999). Wnt signaling in Xenopus embryos inhibits bmp4 expression and activates neural development. *Genes Dev* **13**, 3149-3159.

- Barembaum, M., and Bronner-Fraser, M. (2005). Early steps in neural crest specification. *Semin Cell Dev Biol* 16, 642-646.
- Battle, E., Sancho, E., Franci, C., Dominguez, D., Monfar, M., Baulida, J., and Garcia De Herreros, A. (2000). The transcription factor snail is a repressor of E-cadherin gene expression in epithelial tumour cells. *Nat Cell Biol* 2, 84-89.
- Behrens, J., von Kries, J.P., Kuhl, M., Bruhn, L., Wedlich, D., Grosschedl, R., and Birchmeier, W. (1996). Functional interaction of beta-catenin with the transcription factor LEF-1. *Nature* 382, 638-642.
- Bekman, E., and Henrique, D. (2002). Embryonic expression of three mouse genes with homology to the *Drosophila melanogaster* prickle gene. *Gene Expr Patterns* 2, 73-77.
- Belmadani, A., Tran, P.B., Ren, D., Assimacopoulos, S., Grove, E.A., and Miller, R.J. (2005). The chemokine stromal cell-derived factor-1 regulates the migration of sensory neuron progenitors. *J Neurosci* 25, 3995-4003.
- Berndt, J.D., and Halloran, M.C. (2006). Semaphorin 3d promotes cell proliferation and neural crest cell development downstream of TCF in the zebrafish hindbrain. *Development* 133, 3983-3992.
- Bilder, D., and Perrimon, N. (2000). Localization of apical epithelial determinants by the basolateral PDZ protein Scribble. *Nature* 403, 676-680.
- Borchers, A., David, R., and Wedlich, D. (2001). *Xenopus* cadherin-11 restrains cranial neural crest migration and influences neural crest specification. *Development* 128, 3049-3060.
- Borchers, A., Epperlein, H.H., and Wedlich, D. (2000). An assay system to study migratory behavior of cranial neural crest cells in *Xenopus*. *Dev Genes Evol* 210, 217-222.
- Boudeau, J., Miranda-Saavedra, D., Barton, G.J., and Alessi, D.R. (2006). Emerging roles of pseudokinases. *Trends Cell Biol* 16, 443-452.
- Boutros, M., Paricio, N., Strutt, D.I., and Mlodzik, M. (1998). Dishevelled activates JNK and discriminates between JNK pathways in planar polarity and wingless signaling. *Cell* 94, 109-118.
- Bronner-Fraser, M., Stern, C.D., and Fraser, S. (1991). Analysis of neural crest cell lineage and migration. *J Craniofac Genet Dev Biol* 11, 214-222.
- Brown, C.B., Feiner, L., Lu, M.M., Li, J., Ma, X., Webber, A.L., Jia, L., Raper, J.A., and Epstein, J.A. (2001). PlexinA2 and semaphorin signaling during cardiac neural crest development. *Development* 128, 3071-3080.
- Cai, D.H., Vollberg, T.M., Sr., Hahn-Dantona, E., Quigley, J.P., and Brauer, P.R. (2000). MMP-2 expression during early avian cardiac and neural crest morphogenesis. *Anat Rec* 259, 168-179.
- Calmont, A., Ivins, S., Van Bueren, K.L., Papangelis, I., Kyriakopoulou, V., Andrews, W.D., Martin, J.F., Moon, A.M., Illingworth, E.A., Basson, M.A., *et al.* (2009). Tbx1 controls cardiac neural crest cell migration during arch artery development by regulating Gbx2 expression in the pharyngeal ectoderm. *Development* 136, 3173-3183.
- Caneparo, L., Huang, Y.L., Staudt, N., Tada, M., Ahrendt, R., Kazanskaya, O., Niehrs, C., and Houart, C. (2007). Dickkopf-1 regulates gastrulation movements by coordinated modulation of Wnt/beta catenin and Wnt/PCP activities, through interaction with the Dally-like homolog Knypek. *Genes Dev* 21, 465-480.
- Cano, A., Perez-Moreno, M.A., Rodrigo, I., Locascio, A., Blanco, M.J., del Barrio, M.G., Portillo, F., and Nieto, M.A. (2000). The transcription factor snail controls epithelial-mesenchymal transitions by repressing E-cadherin expression. *Nat Cell Biol* 2, 76-83.
- Cantemir, V., Cai, D.H., Reedy, M.V., and Brauer, P.R. (2004). Tissue inhibitor of metalloproteinase-2 (TIMP-2) expression during cardiac neural crest cell migration and its role in proMMP-2 activation. *Dev Dyn* 231, 709-719.
- Capelluto, D.G., Kutateladze, T.G., Habas, R., Finkielstein, C.V., He, X., and Overduin, M. (2002). The DIX domain targets dishevelled to actin stress fibres and vesicular membranes. *Nature* 419, 726-729.
- Carl, T.F., Dufton, C., Hanken, J., and Klymkowsky, M.W. (1999). Inhibition of neural crest migration in *Xenopus* using antisense slug RNA. *Dev Biol* 213, 101-115.

- Carmona-Fontaine, C., Matthews, H.K., Kuriyama, S., Moreno, M., Dunn, G.A., Parsons, M., Stern, C.D., and Mayor, R. (2008). Contact inhibition of locomotion in vivo controls neural crest directional migration. *Nature* 456, 957-961.
- Carreira-Barbosa, F., Concha, M.L., Takeuchi, M., Ueno, N., Wilson, S.W., and Tada, M. (2003). Prickle 1 regulates cell movements during gastrulation and neuronal migration in zebrafish. *Development* 130, 4037-4046.
- Casal, J., Lawrence, P.A., and Struhl, G. (2006). Two separate molecular systems, Dachshous/Fat and Starry night/Frizzled, act independently to confer planar cell polarity. *Development* 133, 4561-4572.
- Cheung, M., Chaboissier, M.C., Mynett, A., Hirst, E., Schedl, A., and Briscoe, J. (2005). The transcriptional control of trunk neural crest induction, survival, and delamination. *Dev Cell* 8, 179-192.
- Choi, K.W., and Benzer, S. (1994). Rotation of photoreceptor clusters in the developing *Drosophila* eye requires the nemo gene. *Cell* 78, 125-136.
- Choi, S.C., and Han, J.K. (2002). *Xenopus* Cdc42 regulates convergent extension movements during gastrulation through Wnt/Ca<sup>2+</sup> signaling pathway. *Dev Biol* 244, 342-357.
- Chou, Y.H., and Hayman, M.J. (1991). Characterization of a member of the immunoglobulin gene superfamily that possibly represents an additional class of growth factor receptor. *Proc Natl Acad Sci U S A* 88, 4897-4901.
- Chu, Y.S., Eder, O., Thomas, W.A., Simcha, I., Pincet, F., Ben-Ze'ev, A., Perez, E., Thiery, J.P., and Dufour, S. (2006). Prototypical type I E-cadherin and type II cadherin-7 mediate very distinct adhesiveness through their extracellular domains. *J Biol Chem* 281, 2901-2910.
- Ciruna, B., Jenny, A., Lee, D., Mlodzik, M., and Schier, A.F. (2006). Planar cell polarity signalling couples cell division and morphogenesis during neurulation. *Nature* 439, 220-224.
- Collazo, A., Bronner-Fraser, M., and Fraser, S.E. (1993). Vital dye labelling of *Xenopus laevis* trunk neural crest reveals multipotency and novel pathways of migration. *Development* 118, 363-376.
- Collier, S., and Gubb, D. (1997). *Drosophila* tissue polarity requires the cell-autonomous activity of the fuzzy gene, which encodes a novel transmembrane protein. *Development* 124, 4029-4037.
- Collier, S., Lee, H., Burgess, R., and Adler, P. (2005). The WD40 repeat protein fritz links cytoskeletal planar polarity to frizzled subcellular localization in the *Drosophila* epidermis. *Genetics* 169, 2035-2045.
- Cong, F., Schweizer, L., and Varmus, H. (2004). Casein kinase Iε modulates the signaling specificities of dishevelled. *Mol Cell Biol* 24, 2000-2011.
- Cooper, M.T., and Bray, S.J. (1999). Frizzled regulation of Notch signalling polarizes cell fate in the *Drosophila* eye. *Nature* 397, 526-530.
- Dabdoub, A., Donohue, M.J., Brennan, A., Wolf, V., Montcouquiol, M., Sassoon, D.A., Hseih, J.C., Rubin, J.S., Salinas, P.C., and Kelley, M.W. (2003). Wnt signaling mediates reorientation of outer hair cell stereociliary bundles in the mammalian cochlea. *Development* 130, 2375-2384.
- Damianitsch, K., Melchert, J., and Pieler, T. (2009). XsFRP5 modulates endodermal organogenesis in *Xenopus laevis*. *Dev Biol* 329, 327-337.
- Das, G., Reynolds-Kenneally, J., and Mlodzik, M. (2002). The atypical cadherin Flamingo links Frizzled and Notch signaling in planar polarity establishment in the *Drosophila* eye. *Dev Cell* 2, 655-666.
- Davy, A., and Soriano, P. (2007). Ephrin-B2 forward signaling regulates somite patterning and neural crest cell development. *Dev Biol* 304, 182-193.
- De Bellard, M.E., Rao, Y., and Bronner-Fraser, M. (2003). Dual function of Slit2 in repulsion and enhanced migration of trunk, but not vagal, neural crest cells. *J Cell Biol* 162, 269-279.
- De Calisto, J., Araya, C., Marchant, L., Riaz, C.F., and Mayor, R. (2005). Essential role of non-canonical Wnt signalling in neural crest migration. *Development* 132, 2587-2597.
- De Robertis, E.M. (2006). Spemann's organizer and self-regulation in amphibian embryos. *Nat Rev Mol Cell Biol* 7, 296-302.
- De Robertis, E.M., and Kuroda, H. (2004). Dorsal-ventral patterning and neural induction in *Xenopus* embryos. *Annu Rev Cell Dev Biol* 20, 285-308.

- Deardorff, M.A., Tan, C., Conrad, L.J., and Klein, P.S. (1998). Frizzled-8 is expressed in the Spemann organizer and plays a role in early morphogenesis. *Development* *125*, 2687-2700.
- Delaune, E., Lemaire, P., and Kodjabachian, L. (2005). Neural induction in *Xenopus* requires early FGF signalling in addition to BMP inhibition. *Development* *132*, 299-310.
- Dickson, B.J., and Gilestro, G.F. (2006). Regulation of commissural axon pathfinding by slit and its Robo receptors. *Annu Rev Cell Dev Biol* *22*, 651-675.
- Djiane, A., Riou, J., Umbhauer, M., Boucaut, J., and Shi, D. (2000). Role of frizzled 7 in the regulation of convergent extension movements during gastrulation in *Xenopus laevis*. *Development* *127*, 3091-3100.
- Du, S.J., Purcell, S.M., Christian, J.L., McGrew, L.L., and Moon, R.T. (1995). Identification of distinct classes and functional domains of Wnts through expression of wild-type and chimeric proteins in *Xenopus* embryos. *Mol Cell Biol* *15*, 2625-2634.
- Eaton, S., Wepf, R., and Simons, K. (1996). Roles for Rac1 and Cdc42 in planar polarization and hair outgrowth in the wing of *Drosophila*. *J Cell Biol* *135*, 1277-1289.
- Endo, Y., Wolf, V., Muraiso, K., Kamijo, K., Soon, L., Uren, A., Barshishat-Kupper, M., and Rubin, J.S. (2005). Wnt-3a-dependent cell motility involves RhoA activation and is specifically regulated by dishevelled-2. *J Biol Chem* *280*, 777-786.
- Erickson, C.A., Duong, T.D., and Tosney, K.W. (1992). Descriptive and experimental analysis of the dispersion of neural crest cells along the dorsolateral path and their entry into ectoderm in the chick embryo. *Dev Biol* *151*, 251-272.
- Ewald, A.J., Peyrot, S.M., Tyszka, J.M., Fraser, S.E., and Wallingford, J.B. (2004). Regional requirements for Dishevelled signaling during *Xenopus* gastrulation: separable effects on blastopore closure, mesendoderm internalization and archenteron formation. *Development* *131*, 6195-6209.
- Fagotto, F., Gluck, U., and Gumbiner, B.M. (1998). Nuclear localization signal-independent and importin/karyopherin-independent nuclear import of beta-catenin. *Curr Biol* *8*, 181-190.
- Fainsod, A., Steinbeisser, H., and De Robertis, E.M. (1994). On the function of BMP-4 in patterning the marginal zone of the *Xenopus* embryo. *EMBO J* *13*, 5015-5025.
- Fanto, M., Weber, U., Strutt, D.I., and Mlodzik, M. (2000). Nuclear signaling by Rac and Rho GTPases is required in the establishment of epithelial planar polarity in the *Drosophila* eye. *Curr Biol* *10*, 979-988.
- Gammill, L.S., Gonzalez, C., and Bronner-Fraser, M. (2007). Neuropilin 2/semaphorin 3F signaling is essential for cranial neural crest migration and trigeminal ganglion condensation. *Dev Neurobiol* *67*, 47-56.
- Gammill, L.S., Gonzalez, C., Gu, C., and Bronner-Fraser, M. (2006). Guidance of trunk neural crest migration requires neuropilin 2/semaphorin 3F signaling. *Development* *133*, 99-106.
- Gitler, A.D., Brown, C.B., Kochilas, L., Li, J., and Epstein, J.A. (2002). Neural crest migration and mouse models of congenital heart disease. *Cold Spring Harb Symp Quant Biol* *67*, 57-62.
- Goto, T., Davidson, L., Asashima, M., and Keller, R. (2005). Planar cell polarity genes regulate polarized extracellular matrix deposition during frog gastrulation. *Curr Biol* *15*, 787-793.
- Goto, T., and Keller, R. (2002). The planar cell polarity gene *strabismus* regulates convergence and extension and neural fold closure in *Xenopus*. *Dev Biol* *247*, 165-181.
- Grassot, J., Gouy, M., Perriere, G., and Mouchiroud, G. (2006). Origin and molecular evolution of receptor tyrosine kinases with immunoglobulin-like domains. *Mol Biol Evol* *23*, 1232-1241.
- Guo, N., Hawkins, C., and Nathans, J. (2004). Frizzled6 controls hair patterning in mice. *Proc Natl Acad Sci U S A* *101*, 9277-9281.
- Habas, R., Dawid, I.B., and He, X. (2003). Coactivation of Rac and Rho by Wnt/Frizzled signaling is required for vertebrate gastrulation. *Genes Dev* *17*, 295-309.
- Habas, R., Kato, Y., and He, X. (2001). Wnt/Frizzled activation of Rho regulates vertebrate gastrulation and requires a novel Formin homology protein Daam1. *Cell* *107*, 843-854.
- Hadeball, B., Borchers, A., and Wedlich, D. (1998). *Xenopus* cadherin-11 (Xcadherin-11) expression requires the Wg/Wnt signal. *Mech Dev* *72*, 101-113.

- Hamblet, N.S., Lijam, N., Ruiz-Lozano, P., Wang, J., Yang, Y., Luo, Z., Mei, L., Chien, K.R., Sussman, D.J., and Wynshaw-Boris, A. (2002). Dishevelled 2 is essential for cardiac outflow tract development, somite segmentation and neural tube closure. *Development* 129, 5827-5838.
- Hannus, M., Feiguin, F., Heisenberg, C.P., and Eaton, S. (2002). Planar cell polarization requires Widerborst, a B' regulatory subunit of protein phosphatase 2A. *Development* 129, 3493-3503.
- Harland, R., and Gerhart, J. (1997). Formation and function of Spemann's organizer. *Annu Rev Cell Dev Biol* 13, 611-667.
- Hart, M., Concordet, J.P., Lassot, I., Albert, I., del los Santos, R., Durand, H., Perret, C., Rubinfeld, B., Margottin, F., Benarous, R., *et al.* (1999). The F-box protein beta-TrCP associates with phosphorylated beta-catenin and regulates its activity in the cell. *Curr Biol* 9, 207-210.
- Hatta, K., Takagi, S., Fujisawa, H., and Takeichi, M. (1987). Spatial and temporal expression pattern of N-cadherin cell adhesion molecules correlated with morphogenetic processes of chicken embryos. *Dev Biol* 120, 215-227.
- He, X., Saint-Jeannet, J.P., Wang, Y., Nathans, J., Dawid, I., and Varmus, H. (1997). A member of the Frizzled protein family mediating axis induction by Wnt-5A. *Science* 275, 1652-1654.
- Heisenberg, C.P., Tada, M., Rauch, G.J., Saude, L., Concha, M.L., Geisler, R., Stemple, D.L., Smith, J.C., and Wilson, S.W. (2000). Silberblick/Wnt11 mediates convergent extension movements during zebrafish gastrulation. *Nature* 405, 76-81.
- Helbling, P.M., Tran, C.T., and Brandli, A.W. (1998). Requirement for EphA receptor signaling in the segregation of *Xenopus* third and fourth arch neural crest cells. *Mech Dev* 78, 63-79.
- High, F., and Epstein, J.A. (2007). Signalling pathways regulating cardiac neural crest migration and differentiation. *Novartis Found Symp* 283, 152-161; discussion 161-154, 238-141.
- Himanen, J.P., Chumley, M.J., Lackmann, M., Li, C., Barton, W.A., Jeffrey, P.D., Vearing, C., Geleick, D., Feldheim, D.A., Boyd, A.W., *et al.* (2004). Repelling class discrimination: ephrin-A5 binds to and activates EphB2 receptor signaling. *Nat Neurosci* 7, 501-509.
- Honore, S.M., Aybar, M.J., and Mayor, R. (2003). Sox10 is required for the early development of the prospective neural crest in *Xenopus* embryos. *Dev Biol* 260, 79-96.
- Hopwood, N.D., Pluck, A., and Gurdon, J.B. (1989). A *Xenopus* mRNA related to *Drosophila* twist is expressed in response to induction in the mesoderm and the neural crest. *Cell* 59, 893-903.
- Hsu, D.R., Economides, A.N., Wang, X., Eimon, P.M., and Harland, R.M. (1998). The *Xenopus* dorsalizing factor Gremlin identifies a novel family of secreted proteins that antagonize BMP activities. *Mol Cell* 1, 673-683.
- Huang, G.Y., Cooper, E.S., Waldo, K., Kirby, M.L., Gilula, N.B., and Lo, C.W. (1998). Gap junction-mediated cell-cell communication modulates mouse neural crest migration. *J Cell Biol* 143, 1725-1734.
- Huang, H.C., and Klein, P.S. (2004). The Frizzled family: receptors for multiple signal transduction pathways. *Genome Biol* 5, 234.
- Huh, M.I., Lee, Y.M., Seo, S.K., Kang, B.S., Chang, Y., Lee, Y.S., Fini, M.E., Kang, S.S., and Jung, J.C. (2007). Roles of MMP/TIMP in regulating matrix swelling and cell migration during chick corneal development. *J Cell Biochem* 101, 1222-1237.
- Itoh, K., Brott, B.K., Bae, G.U., Ratcliffe, M.J., and Sokol, S.Y. (2005). Nuclear localization is required for Dishevelled function in Wnt/beta-catenin signaling. *J Biol* 4, 3.
- Itoh, K., Krupnik, V.E., and Sokol, S.Y. (1998). Axis determination in *Xenopus* involves biochemical interactions of axin, glycogen synthase kinase 3 and beta-catenin. *Curr Biol* 8, 591-594.
- Itoh, R.E., Kurokawa, K., Ohba, Y., Yoshizaki, H., Mochizuki, N., and Matsuda, M. (2002). Activation of rac and cdc42 video imaged by fluorescent resonance energy transfer-based single-molecule probes in the membrane of living cells. *Mol Cell Biol* 22, 6582-6591.
- Jenny, A., Darken, R.S., Wilson, P.A., and Mlodzik, M. (2003). Prickle and Strabismus form a functional complex to generate a correct axis during planar cell polarity signaling. *EMBO J* 22, 4409-4420.

- Jenny, A., Reynolds-Kenneally, J., Das, G., Burnett, M., and Mlodzik, M. (2005). Diego and Prickle regulate Frizzled planar cell polarity signalling by competing for Dishevelled binding. *Nat Cell Biol* 7, 691-697.
- Jessen, J.R., Topczewski, J., Bingham, S., Sepich, D.S., Marlow, F., Chandrasekhar, A., and Solnica-Krezel, L. (2002). Zebrafish trilobite identifies new roles for Strabismus in gastrulation and neuronal movements. *Nat Cell Biol* 4, 610-615.
- Jia, L., Cheng, L., and Raper, J. (2005). Slit/Robo signaling is necessary to confine early neural crest cells to the ventral migratory pathway in the trunk. *Dev Biol* 282, 411-421.
- Jiang, Y., Liu, M.T., and Gershon, M.D. (2003). Netrins and DCC in the guidance of migrating neural crest-derived cells in the developing bowel and pancreas. *Dev Biol* 258, 364-384.
- Joos, T.O., Whittaker, C.A., Meng, F., DeSimone, D.W., Gnau, V., and Hausen, P. (1995). Integrin alpha 5 during early development of *Xenopus laevis*. *Mech Dev* 50, 187-199.
- Kadmas, J.L., Smith, M.A., Pronovost, S.M., and Beckerle, M.C. (2007). Characterization of RACK1 function in *Drosophila* development. *Dev Dyn* 236, 2207-2215.
- Karner, C.M., Chirumamilla, R., Aoki, S., Igarashi, P., Wallingford, J.B., and Carroll, T.J. (2009). Wnt9b signaling regulates planar cell polarity and kidney tubule morphogenesis. *Nat Genet* 41, 793-799.
- Kashef, J., Kohler, A., Kuriyama, S., Alfandari, D., Mayor, R., and Wedlich, D. (2009). Cadherin-11 regulates protrusive activity in *Xenopus* cranial neural crest cells upstream of Trio and the small GTPases. *Genes Dev* 23, 1393-1398.
- Katanaev, V.L., Ponzielli, R., Semeriva, M., and Tomlinson, A. (2005). Trimeric G protein-dependent frizzled signaling in *Drosophila*. *Cell* 120, 111-122.
- Katoh, K., Kano, Y., Amano, M., Kaibuchi, K., and Fujiwara, K. (2001a). Stress fiber organization regulated by MLCK and Rho-kinase in cultured human fibroblasts. *Am J Physiol Cell Physiol* 280, C1669-1679.
- Katoh, K., Kano, Y., Amano, M., Onishi, H., Kaibuchi, K., and Fujiwara, K. (2001b). Rho-kinase--mediated contraction of isolated stress fibers. *J Cell Biol* 153, 569-584.
- Kee, Y., Hwang, B.J., Sternberg, P.W., and Bronner-Fraser, M. (2007). Evolutionary conservation of cell migration genes: from nematode neurons to vertebrate neural crest. *Genes Dev* 21, 391-396.
- Keller, R. (2002). Shaping the vertebrate body plan by polarized embryonic cell movements. *Science* 298, 1950-1954.
- Kemp, C.R., Willems, E., Wawrzak, D., Hendrickx, M., Agbor Agbor, T., and Leyns, L. (2007). Expression of Frizzled5, Frizzled7, and Frizzled10 during early mouse development and interactions with canonical Wnt signaling. *Dev Dyn* 236, 2011-2019.
- Kibar, Z., Gauthier, S., Lee, S.H., Vidal, S., and Gros, P. (2003). Rescue of the neural tube defect of loop-tail mice by a BAC clone containing the *Ltap* gene. *Genomics* 82, 397-400.
- Kibar, Z., Vogan, K.J., Groulx, N., Justice, M.J., Underhill, D.A., and Gros, P. (2001). *Ltap*, a mammalian homolog of *Drosophila* Strabismus/Van Gogh, is altered in the mouse neural tube mutant Loop-tail. *Nat Genet* 28, 251-255.
- Kil, S.H., Lallier, T., and Bronner-Fraser, M. (1996). Inhibition of cranial neural crest adhesion in vitro and migration in vivo using integrin antisense oligonucleotides. *Dev Biol* 179, 91-101.
- Kim, G.H., and Han, J.K. (2005). JNK and ROKalpha function in the noncanonical Wnt/RhoA signaling pathway to regulate *Xenopus* convergent extension movements. *Dev Dyn* 232, 958-968.
- Kim, G.H., Her, J.H., and Han, J.K. (2008). Ryk cooperates with Frizzled 7 to promote Wnt11-mediated endocytosis and is essential for *Xenopus laevis* convergent extension movements. *J Cell Biol* 182, 1073-1082.
- Kinoshita, N., Iioka, H., Miyakoshi, A., and Ueno, N. (2003). PKC delta is essential for Dishevelled function in a noncanonical Wnt pathway that regulates *Xenopus* convergent extension movements. *Genes Dev* 17, 1663-1676.
- Kirillova, I., Novikova, I., Auge, J., Audollent, S., Esnault, D., Encha-Razavi, F., Lazjuk, G., Attie-Bitach, T., and Vekemans, M. (2000). Expression of the sonic hedgehog gene in human embryos with neural tube defects. *Teratology* 61, 347-354.



- Kishida, S., Yamamoto, H., Hino, S., Ikeda, S., Kishida, M., and Kikuchi, A. (1999). DIX domains of Dvl and axin are necessary for protein interactions and their ability to regulate beta-catenin stability. *Mol Cell Biol* *19*, 4414-4422.
- Klein, T.J., Jenny, A., Djiane, A., and Mlodzik, M. (2006). CKlepsilon/discs overgrown promotes both Wnt-Fz/beta-catenin and Fz/PCP signaling in *Drosophila*. *Curr Biol* *16*, 1337-1343.
- Klein, T.J., and Mlodzik, M. (2005). Planar cell polarization: an emerging model points in the right direction. *Annu Rev Cell Dev Biol* *21*, 155-176.
- Klisch, T.J., Souopgui, J., Juergens, K., Rust, B., Pieler, T., and Henningfeld, K.A. (2006). Mxi1 is essential for neurogenesis in *Xenopus* and acts by bridging the pan-neural and proneural genes. *Dev Biol* *292*, 470-485.
- Klymkowsky, M.W., and Hanken, J. (1991). Whole-mount staining of *Xenopus* and other vertebrates. *Methods Cell Biol* *36*, 419-441.
- Koblar, S.A., Krull, C.E., Pasquale, E.B., McLennan, R., Peale, F.D., Cerretti, D.P., and Bothwell, M. (2000). Spinal motor axons and neural crest cells use different molecular guides for segmental migration through the rostral half-somite. *J Neurobiol* *42*, 437-447.
- Koestner, U., Shnitsar, I., Linnemannstons, K., Hufton, A.L., and Borchers, A. (2008). Semaphorin and neuropilin expression during early morphogenesis of *Xenopus laevis*. *Dev Dyn* *237*, 3853-3863.
- Kolodkin, A.L. (1998). Semaphorin-mediated neuronal growth cone guidance. *Prog Brain Res* *117*, 115-132.
- Komiya, Y., and Habas, R. (2008). Wnt signal transduction pathways. *Organogenesis* *4*, 68-75.
- Krotoski, D.M., and Bronner-Fraser, M. (1986). Mapping of neural crest pathways in *Xenopus laevis*. *Prog Clin Biol Res* *217B*, 229-233.
- Krotoski, D.M., Fraser, S.E., and Bronner-Fraser, M. (1988). Mapping of neural crest pathways in *Xenopus laevis* using inter- and intra-specific cell markers. *Dev Biol* *127*, 119-132.
- Kruger, R.P., Aurandt, J., and Guan, K.L. (2005). Semaphorins command cells to move. *Nat Rev Mol Cell Biol* *6*, 789-800.
- Krull, C.E., Lansford, R., Gale, N.W., Collazo, A., Marcelle, C., Yancopoulos, G.D., Fraser, S.E., and Bronner-Fraser, M. (1997). Interactions of Eph-related receptors and ligands confer rostrocaudal pattern to trunk neural crest migration. *Curr Biol* *7*, 571-580.
- Kuphal, S., Palm, H.G., Poser, I., and Bosserhoff, A.K. (2005). Snail-regulated genes in malignant melanoma. *Melanoma Res* *15*, 305-313.
- Kuriyama, S., and Mayor, R. (2008). Molecular analysis of neural crest migration. *Philos Trans R Soc Lond B Biol Sci* *363*, 1349-1362.
- Kwon, H.J., Bae, S., Son, Y.H., and Chung, H.M. (2001). Expression of the *Xenopus* homologue of the receptor for activated C-kinase 1 (RACK1) in the *Xenopus* embryo. *Dev Genes Evol* *211*, 195-197.
- LaBonne, C., and Bronner-Fraser, M. (2000). Snail-related transcriptional repressors are required in *Xenopus* for both the induction of the neural crest and its subsequent migration. *Dev Biol* *221*, 195-205.
- Lallier, T.E., Whittaker, C.A., and DeSimone, D.W. (1996). Integrin alpha 6 expression is required for early nervous system development in *Xenopus laevis*. *Development* *122*, 2539-2554.
- Lawrence, P.A., Casal, J., and Struhl, G. (2004). Cell interactions and planar polarity in the abdominal epidermis of *Drosophila*. *Development* *131*, 4651-4664.
- Lawrence, P.A., Struhl, G., and Casal, J. (2007). Planar cell polarity: one or two pathways? *Nat Rev Genet* *8*, 555-563.
- Lee, J.S., Ishimoto, A., and Yanagawa, S. (1999). Characterization of mouse dishevelled (Dvl) proteins in Wnt/Wingless signaling pathway. *J Biol Chem* *274*, 21464-21470.
- Lele, Z., Bakkers, J., and Hammerschmidt, M. (2001). Morpholino phenocopies of the swirl, snailhouse, somitabun, minifin, silberblick, and pipetail mutations. *Genesis* *30*, 190-194.
- Lepore, J.J., Mericko, P.A., Cheng, L., Lu, M.M., Morrisey, E.E., and Parmacek, M.S. (2006). GATA-6 regulates semaphorin 3C and is required in cardiac neural crest for cardiovascular morphogenesis. *J Clin Invest* *116*, 929-939.

- Linker, C., and Stern, C.D. (2004). Neural induction requires BMP inhibition only as a late step, and involves signals other than FGF and Wnt antagonists. *Development* *131*, 5671-5681.
- Logan, C.Y., and Nusse, R. (2004). The Wnt signaling pathway in development and disease. *Annu Rev Cell Dev Biol* *20*, 781-810.
- Lopez-Bergami, P., Habelhah, H., Bhoumik, A., Zhang, W., Wang, L.H., and Ronai, Z. (2005). RACK1 mediates activation of JNK by protein kinase C [corrected]. *Mol Cell* *19*, 309-320.
- Lu, X., Borchers, A.G., Jolicoeur, C., Rayburn, H., Baker, J.C., and Tessier-Lavigne, M. (2004). PTK7/CCK-4 is a novel regulator of planar cell polarity in vertebrates. *Nature* *430*, 93-98.
- MacDonald, B.T., Tamai, K., and He, X. (2009). Wnt/beta-catenin signaling: components, mechanisms, and diseases. *Dev Cell* *17*, 9-26.
- Mancilla, A., and Mayor, R. (1996). Neural crest formation in *Xenopus laevis*: mechanisms of Xslug induction. *Dev Biol* *177*, 580-589.
- Marchant, L., Linker, C., Ruiz, P., Guerrero, N., and Mayor, R. (1998). The inductive properties of mesoderm suggest that the neural crest cells are specified by a BMP gradient. *Dev Biol* *198*, 319-329.
- Marlow, F., Topczewski, J., Sepich, D., and Solnica-Krezel, L. (2002). Zebrafish Rho kinase 2 acts downstream of Wnt11 to mediate cell polarity and effective convergence and extension movements. *Curr Biol* *12*, 876-884.
- Marlow, F., Zwartkuis, F., Malicki, J., Neuhaus, S.C., Abbas, L., Weaver, M., Driever, W., and Solnica-Krezel, L. (1998). Functional interactions of genes mediating convergent extension, knypek and trilobite, during the partitioning of the eye primordium in zebrafish. *Dev Biol* *203*, 382-399.
- Matakatsu, H., and Blair, S.S. (2004). Interactions between Fat and Dachshous and the regulation of planar cell polarity in the *Drosophila* wing. *Development* *131*, 3785-3794.
- Matsui, T., Raya, A., Kawakami, Y., Callol-Massot, C., Capdevila, J., Rodriguez-Esteban, C., and Izpisua Belmonte, J.C. (2005). Noncanonical Wnt signaling regulates midline convergence of organ primordia during zebrafish development. *Genes Dev* *19*, 164-175.
- Matthews, H.K., Broders-Bondon, F., Thiery, J.P., and Mayor, R. (2008a). Wnt11r is required for cranial neural crest migration. *Dev Dyn* *237*, 3404-3409.
- Matthews, H.K., Marchant, L., Carmona-Fontaine, C., Kuriyama, S., Larrain, J., Holt, M.R., Parsons, M., and Mayor, R. (2008b). Directional migration of neural crest cells in vivo is regulated by Syndecan-4/Rac1 and non-canonical Wnt signaling/RhoA. *Development* *135*, 1771-1780.
- Matusek, T., Djiane, A., Jankovics, F., Brunner, D., Mlodzik, M., and Mihaly, J. (2006). The *Drosophila* formin DAAM regulates the tracheal cuticle pattern through organizing the actin cytoskeleton. *Development* *133*, 957-966.
- Mayor, R., Morgan, R., and Sargent, M.G. (1995). Induction of the prospective neural crest of *Xenopus*. *Development* *121*, 767-777.
- Mayor, R., Young, R., and Vargas, A. (1999). Development of neural crest in *Xenopus*. *Curr Top Dev Biol* *43*, 85-113.
- McCahill, A., Warwicker, J., Bolger, G.B., Houslay, M.D., and Yarwood, S.J. (2002). The RACK1 scaffold protein: a dynamic cog in cell response mechanisms. *Mol Pharmacol* *62*, 1261-1273.
- McCusker, C., Cousin, H., Neuner, R., and Alfandari, D. (2009). Extracellular cleavage of cadherin-11 by ADAM metalloproteases is essential for *Xenopus* cranial neural crest cell migration. *Mol Biol Cell* *20*, 78-89.
- McKay, R.M., Peters, J.M., and Graff, J.M. (2001). The casein kinase I family: roles in morphogenesis. *Dev Biol* *235*, 378-387.
- McLennan, R., and Krull, C.E. (2002). Ephrin-as cooperate with EphA4 to promote trunk neural crest migration. *Gene Expr* *10*, 295-305.
- Medina, A., Reintsch, W., and Steinbeisser, H. (2000). *Xenopus* frizzled 7 can act in canonical and non-canonical Wnt signaling pathways: implications on early patterning and morphogenesis. *Mech Dev* *92*, 227-237.

- Medina, A., and Steinbeisser, H. (2000). Interaction of Frizzled 7 and Dishevelled in *Xenopus*. *Dev Dyn* **218**, 671-680.
- Mellitzer, G., Xu, Q., and Wilkinson, D.G. (1999). Eph receptors and ephrins restrict cell intermingling and communication. *Nature* **400**, 77-81.
- Mellott, D.O., and Burke, R.D. (2008). Divergent roles for Eph and ephrin in avian cranial neural crest. *BMC Dev Biol* **8**, 56.
- Merrill, A.E., Bochukova, E.G., Brugger, S.M., Ishii, M., Pilz, D.T., Wall, S.A., Lyons, K.M., Wilkie, A.O., and Maxson, R.E., Jr. (2006). Cell mixing at a neural crest-mesoderm boundary and deficient ephrin-Eph signaling in the pathogenesis of craniosynostosis. *Hum Mol Genet* **15**, 1319-1328.
- Miller, J.R., Rowning, B.A., Larabell, C.A., Yang-Snyder, J.A., Bates, R.L., and Moon, R.T. (1999). Establishment of the dorsal-ventral axis in *Xenopus* embryos coincides with the dorsal enrichment of dishevelled that is dependent on cortical rotation. *J Cell Biol* **146**, 427-437.
- Miller, M.A., and Steele, R.E. (2000). Lemon encodes an unusual receptor protein-tyrosine kinase expressed during gametogenesis in *Hydra*. *Dev Biol* **224**, 286-298.
- Mlodzik, M. (1999). Planar polarity in the *Drosophila* eye: a multifaceted view of signaling specificity and cross-talk. *EMBO J* **18**, 6873-6879.
- Mochly-Rosen, D., Khaner, H., and Lopez, J. (1991). Identification of intracellular receptor proteins for activated protein kinase C. *Proc Natl Acad Sci U S A* **88**, 3997-4000.
- Moeller, H., Jenny, A., Schaeffer, H.J., Schwarz-Romond, T., Mlodzik, M., Hammerschmidt, M., and Birchmeier, W. (2006). Diversin regulates heart formation and gastrulation movements in development. *Proc Natl Acad Sci U S A* **103**, 15900-15905.
- Molenaar, M., van de Wetering, M., Oosterwegel, M., Peterson-Maduro, J., Godsave, S., Korinek, V., Roose, J., Destree, O., and Clevers, H. (1996). XTcf-3 transcription factor mediates beta-catenin-induced axis formation in *Xenopus* embryos. *Cell* **86**, 391-399.
- Montcouquiol, M., Crenshaw, E.B., 3rd, and Kelley, M.W. (2006). Noncanonical Wnt signaling and neural polarity. *Annu Rev Neurosci* **29**, 363-386.
- Montcouquiol, M., and Kelley, M.W. (2003). Planar and vertical signals control cellular differentiation and patterning in the mammalian cochlea. *J Neurosci* **23**, 9469-9478.
- Montcouquiol, M., Rachel, R.A., Lanford, P.J., Copeland, N.G., Jenkins, N.A., and Kelley, M.W. (2003). Identification of *Vangl2* and *Scrb1* as planar polarity genes in mammals. *Nature* **423**, 173-177.
- Moon, R.T., Campbell, R.M., Christian, J.L., McGrew, L.L., Shih, J., and Fraser, S. (1993). Xwnt-5A: a maternal Wnt that affects morphogenetic movements after overexpression in embryos of *Xenopus laevis*. *Development* **119**, 97-111.
- Moriguchi, T., Kawachi, K., Kamakura, S., Masuyama, N., Yamanaka, H., Matsumoto, K., Kikuchi, A., and Nishida, E. (1999). Distinct domains of mouse dishevelled are responsible for the c-Jun N-terminal kinase/stress-activated protein kinase activation and the axis formation in vertebrates. *J Biol Chem* **274**, 30957-30962.
- Mossie, K., Jallal, B., Alves, F., Sures, I., Plowman, G.D., and Ullrich, A. (1995). Colon carcinoma kinase-4 defines a new subclass of the receptor tyrosine kinase family. *Oncogene* **11**, 2179-2184.
- Mullis, K., Faloona, F., Scharf, S., Saiki, R., Horn, G., and Erlich, H. (1986). Specific enzymatic amplification of DNA in vitro: the polymerase chain reaction. *Cold Spring Harb Symp Quant Biol* **51 Pt 1**, 263-273.
- Murdoch, J.N., Henderson, D.J., Doudney, K., Gaston-Massuet, C., Phillips, H.M., Paternotte, C., Arkell, R., Stanier, P., and Copp, A.J. (2003). Disruption of scribble (*Scrb1*) causes severe neural tube defects in the circletail mouse. *Hum Mol Genet* **12**, 87-98.
- Murdoch, J.N., Rachel, R.A., Shah, S., Beermann, F., Stanier, P., Mason, C.A., and Copp, A.J. (2001). Circletail, a new mouse mutant with severe neural tube defects: chromosomal localization and interaction with the loop-tail mutation. *Genomics* **78**, 55-63.
- Myers, D.C., Sepich, D.S., and Solnica-Krezel, L. (2002). Convergence and extension in vertebrate gastrulae: cell movements according to or in search of identity? *Trends Genet* **18**, 447-455.

- Nakagawa, S., and Takeichi, M. (1995). Neural crest cell-cell adhesion controlled by sequential and subpopulation-specific expression of novel cadherins. *Development* *121*, 1321-1332.
- Nakagawa, S., and Takeichi, M. (1998). Neural crest emigration from the neural tube depends on regulated cadherin expression. *Development* *125*, 2963-2971.
- Nakaya, M.A., Habas, R., Biris, K., Dunty, W.C., Jr., Kato, Y., He, X., and Yamaguchi, T.P. (2004). Identification and comparative expression analyses of Daam genes in mouse and *Xenopus*. *Gene Expr Patterns* *5*, 97-105.
- Narimatsu, M., Bose, R., Pye, M., Zhang, L., Miller, B., Ching, P., Sakuma, R., Luga, V., Roncari, L., Attisano, L., *et al.* (2009). Regulation of planar cell polarity by Smurf ubiquitin ligases. *Cell* *137*, 295-307.
- Natarajan, D., Marcos-Gutierrez, C., Pachnis, V., and de Graaff, E. (2002). Requirement of signalling by receptor tyrosine kinase RET for the directed migration of enteric nervous system progenitor cells during mammalian embryogenesis. *Development* *129*, 5151-5160.
- Neuner, R., Cousin, H., McCusker, C., Coyne, M., and Alfandari, D. (2009). *Xenopus* ADAM19 is involved in neural, neural crest and muscle development. *Mech Dev* *126*, 240-255.
- Newgreen, D., and Gibbins, I. (1982). Factors controlling the time of onset of the migration of neural crest cells in the fowl embryo. *Cell Tissue Res* *224*, 145-160.
- Nieto, M.A., Sargent, M.G., Wilkinson, D.G., and Cooke, J. (1994). Control of cell behavior during vertebrate development by Slug, a zinc finger gene. *Science* *264*, 835-839.
- Niewkoop P.D., F.J. (1956). Normal table of *Xenopus laevis*. Amsterdam: North Holland Publishing.
- Nilsson, J., Sengupta, J., Frank, J., and Nissen, P. (2004). Regulation of eukaryotic translation by the RACK1 protein: a platform for signalling molecules on the ribosome. *EMBO Rep* *5*, 1137-1141.
- Nusslein-Volhard, C., and Wieschaus, E. (1980). Mutations affecting segment number and polarity in *Drosophila*. *Nature* *287*, 795-801.
- Offen, N., Meyer, A., and Begemann, G. (2009). Identification of novel genes involved in the development of the sword and gonopodium in swordtail fish. *Dev Dyn* *238*, 1674-1687.
- Ohkawara, B., Yamamoto, T.S., Tada, M., and Ueno, N. (2003). Role of glypican 4 in the regulation of convergent extension movements during gastrulation in *Xenopus laevis*. *Development* *130*, 2129-2138.
- Orioli, D., and Klein, R. (1997). The Eph receptor family: axonal guidance by contact repulsion. *Trends Genet* *13*, 354-359.
- Osborne, N.J., Begbie, J., Chilton, J.K., Schmidt, H., and Eickholt, B.J. (2005). Semaphorin/neuropilin signaling influences the positioning of migratory neural crest cells within the hindbrain region of the chick. *Dev Dyn* *232*, 939-949.
- Ossipova, O., Dhawan, S., Sokol, S., and Green, J.B. (2005). Distinct PAR-1 proteins function in different branches of Wnt signaling during vertebrate development. *Dev Cell* *8*, 829-841.
- Pan, F.C., Chen, Y., Loeber, J., Henningfeld, K., and Pieler, T. (2006). I-SceI meganuclease-mediated transgenesis in *Xenopus*. *Dev Dyn* *235*, 247-252.
- Pan, W.J., Pang, S.Z., Huang, T., Guo, H.Y., Wu, D., and Li, L. (2004). Characterization of function of three domains in dishevelled-1: DEP domain is responsible for membrane translocation of dishevelled-1. *Cell Res* *14*, 324-330.
- Paricio, N., Feiguin, F., Boutros, M., Eaton, S., and Mlodzik, M. (1999). The *Drosophila* STE20-like kinase misshapen is required downstream of the Frizzled receptor in planar polarity signaling. *EMBO J* *18*, 4669-4678.
- Park, S.K., Lee, H.S., and Lee, S.T. (1996a). Characterization of the human full-length PTK7 cDNA encoding a receptor protein tyrosine kinase-like molecule closely related to chick KLG. *J Biochem* *119*, 235-239.
- Park, T.J., Gray, R.S., Sato, A., Habas, R., and Wallingford, J.B. (2005). Subcellular localization and signaling properties of dishevelled in developing vertebrate embryos. *Curr Biol* *15*, 1039-1044.
- Park, T.J., Haigo, S.L., and Wallingford, J.B. (2006). Ciliogenesis defects in embryos lacking inturned or fuzzy function are associated with failure of planar cell polarity and Hedgehog signaling. *Nat Genet* *38*, 303-311.
- Park, W.J., Liu, J., Sharp, E.J., and Adler, P.N. (1996b). The *Drosophila* tissue polarity gene inturned acts cell autonomously and encodes a novel protein. *Development* *122*, 961-969.

- Pasquale, E.B. (1997). The Eph family of receptors. *Curr Opin Cell Biol* 9, 608-615.
- Penton, A., Wodarz, A., and Nusse, R. (2002). A mutational analysis of dishevelled in *Drosophila* defines novel domains in the dishevelled protein as well as novel suppressing alleles of axin. *Genetics* 161, 747-762.
- Perrimon, N., and Mahowald, A.P. (1987). Multiple functions of segment polarity genes in *Drosophila*. *Dev Biol* 119, 587-600.
- Pertz, O., Hodgson, L., Klemke, R.L., and Hahn, K.M. (2006). Spatiotemporal dynamics of RhoA activity in migrating cells. *Nature* 440, 1069-1072.
- Phillips, H.M., Murdoch, J.N., Chaudhry, B., Copp, A.J., and Henderson, D.J. (2005). Vangl2 acts via RhoA signaling to regulate polarized cell movements during development of the proximal outflow tract. *Circ Res* 96, 292-299.
- Pulido, D., Campuzano, S., Koda, T., Modolell, J., and Barbacid, M. (1992). Dtrk, a *Drosophila* gene related to the trk family of neurotrophin receptors, encodes a novel class of neural cell adhesion molecule. *EMBO J* 11, 391-404.
- Ransom, D.G., Hens, M.D., and DeSimone, D.W. (1993). Integrin expression in early amphibian embryos: cDNA cloning and characterization of *Xenopus* beta 1, beta 2, beta 3, and beta 6 subunits. *Dev Biol* 160, 265-275.
- Rawls, A.S., Guinto, J.B., and Wolff, T. (2002). The cadherins fat and dachsous regulate dorsal/ventral signaling in the *Drosophila* eye. *Curr Biol* 12, 1021-1026.
- Reaume, A.G., de Sousa, P.A., Kulkarni, S., Langille, B.L., Zhu, D., Davies, T.C., Juneja, S.C., Kidder, G.M., and Rossant, J. (1995). Cardiac malformation in neonatal mice lacking connexin43. *Science* 267, 1831-1834.
- Robinson, V., Smith, A., Flenniken, A.M., and Wilkinson, D.G. (1997). Roles of Eph receptors and ephrins in neural crest pathfinding. *Cell Tissue Res* 290, 265-274.
- Ross, A.J., May-Simera, H., Eichers, E.R., Kai, M., Hill, J., Jagger, D.J., Leitch, C.C., Chapple, J.P., Munro, P.M., Fisher, S., *et al.* (2005). Disruption of Bardet-Biedl syndrome ciliary proteins perturbs planar cell polarity in vertebrates. *Nat Genet* 37, 1135-1140.
- Rothbacher, U., Laurent, M.N., Deardorff, M.A., Klein, P.S., Cho, K.W., and Fraser, S.E. (2000). Dishevelled phosphorylation, subcellular localization and multimerization regulate its role in early embryogenesis. *EMBO J* 19, 1010-1022.
- Rukstalis, J.M., and Habener, J.F. (2007). Snail2, a mediator of epithelial-mesenchymal transitions, expressed in progenitor cells of the developing endocrine pancreas. *Gene Expr Patterns* 7, 471-479.
- Sadaghiani, B., and Thiebaud, C.H. (1987). Neural crest development in the *Xenopus laevis* embryo, studied by interspecific transplantation and scanning electron microscopy. *Dev Biol* 124, 91-110.
- Sagot, I., Rodal, A.A., Moseley, J., Goode, B.L., and Pellman, D. (2002). An actin nucleation mechanism mediated by Bni1 and profilin. *Nat Cell Biol* 4, 626-631.
- Sanger, F., Nicklen, S., and Coulson, A.R. (1977). DNA sequencing with chain-terminating inhibitors. *Proc Natl Acad Sci U S A* 74, 5463-5467.
- Santiago, A., and Erickson, C.A. (2002). Ephrin-B ligands play a dual role in the control of neural crest cell migration. *Development* 129, 3621-3632.
- Saraga-Babic, M., Sapunar, D., and Stefanovic, V. (1993). Histological features of axial structures during embryonic and fetal stages of human craniorachischisis. *Acta Neuropathol* 86, 289-294.
- Sasai, N., Nakazawa, Y., Haraguchi, T., and Sasai, Y. (2004). The neurotrophin-receptor-related protein NRH1 is essential for convergent extension movements. *Nat Cell Biol* 6, 741-748.
- Sato, M., Tsai, H.J., and Yost, H.J. (2006). Semaphorin3D regulates invasion of cardiac neural crest cells into the primary heart field. *Dev Biol* 298, 12-21.
- Sauka-Spengler, T., and Bronner-Fraser, M. (2008). A gene regulatory network orchestrates neural crest formation. *Nat Rev Mol Cell Biol* 9, 557-568.
- Savagner, P., Yamada, K.M., and Thiery, J.P. (1997). The zinc-finger protein slug causes desmosome dissociation, an initial and necessary step for growth factor-induced epithelial-mesenchymal transition. *J Cell Biol* 137, 1403-1419.

- Schambony, A., and Wedlich, D. (2007). Wnt-5A/Ror2 regulate expression of XPAPC through an alternative noncanonical signaling pathway. *Dev Cell* *12*, 779-792.
- Schwarz-Romond, T., Asbrand, C., Bakkers, J., Kuhl, M., Schaeffer, H.J., Huelsken, J., Behrens, J., Hammerschmidt, M., and Birchmeier, W. (2002). The ankyrin repeat protein Diversin recruits Casein kinase I $\epsilon$  to the beta-catenin degradation complex and acts in both canonical Wnt and Wnt/JNK signaling. *Genes Dev* *16*, 2073-2084.
- Schwarz, Q., Maden, C.H., Davidson, K., and Ruhrberg, C. (2009a). Neuropilin-mediated neural crest cell guidance is essential to organise sensory neurons into segmented dorsal root ganglia. *Development* *136*, 1785-1789.
- Schwarz, Q., Maden, C.H., Vieira, J.M., and Ruhrberg, C. (2009b). Neuropilin 1 signaling guides neural crest cells to coordinate pathway choice with cell specification. *Proc Natl Acad Sci U S A* *106*, 6164-6169.
- Schwarz, Q., Vieira, J.M., Howard, B., Eickholt, B.J., and Ruhrberg, C. (2008). Neuropilin 1 and 2 control cranial gangliogenesis and axon guidance through neural crest cells. *Development* *135*, 1605-1613.
- Seifert, J.R., and Mlodzik, M. (2007). Frizzled/PCP signalling: a conserved mechanism regulating cell polarity and directed motility. *Nat Rev Genet* *8*, 126-138.
- Selleck, M.A., and Bronner-Fraser, M. (1996). The genesis of avian neural crest cells: a classic embryonic induction. *Proc Natl Acad Sci U S A* *93*, 9352-9357.
- Shao, M., Liu, Z.Z., Wang, C.D., Li, H.Y., Carron, C., Zhang, H.W., and Shi, D.L. (2009). Down syndrome critical region protein 5 regulates membrane localization of Wnt receptors, Dishevelled stability and convergent extension in vertebrate embryos. *Development* *136*, 2121-2131.
- Sharp, P.A., Sugden, B., and Sambrook, J. (1973). Detection of two restriction endonuclease activities in *Haemophilus parainfluenzae* using analytical agarose-ethidium bromide electrophoresis. *Biochemistry* *12*, 3055-3063.
- Shevchenko, A., Wilm, M., Vorm, O., and Mann, M. (1996). Mass spectrometric sequencing of proteins silver-stained polyacrylamide gels. *Anal Chem* *68*, 850-858.
- Shiau, C.E., Lwigale, P.Y., Das, R.M., Wilson, S.A., and Bronner-Fraser, M. (2008). Robo2-Slit1 dependent cell-cell interactions mediate assembly of the trigeminal ganglion. *Nat Neurosci* *11*, 269-276.
- Shimada, Y., Usui, T., Yanagawa, S., Takeichi, M., and Uemura, T. (2001). Asymmetric colocalization of Flamingo, a seven-pass transmembrane cadherin, and Dishevelled in planar cell polarization. *Curr Biol* *11*, 859-863.
- Simons, M., Gloy, J., Ganner, A., Bullerkotte, A., Bashkurov, M., Kronig, C., Schermer, B., Benzing, T., Cabello, O.A., Jenny, A., *et al.* (2005). Inversin, the gene product mutated in nephronophthisis type II, functions as a molecular switch between Wnt signaling pathways. *Nat Genet* *37*, 537-543.
- Simons, M., and Mlodzik, M. (2008). Planar cell polarity signaling: from fly development to human disease. *Annu Rev Genet* *42*, 517-540.
- Simons, M., and Walz, G. (2006). Polycystic kidney disease: cell division without a cilium? *Kidney Int* *70*, 854-864.
- Singla, V., and Reiter, J.F. (2006). The primary cilium as the cell's antenna: signaling at a sensory organelle. *Science* *313*, 629-633.
- Sisson, B.E., and Topczewski, J. (2009). Expression of five frizzleds during zebrafish craniofacial development. *Gene Expr Patterns*.
- Sivak, J.M., Petersen, L.F., and Amaya, E. (2005). FGF signal interpretation is directed by Sprouty and Spred proteins during mesoderm formation. *Dev Cell* *8*, 689-701.
- Sklan, E.H., Podoly, E., and Soreq, H. (2006). RACK1 has the nerve to act: structure meets function in the nervous system. *Prog Neurobiol* *78*, 117-134.
- Smalley, M.J., Sara, E., Paterson, H., Naylor, S., Cook, D., Jayatilake, H., Fryer, L.G., Hutchinson, L., Fry, M.J., and Dale, T.C. (1999). Interaction of axin and Dvl-2 proteins regulates Dvl-2-stimulated TCF-dependent transcription. *EMBO J* *18*, 2823-2835.

- Smith, A., Robinson, V., Patel, K., and Wilkinson, D.G. (1997). The EphA4 and EphB1 receptor tyrosine kinases and ephrin-B2 ligand regulate targeted migration of branchial neural crest cells. *Curr Biol* 7, 561-570.
- Sokol, S.Y. (1996). Analysis of Dishevelled signalling pathways during *Xenopus* development. *Curr Biol* 6, 1456-1467.
- Steventon, B., Carmona-Fontaine, C., and Mayor, R. (2005). Genetic network during neural crest induction: from cell specification to cell survival. *Semin Cell Dev Biol* 16, 647-654.
- Strachan, L.R., and Condic, M.L. (2003). Neural crest motility and integrin regulation are distinct in cranial and trunk populations. *Dev Biol* 259, 288-302.
- Strachan, L.R., and Condic, M.L. (2008). Neural crest motility on fibronectin is regulated by integrin activation. *Exp Cell Res* 314, 441-452.
- Strutt, D. (2003). Frizzled signalling and cell polarisation in *Drosophila* and vertebrates. *Development* 130, 4501-4513.
- Strutt, D., Johnson, R., Cooper, K., and Bray, S. (2002). Asymmetric localization of frizzled and the determination of notch-dependent cell fate in the *Drosophila* eye. *Curr Biol* 12, 813-824.
- Strutt, D.I., Weber, U., and Mlodzik, M. (1997). The role of RhoA in tissue polarity and Frizzled signalling. *Nature* 387, 292-295.
- Strutt, H., Mundy, J., Hofstra, K., and Strutt, D. (2004). Cleavage and secretion is not required for Four-jointed function in *Drosophila* patterning. *Development* 131, 881-890.
- Strutt, H., Price, M.A., and Strutt, D. (2006). Planar polarity is positively regulated by casein kinase Iepsilon in *Drosophila*. *Curr Biol* 16, 1329-1336.
- Sullivan, R., Huang, G.Y., Meyer, R.A., Wessels, A., Linask, K.K., and Lo, C.W. (1998). Heart malformations in transgenic mice exhibiting dominant negative inhibition of gap junctional communication in neural crest cells. *Dev Biol* 204, 224-234.
- Sun, T.Q., Lu, B., Feng, J.J., Reinhard, C., Jan, Y.N., Fantl, W.J., and Williams, L.T. (2001). PAR-1 is a Dishevelled-associated kinase and a positive regulator of Wnt signalling. *Nat Cell Biol* 3, 628-636.
- Sussman, D.J., Klingensmith, J., Salinas, P., Adams, P.S., Nusse, R., and Perrimon, N. (1994). Isolation and characterization of a mouse homolog of the *Drosophila* segment polarity gene *dishevelled*. *Dev Biol* 166, 73-86.
- Tada, M., and Smith, J.C. (2000). *Xwnt11* is a target of *Xenopus* Brachyury: regulation of gastrulation movements via Dishevelled, but not through the canonical Wnt pathway. *Development* 127, 2227-2238.
- Tahinci, E., and Symes, K. (2003). Distinct functions of Rho and Rac are required for convergent extension during *Xenopus* gastrulation. *Dev Biol* 259, 318-335.
- Tahinci, E., Thorne, C.A., Franklin, J.L., Salic, A., Christian, K.M., Lee, L.A., Coffey, R.J., and Lee, E. (2007). *Lrp6* is required for convergent extension during *Xenopus* gastrulation. *Development* 134, 4095-4106.
- Takada, R., Hijikata, H., Kondoh, H., and Takada, S. (2005). Analysis of combinatorial effects of Wnts and Frizzleds on beta-catenin/armadillo stabilization and Dishevelled phosphorylation. *Genes Cells* 10, 919-928.
- Tamagnone, L., and Comoglio, P.M. (2004). To move or not to move? Semaphorin signalling in cell migration. *EMBO Rep* 5, 356-361.
- Taneyhill, L.A. (2008). To adhere or not to adhere: the role of Cadherins in neural crest development. *Cell Adh Migr* 2, 223-230.
- Taneyhill, L.A., Coles, E.G., and Bronner-Fraser, M. (2007). *Snail2* directly represses *cadherin6B* during epithelial-to-mesenchymal transitions of the neural crest. *Development* 134, 1481-1490.
- Tanihara, H., Sano, K., Heimark, R.L., St John, T., and Suzuki, S. (1994). Cloning of five human cadherins clarifies characteristic features of cadherin extracellular domain and provides further evidence for two structurally different types of cadherin. *Cell Adhes Commun* 2, 15-26.
- Taylor, J., Abramova, N., Charlton, J., and Adler, P.N. (1998). *Van Gogh*: a new *Drosophila* tissue polarity gene. *Genetics* 150, 199-210.
- Theisen, H., Purcell, J., Bennett, M., Kansagara, D., Syed, A., and Marsh, J.L. (1994). *dishevelled* is required during wingless signaling to establish both cell polarity and cell identity. *Development* 120, 347-360.

- Thiery, J.P. (2002). Epithelial-mesenchymal transitions in tumour progression. *Nat Rev Cancer* 2, 442-454.
- Thorpe, C.J., and Moon, R.T. (2004). nemo-like kinase is an essential co-activator of Wnt signaling during early zebrafish development. *Development* 131, 2899-2909.
- Ting, M.C., Wu, N.L., Roybal, P.G., Sun, J., Liu, L., Yen, Y., and Maxson, R.E., Jr. (2009). EphA4 as an effector of Twist1 in the guidance of osteogenic precursor cells during calvarial bone growth and in craniosynostosis. *Development* 136, 855-864.
- Tomlinson, M.L., Guan, P., Morris, R.J., Fidock, M.D., Rejzek, M., Garcia-Morales, C., Field, R.A., and Wheeler, G.N. (2009). A chemical genomic approach identifies matrix metalloproteinases as playing an essential and specific role in *Xenopus* melanophore migration. *Chem Biol* 16, 93-104.
- Topczewski, J., Sepich, D.S., Myers, D.C., Walker, C., Amores, A., Lele, Z., Hammerschmidt, M., Postlethwait, J., and Solnica-Krezel, L. (2001). The zebrafish glypican knypek controls cell polarity during gastrulation movements of convergent extension. *Dev Cell* 1, 251-264.
- Toyofuku, T., Yoshida, J., Sugimoto, T., Yamamoto, M., Makino, N., Takamatsu, H., Takegahara, N., Suto, F., Hori, M., Fujisawa, H., *et al.* (2008). Repulsive and attractive semaphorins cooperate to direct the navigation of cardiac neural crest cells. *Dev Biol* 321, 251-262.
- Tree, D.R., Shulman, J.M., Rousset, R., Scott, M.P., Gubb, D., and Axelrod, J.D. (2002). Prickle mediates feedback amplification to generate asymmetric planar cell polarity signaling. *Cell* 109, 371-381.
- Tucker, R.P. (2004). Neural crest cells: a model for invasive behavior. *Int J Biochem Cell Biol* 36, 173-177.
- Tuzi, N.L., and Gullick, W.J. (1994). eph, the largest known family of putative growth factor receptors. *Br J Cancer* 69, 417-421.
- Twigg, S.R., Kan, R., Babbs, C., Bochukova, E.G., Robertson, S.P., Wall, S.A., Morriss-Kay, G.M., and Wilkie, A.O. (2004). Mutations of ephrin-B1 (EFNB1), a marker of tissue boundary formation, cause craniofrontonasal syndrome. *Proc Natl Acad Sci U S A* 101, 8652-8657.
- Ungar, A.R., Kelly, G.M., and Moon, R.T. (1995). Wnt4 affects morphogenesis when misexpressed in the zebrafish embryo. *Mech Dev* 52, 153-164.
- Unterseher, F., Hefele, J.A., Giehl, K., De Robertis, E.M., Wedlich, D., and Schambony, A. (2004). Paraxial protocadherin coordinates cell polarity during convergent extension via Rho A and JNK. *EMBO J* 23, 3259-3269.
- Usui, T., Shima, Y., Shimada, Y., Hirano, S., Burgess, R.W., Schwarz, T.L., Takeichi, M., and Uemura, T. (1999). Flamingo, a seven-pass transmembrane cadherin, regulates planar cell polarity under the control of Frizzled. *Cell* 98, 585-595.
- Vallejo-Illarramendi, A., Zang, K., and Reichardt, L.F. (2009). Focal adhesion kinase is required for neural crest cell morphogenesis during mouse cardiovascular development. *J Clin Invest* 119, 2218-2230.
- Vallin, J., Thuret, R., Giacomello, E., Faraldo, M.M., Thiery, J.P., and Broders, F. (2001). Cloning and characterization of three *Xenopus* slug promoters reveal direct regulation by Lef/beta-catenin signaling. *J Biol Chem* 276, 30350-30358.
- Veeman, M.T., Axelrod, J.D., and Moon, R.T. (2003a). A second canon. Functions and mechanisms of beta-catenin-independent Wnt signaling. *Dev Cell* 5, 367-377.
- Veeman, M.T., Slusarski, D.C., Kaykas, A., Louie, S.H., and Moon, R.T. (2003b). Zebrafish prickle, a modulator of noncanonical Wnt/Fz signaling, regulates gastrulation movements. *Curr Biol* 13, 680-685.
- Vinson, C.R., and Adler, P.N. (1987). Directional non-cell autonomy and the transmission of polarity information by the frizzled gene of *Drosophila*. *Nature* 329, 549-551.
- Wallingford, J.B. (2004). Closing in on vertebrate planar polarity. *Nat Cell Biol* 6, 687-689.
- Wallingford, J.B., and Habas, R. (2005). The developmental biology of Dishevelled: an enigmatic protein governing cell fate and cell polarity. *Development* 132, 4421-4436.
- Wallingford, J.B., and Harland, R.M. (2001). *Xenopus* Dishevelled signaling regulates both neural and mesodermal convergent extension: parallel forces elongating the body axis. *Development* 128, 2581-2592.
- Wallingford, J.B., and Harland, R.M. (2002). Neural tube closure requires Dishevelled-dependent convergent extension of the midline. *Development* 129, 5815-5825.



- Wallingford, J.B., Rowning, B.A., Vogeli, K.M., Rothbacher, U., Fraser, S.E., and Harland, R.M. (2000). Dishevelled controls cell polarity during *Xenopus* gastrulation. *Nature* *405*, 81-85.
- Wang, H.U., and Anderson, D.J. (1997). Eph family transmembrane ligands can mediate repulsive guidance of trunk neural crest migration and motor axon outgrowth. *Neuron* *18*, 383-396.
- Wang, J., Hamblet, N.S., Mark, S., Dickinson, M.E., Brinkman, B.C., Segil, N., Fraser, S.E., Chen, P., Wallingford, J.B., and Wynshaw-Boris, A. (2006a). Dishevelled genes mediate a conserved mammalian PCP pathway to regulate convergent extension during neurulation. *Development* *133*, 1767-1778.
- Wang, Y., Guo, N., and Nathans, J. (2006b). The role of Frizzled3 and Frizzled6 in neural tube closure and in the planar polarity of inner-ear sensory hair cells. *J Neurosci* *26*, 2147-2156.
- Wang, Y., Janicki, P., Koster, I., Berger, C.D., Wenzl, C., Grosshans, J., and Steinbeisser, H. (2008). *Xenopus* Paraxial Protocadherin regulates morphogenesis by antagonizing Sprouty. *Genes Dev* *22*, 878-883.
- Wang, Y., and Nathans, J. (2007). Tissue/planar cell polarity in vertebrates: new insights and new questions. *Development* *134*, 647-658.
- Wang, Y., Zhang, J., Mori, S., and Nathans, J. (2006c). Axonal growth and guidance defects in Frizzled3 knock-out mice: a comparison of diffusion tensor magnetic resonance imaging, neurofilament staining, and genetically directed cell labeling. *J Neurosci* *26*, 355-364.
- Watanabe, N., and Higashida, C. (2004). Formins: processive cappers of growing actin filaments. *Exp Cell Res* *301*, 16-22.
- Wehrli, M., Dougan, S.T., Caldwell, K., O'Keefe, L., Schwartz, S., Vaizel-Ohayon, D., Schejter, E., Tomlinson, A., and DiNardo, S. (2000). arrow encodes an LDL-receptor-related protein essential for Wingless signalling. *Nature* *407*, 527-530.
- Wells, C.M., and Ridley, A.J. (2005). Analysis of cell migration using the Dunn chemotaxis chamber and time-lapse microscopy. *Methods Mol Biol* *294*, 31-41.
- Whittaker, C.A., and DeSimone, D.W. (1993). Integrin alpha subunit mRNAs are differentially expressed in early *Xenopus* embryos. *Development* *117*, 1239-1249.
- Wiggin, O., and Hamel, P.A. (2002). Pax3 regulates morphogenetic cell behavior in vitro coincident with activation of a PCP/non-canonical Wnt-signaling cascade. *J Cell Sci* *115*, 531-541.
- Willert, K., Brink, M., Wodarz, A., Varmus, H., and Nusse, R. (1997). Casein kinase 2 associates with and phosphorylates dishevelled. *EMBO J* *16*, 3089-3096.
- Winberg, M.L., Tamagnone, L., Bai, J., Comoglio, P.M., Montell, D., and Goodman, C.S. (2001). The transmembrane protein Off-track associates with Plexins and functions downstream of Semaphorin signaling during axon guidance. *Neuron* *32*, 53-62.
- Winklbauer, R., Medina, A., Swain, R.K., and Steinbeisser, H. (2001). Frizzled-7 signalling controls tissue separation during *Xenopus* gastrulation. *Nature* *413*, 856-860.
- Winter, C.G., Wang, B., Ballew, A., Royou, A., Kares, R., Axelrod, J.D., and Luo, L. (2001). *Drosophila* Rho-associated kinase (Drok) links Frizzled-mediated planar cell polarity signaling to the actin cytoskeleton. *Cell* *105*, 81-91.
- Wolff, T., and Rubin, G.M. (1998). Strabismus, a novel gene that regulates tissue polarity and cell fate decisions in *Drosophila*. *Development* *125*, 1149-1159.
- Wong, H.C., Bourdelas, A., Krauss, A., Lee, H.J., Shao, Y., Wu, D., Mlodzik, M., Shi, D.L., and Zheng, J. (2003). Direct binding of the PDZ domain of Dishevelled to a conserved internal sequence in the C-terminal region of Frizzled. *Mol Cell* *12*, 1251-1260.
- Wong, H.C., Mao, J., Nguyen, J.T., Srinivas, S., Zhang, W., Liu, B., Li, L., Wu, D., and Zheng, J. (2000). Structural basis of the recognition of the dishevelled DEP domain in the Wnt signaling pathway. *Nat Struct Biol* *7*, 1178-1184.
- Wong, L.L., and Adler, P.N. (1993). Tissue polarity genes of *Drosophila* regulate the subcellular location for prehair initiation in pupal wing cells. *J Cell Biol* *123*, 209-221.
- Wu, J., Jenny, A., Mirkovic, I., and Mlodzik, M. (2008). Frizzled-Dishevelled signaling specificity outcome can be modulated by Diego in *Drosophila*. *Mech Dev* *125*, 30-42.

- Xu, X., Francis, R., Wei, C.J., Linask, K.L., and Lo, C.W. (2006). Connexin 43-mediated modulation of polarized cell movement and the directional migration of cardiac neural crest cells. *Development* 133, 3629-3639.
- Yamaguchi, Y., Katoh, H., Yasui, H., Mori, K., and Negishi, M. (2001). RhoA inhibits the nerve growth factor-induced Rac1 activation through Rho-associated kinase-dependent pathway. *J Biol Chem* 276, 18977-18983.
- Yamanaka, H., Moriguchi, T., Masuyama, N., Kusakabe, M., Hanafusa, H., Takada, R., Takada, S., and Nishida, E. (2002). JNK functions in the non-canonical Wnt pathway to regulate convergent extension movements in vertebrates. *EMBO Rep* 3, 69-75.
- Yan, J., Huen, D., Morely, T., Johnson, G., Gubb, D., Roote, J., and Adler, P.N. (2008). The multiple-wing-hairs gene encodes a novel GBD-FH3 domain-containing protein that functions both prior to and after wing hair initiation. *Genetics* 180, 219-228.
- Yanagawa, S., van Leeuwen, F., Wodarz, A., Klingensmith, J., and Nusse, R. (1995). The dishevelled protein is modified by wingless signaling in *Drosophila*. *Genes Dev* 9, 1087-1097.
- Yang-Snyder, J., Miller, J.R., Brown, J.D., Lai, C.J., and Moon, R.T. (1996). A frizzled homolog functions in a vertebrate Wnt signaling pathway. *Curr Biol* 6, 1302-1306.
- Yang, C.H., Axelrod, J.D., and Simon, M.A. (2002). Regulation of Frizzled by fat-like cadherins during planar polarity signaling in the *Drosophila* compound eye. *Cell* 108, 675-688.
- Yen, W.W., Williams, M., Periasamy, A., Conaway, M., Burdsal, C., Keller, R., Lu, X., and Sutherland, A. (2009). PTK7 is essential for polarized cell motility and convergent extension during mouse gastrulation. *Development* 136, 2039-2048.
- Yin, C., Kiskowski, M., Pouille, P.A., Farge, E., and Solnica-Krezel, L. (2008). Cooperation of polarized cell intercalations drives convergence and extension of presomitic mesoderm during zebrafish gastrulation. *J Cell Biol* 180, 221-232.
- Young, H.M., Hearn, C.J., Farlie, P.G., Canty, A.J., Thomas, P.Q., and Newgreen, D.F. (2001). GDNF is a chemoattractant for enteric neural cells. *Dev Biol* 229, 503-516.
- Yu, H.H., and Moens, C.B. (2005). Semaphorin signaling guides cranial neural crest cell migration in zebrafish. *Dev Biol* 280, 373-385.
- Yun, U.J., Kim, S.Y., Liu, J., Adler, P.N., Bae, E., Kim, J., and Park, W.J. (1999). The intumed protein of *Drosophila melanogaster* is a cytoplasmic protein located at the cell periphery in wing cells. *Dev Genet* 25, 297-305.
- Zeidler, M.P., Perrimon, N., and Strutt, D.I. (1999). The four-jointed gene is required in the *Drosophila* eye for ommatidial polarity specification. *Curr Biol* 9, 1363-1372.
- Zisch, A.H., and Pasquale, E.B. (1997). The Eph family: a multitude of receptors that mediate cell recognition signals. *Cell Tissue Res* 290, 217-226

**Curriculum vitae**

**Name:** Iryna Shnitsar

**Date of birth:** 25<sup>th</sup> September 1981

**Address:** Albrecht-Thaer-Weg 26/14, 37075 Göttingen, Germany

**E-mail:** ira.shnitsar@gmail.com

**Marital status:** married, 1 child

**Educational background**

**1988-1998** Primary and secondary schools, Smila, Ukraine

**1998-2002** Bachelor program in biology, The University of Kyiv-Mohyla Academy, Kyiv, Ukraine, BSc, June 2002

**2002-2004** Master program in biology, The University of Kyiv-Mohyla Academy, Kyiv, Ukraine, MSc, June 2004

**2005-2009** MSc/PhD Molecular biology program, University of Göttingen and International Max Plank Research School, Göttingen, Germany

**2006-2009** PhD work in the Dept. of Developmental Biochemistry, GZMB, Göttingen, Germany

**Experimental skills**

**2001-2002** The expression of beta-defensins in human cervical and vulval malignancies. Dept. of Tumor Cell Biology, Institute of Experimental Pathology, Oncology and Radiobiology, NAS of Ukraine, Kyiv, Ukraine.

**2002-2004** Generation and characterization of the monoclonal antibodies to human beta-defensin 2. Dept. of Tumor Cell Biology, Institute of Experimental Pathology, Oncology and Radiobiology, NAS of Ukraine, Kyiv, Ukraine.

**2006-2009** The function of PTK7 during *Xenopus* neural crest migration (PhD thesis). Dept. of Developmental Biochemistry, Center for biochemistry and molecular cell biology, Georg August University Göttingen.

**Scholarships;**

1. International Max Plank Research School Stipend (2005-2006)
2. Lichtenberg Stipend (2006-2008)
3. The Stipend of Christiane Nüsslein-Volhard foundation (2007-2009)
4. The Stipend of Graduate School for Neurosciences and Molecular Biosciences (2009)